Studies of ATF7IP as a novel interaction partner of c-Myb - epigenetic repressor or co-activator?

Flavia Söllner

Master thesis at the Department of Biosciences
Faculty of Mathematics and Natural Sciences

UNIVERSITY OF OSLO
August 2014

Studies of ATF7IP as a novel interaction partner of c-Myb
- epigenetic repressor or co-activator?

Flavia Söllner

http://www.duo.uio.no

Print: Reprosentralen, Universitetet i Oslo

Acknowledgements

The work for this thesis was carried out at the Department of Biosciences, University of Oslo in the period from May 2013 to August 2014.

First and foremost, I would like to thank my supervisor Professor Odd Stokke Gabrielsen for providing me with this project and for letting me work and study in his group. His guidance and encouragement have meant a lot to me.

I would like to particularly thank my co-supervisors: Vilborg Matre and Marit Ledsaak. Their help both in the lab and later during the writing process has been invaluable to me. I want to thank them for always having an open ear and for sharing their knowledge and expertise so freely and enthusiastically with me. I would also like to thank Ragnhild Eskeland for her input and advice.

Further, I would like to thank all the Myb group members present and past; they have made being part of this group feel like hitting the jackpot.

Next, I would like to thank my friends: Gro and Trine, Astri and Chrissie, Markus and Tom. A special thank you goes to Margrete; being able to study beside her has been fantastic.

Finally, I would like to thank my grandparents Magdalena and Josef, Stefan and Maria, my parents Hildegard and Walter, my brother Immo, my sister Antonia (&co.), and Benjamin. Without you none of this would have been possible.

Oslo, August 2014
Flavia Söllner

Abstract

The c-Myb transcription factor is a key regulator of haematopoiesis. Its activity is regulated by a large network of protein interactions and post-translational modifications. ATF7IP is a transcriptional cofactor previously implicated both as a repressive and activating modulator of other transcription factors, depending on site and context. A recent yeast two-hybrid screening in our lab identified ATF7IP as a putative interaction partner of c-Myb.

In this thesis, the interaction between ATF7IP and c-Myb was investigated and validated using GST-pulldown analyses. We found ATF7IP to associate with c-Myb in a SUMO-enhanced manner. Initially we proposed two hypothetical models for the functional consequences of how ATF7IP modulates c-Myb function: The Epigenetic Repressor Model and The Mediator-like Activation Model. Using various reporter gene assays, we found no evidence for the first model, but ATF7IP-induced activation in two different reporter assays. We conclude that ATF7IP acts as a novel c-Myb co-activator, presumably by bridging enhancer-bound c-Myb to the general transcription apparatus, thereby promoting the initiation of c-Myb target gene expression.

Table of Contents

1. Introduction 11
1.1. Transcription 11
1.2. c-Myb 12
1.2.1. Molecular properties of c-Myb 13
1.2.1.1. The DNA binding domain of c-Myb 14
1.2.1.2. The transactivation domain of c-Myb 14
1.2.1.3. The C-terminal regulatory domain of c-Myb 15
1.2.2. c-Myb protein and post-translational modifications 15
1.2.2.1. PTMs in the DBD region of c-Myb 16
1.2.2.2. Motif in the TAD region of c-Myb 16
1.2.2.3. PTMs in the CRD region of c-Myb 17
1.2.3. c-Myb protein-protein interactions 17
1.2.4. c-Myb and epigenetic effects 19
1.2.5. c-Myb targets 20
1.2.6. The biological function of c-Myb 21
1.3. SUMO 22
1.3.1. Non-covalent and covalent SUMO interactions 22
1.3.2. The SUMO paradox 24
1.3.3. SUMO and c-Myb 24
1.4. ATF7IP 25
1.4.1. Molecular properties of ATF7IP 26
1.4.2. ATF7IP and PTMs 26
1.4.3. ATF7IP and interacting proteins 27
1.4.3.1. Protein‐Protein interactions with ATF7IP-Domain 1 27
1.4.3.2. Protein‐Protein interactions with ATF7IP-Domain 2 27
1.4.3.3. Protein‐Protein interactions involving unknown region of ATF7IP 28
1.4.3.4. The strong SIM domain of ATF7IP 28
1.4.4. ATF7IP and interacting proteins in repression 28
1.4.5. ATF7IP and interacting proteins in activation 29
1.5. Aim of the Study 30

2. Methods 33
2.1. Nucleic acid and Subcloning Techniques 33
2.1.1. Transformation of bacterial cells 33
2.1.2. DNA extraction from bacterial cells 35
2.1.3. RNA extraction from mammalian cells 35
2.1.4. DNA/RNA concentration assessment 36
2.1.5. DNA restriction digest 37
2.1.6. DNA separation by agarose gel electrophoresis 38
2.1.7. DNA purification from agarose gel 40
2.1.8. DNA ligation 40
2.1.9. Gateway recombination cloning 41
2.1.10. Polymerase chain reaction (PCR) 43
2.1.11. quantitative real-time PCR (qRT-PCR) 43
2.1.12. DNA mutagenesis 45
2.1.13. cDNA synthesis 48
2.1.14. DNA sequencing 49
2.1.15. Plasmid Stem Culturing 49
2.2. Mammalian Cell Culturing 50
2.2.1. Routine Maintenance of Cells 50
2.2.1.1. COS-1 52
2.2.1.2. CV-1 52
2.2.1.3. HEK293-c1 52
2.2.1.4. HD11 52

2.2.2. Counting Cells 53
2.2.3. Transfecting Cells 53
2.2.3.1. COS-1 55
2.2.3.2. CV-1 55
2.2.3.3. HEK293-c1 56
2.2.3.4. HD11 56
2.3. Protein Techniques *57*
2.3.1. GST-protein purification and GST-pulldown 57
2.3.2. Luciferase Reporter Gene Assay 60
2.3.2.1. Luciferase Assays using Transiently Transfected Reporters 62
2.3.2.2. Luciferase Assays using Stably Integrated Reporters 62
2.3.3. HD11 mim-1 Reporter Gene Assay 63
2.3.4. Protein Phosphatase treatment 65
2.3.5. SDS-PAGE 66
2.3.6. Semi-dry Western blotting 68

3. Results 71
3.1. Development of tools *71*
3.1.1. Generating plasmids for expression of ATF7IP and its partners 71
3.1.1.1. Subcloning of the 3FLAG-tagged ATF7IP construct 71
3.1.1.2. Mutagenizing the ATF7IP construct 72
3.1.1.3. Subcloning of the HA tagged hMBD1 construct 73
3.1.1.4. Gateway cloning of SETDB1 into an expression vector 74
3.1.2. Protein expression and Antibody detection 75
3.1.2.1. Detecting 3FLAG-tagged COS-1 cell lysates 75
3.1.2.2. Detecting ectopic and endogenous ATF7IP in HEK293-c1 cell lysates 76
3.1.2.3. Detecting 3FG-ATF7IP in CV-1 cell lysate after Phosphatase treatment 77
3.1.2.4. Detecting HA- hMBD1 in COS-1 cell lysate 78
3.1.2.5. Detecting hSETDB1 in COS-1 cell lysate 79
3.1.3. Dosage Response for Luciferase Assays 79
3.1.3.1. c-Myb dosage in transient reporter models 80
3.1.3.2. hSUMO1-Q94P and hSUMO2-Q90P dosage response in transient reporter models 81
3.2. Validation of the interaction between c-Myb and ATF7IP. *84*
3.2.1. Do c-Myb and ATF7IP interact, if so is this interaction SUMO dependent? 84
3.2.2. Does ATF7IP preferentially interact with SUMO1 or SUMO2-conjugated substrates 86
3.3. What are the functional implications of the c-Myb – ATF7IP interaction? Is there a functional difference between ATF7IP wild-type and an ATF7IP SIM mutant? *89*
3.3.1. Luciferase Assays in CV-1 cells using transiently transfected reporters 89
3.3.2. Luciferase Assays in HEK293-c1 cells containing a stably integrated reporter 91
3.4. Does an increase in the SUMOylation level of c-Myb increase the functional effects of the c-Myb - ATF7IP interaction? *94*
3.5. Does co-transfection with known ATF7IP interactants SETDB1 and MBD1 increase the functional effects of the c-Myb – ATF7IP interaction? *95*
3.5.1. Luciferase Assays in CV-1 cells using a transiently transfected reporter 96
3.5.2. Luciferase Assays in HEK293-c1 cells containing a stably integrated reporter 98
3.6. Is the observed MBD1 effect c-Myb specific? *101*
3.7. Is the observed activational effect of MBD1 on c-Myb regulated transcription SUMO dependent? *102*
3.8. What are the functional implications of ATF7IP and MBD1 on c-Myb regulated transcription using a more endogenous assay approach? *103*

4. Discussion 106
4.1. Interaction Studies - Confirming and characterizing the interaction between c-Myb and ATF7IP *106*
4.1.1. ATF7IP and c-Myb interact 107
4.1.2. The interaction between ATF7IP and c-Myb is SUMO enhanced. 107

4.1.3. ATF7IP shows a preference for SUMO2 over SUMO1.....107
4.1.4. ATF7IP shows a preference for poly-SUMO over mono-SUMO.....110
4.2. Functional Studies – The effect ATF7IP has on c-Myb 112
4.2.1. Choice of different functional reporter gene assays 112
4.2.2. Disproving Model 1 - The interaction between c-Myb and ATF7IP does not lead to repression of c-Myb target genes.....115
4.2.3. Expression levels - Endogenous versus transfected ATF7IP 116
4.2.4. PTMs of ATF7IP - The migration paradox 117
4.3. Functional studies - How ATF7IP interaction partners affect c-Myb 119
4.4. Functional Studies - Model 1 versus Model 2.....119

5. Summary of findings 121
5.1. Conclusions - Part 1.....121
5.2. Conclusions - Part 2.....121
5.3. Conclusions - Part 3.....122

6. Future Work 123
6.1. Further studies - Part 1.....123
6.2. Further studies - Part 2.....123
6.3. Further studies - Part 3.....124

7. References 125

1. Introduction

Every single multicellular organism is made up of a multitude of different cells and tissue types. While these cells have diverse physiological and functional characteristics and properties, the DNA sequence of each singular cell is identical. When thinking on an interspecies level: the roundworm has roughly 20000 genes [69]; the fruit fly has less than 14000 [1], yet the roundworm lacks cell types and tissues observable in the fruit fly [42]. A greater number of genes do not seem to necessitate a greater complexity. Neither does an identical genome indicate an identical cellular outcome.

The complexity and differentiation both within one organism and comparatively with another can be explained by the number of ways in which a seemingly small number of genes can be expressed, resulting in different sets of proteins and thus different cell types. Mechanisms such as alternative splicing and DNA re-arrangement are well known. However, it has also been suggested that complexity might have far more to do with differential gene expression patterns than was initially expected [42]. This postulate is supported by the estimation that 10% of the genes found in a multicellular organism encode proteins involved in gene expression regulation [9].

1.1. Transcription

The first step in gene expression is transcription, the copying of a DNA strand into a complementary RNA strand. This process is facilitated by the RNA polymerase enzymes in conjunction with: general transcription factors, activating transcription factors, transcriptional repressors, as well as co-activators, co-repressors, histone-modifying enzymes, and chromatin remodelling complexes.

Eukaryotic cells contain three different types of RNA polymerase (I – III). Although these are structurally very similar to each other, only RNA polymerase II (**RNAPII**) transcribes genes resulting in proteins. Transcription factors are sequence specific DNA-binding proteins that can directly associate with promoter regions in the proximity of genes or with enhancers further away, thereby regulating their target genes. Depending on the specific transcription factor, as well as their interaction

partners and post-translational modifications, the expression of the gene in question can either be ‘up’ or ‘down’ regulated. In differential expression regulation, various diverse mechanisms are at play. The transcription factors might block or enhance the ability of the RNA polymerase to interact with the coding DNA, they might recruit co-activators or co-repressors to the transcription complexes [92], or possibly influence DNA compaction and thus accessibility – either through catalytic function or ability to recruit other epigenetic players [58].

It is the synergistic interplay of necessary transcription factors, polymerase and additional gene regulating proteins, that determines whether or not a specific gene is expressed (and the level of this expression) - both spatially (in a specific cell) and temporally (at a specific time). This culminates in multipart pathways of protein interactions and post-translational modifications controlling cell proliferation and differentiation, thus driving the generation of different and complex tissues.

1.2. c-Myb

The focus of this section is the human c-Myb (**hcM**) transcription factor. Special attention will be paid to its structural and functional domains (section 1.2.1), its post-translational modifications (**PTMs**) (section 1.2.2) and interactions with other proteins (section 1.2.3). The effect of these interactions on chromatin packaging will also be covered (section 1.2.4). Subsequently, a closer look will be directed at the functional role of c-Myb in both normal and malignant cells (sections 1.2.5 and 1.2.6).

The *Myb* proto-oncogene was initially identified as the normal cellular counterpart of the oncogenes carried by the chicken leukaemia viruses: Avian Myeblastosis Virus (**AMV**) and E26 [39]. The viral v-Myb proteins have C-terminal truncations of the normal cellular c-Myb protein. v-Myb^{AMV} was identified as a truncated version of c-Myb. Instead of 75 kDa it weighed 45 kDa and was made up of 370 c-Myb amino acids with an additional 6 and 11 gag and env residue, as well as 10 amino acid (**aa**) substitutions. The *v-myb*^{E26} gene was found to code for a 135 kDa gag-Myb-Ets-1 fusion protein, with a one aa substitution in the Myb region. C-terminal deletions play vital roles in the oncogenicity of these proteins (as reviewed by Lipsick *et al* [44] and Oh *et al* [61]).

As the *v-myb* viruses were known to be severely oncogenic and capable of transforming immature hematopoietic cells *in vitro* and inducing acute leukaemia in chicken [93], concerted efforts into their characterization and biology were initiated. Due to v-Myb protein's role in chicken leukaemia, c-Myb was mainly studied in association with its functions in hematopoietic cells and hematopoietic malignancies. Further investigations into the transcription factor have implicated aberrant c-Myb function in several human cancers (see section 1.2.6).

Interest in c-Myb further led to the discovery of two additional *MYB* gene family members: *MYBL1* and *MYBL2*, which, like *MYB* also encode nuclear proteins, sharing a high degree of sequence similarity and nearly identical DNA-binding specificities [61, 68]. While these members may be similar, it seems that they are subject to different expression patterns [61]. In spite of their high sequence homology with c-Myb as well as both being transcription factors [53, 50], neither A-myb nor B-myb have been shown to be oncogenic, nor be capable of *in vitro* transformation [93].

1.2.1. Molecular properties of c-Myb

The *MYB* gene encodes the nuclear c-Myb protein, spanning 640 amino acid residues arranged in a tripartite structure, which is made up of the DNA binding N-terminal domain (**DBD**), a central transactivation domain (**TAD**), and a regulatory C-terminal domain (**CRD**) (see figure 1.1).

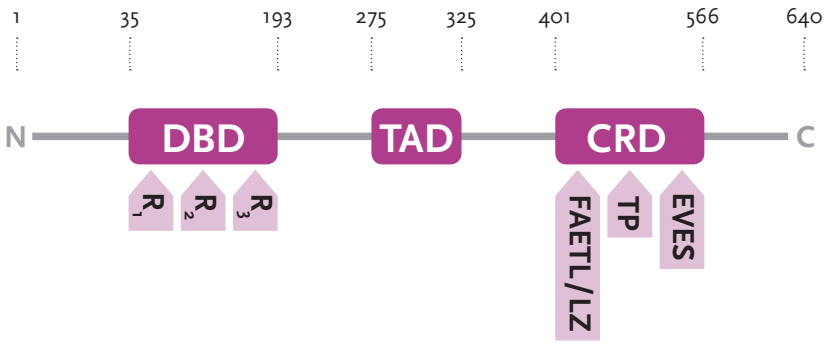

Figure 1.1: Structural and functional domains of c-Myb. The c-Myb protein is a nuclear protein spanning 640 amino acid residues and weighing 75 kDa. Its N-terminal region is comprised of a DBD, a TAD downstream from the DBD, and a CRD. Both the DBD and the CRD are comprised of three subdomains: R1, R2, R3 and FAETL/LZ, TP, EVES, respectively. (See text for further description).

1.2.1.1. The DNA binding domain of c-Myb

The N-terminal region of c-Myb consists of three imperfect tandem direct repeats, **R1**, **R2** and **R3**, which are highly evolutionary conserved and referred to as the **MYB domains**. Each of these repeats consists of 50-53 amino acid residues and they are regularly interspersed with tryptophan residues. Each MYB repeat gives rise to a helix-turn-helix (**HTH**)-related motif. The regularly spaced tryptophan residues form the hydrophobic core of this structure, giving rise to the HTH-related motif [24]. These MYB repeats have been shown to mediate the binding between Myb proteins and DNA. Functional studies of c-Myb revealed that R2 and R3 are both necessary and sufficient for this DNA-protein association, while R1 is dispensable as its function is of a more stabilizing nature [74, 34, 24].

The DNA consensus sequence recognized by these repeats, referred to as the MYB recognition element or **MRE**, was initially characterized in 1988 by Biedenkapp *et al* [6]. Subsequent studies extended the sequence consensus and revealed the MRE to be of bipartite structure, with YAAC as the R3 contacting first half-site and NGHH or GNHH as the R2 contacting second half-site [62, 4, 66] (see appendix: abbreviations: nucleotide codes).

The DBD has also been shown to be of some importance in both protein-protein interactions as well as in chromatin remodelling. Each of the three repeats (R1, R2, R3) carries the architectural signature of the SANT domain, a domain previously characterized in a number of chromatin remodelling proteins [55] (see 1.2.3 and 1.2.4).

1.2.1.2. The transactivation domain of c-Myb

The transactivation domain is found in the central part of the c-Myb tripartite structure (figure 1.1). This section spans 52 amino acids in human c-Myb (aa 275 to 327) and contains clusters of acidic residues, a characteristic generally found in the transactivation domains of transactivation factors (as reviewed by Oh *et al.* [61]).

The transactivational activity of the TAD is constitutive and rooted in the interaction between the TAD domain and the transcriptional co-activators CBP and p300 [68] (also see sections 1.2.3 and 1.2.4).

The TAD domain however, is not the sole source of transactivational activity. Under certain conditions the CRD domain might also function as a transcriptional activator [56].

1.2.1.3. The C-terminal regulatory domain of c-Myb

The C-terminal domain (CRD) of c-Myb contains three subdomains referred to as the **FAETL/LZ**, **TP** and **EVES** subdomains [70] (figure 1.1).

- FAETL/LZ subdomain - a leucine rich region of the protein.
- TP subdomain - a region rich in proline and threonine residues.
- EVES subdomain - an area of the c-Myb protein with various known sites for post-translational modifications.

The CRD was originally known as Negative regulatory domain (NRD), as deletion and interruptions of this domain correlated with an increase of the observed transcriptional activation of the target genes [74]. However, the CRD can also exhibit an activation function, as shown by Molvaersmyr *et al.* [56]. The deSUMOylation of the CRD switches off the negative regulatory function of this domain and the CRD switches into an activating domain. This activation function, or switch, has been termed a SUMO-regulated activation function (**SRAF**) [56] and is thought to depend on the two lysine residues (K503 and K527), shown to be conjugation targets for SUMOylation in the EVES region [19, 8] (figure 1.1 and figure 1.3).

This SUMO-regulated activation function is one of the starting points of the research for this thesis – and will be further discussed in subsequent subchapters (subchapter 1.5).

1.2.2. c-Myb protein and post-translational modifications

The PTM sites found on c-Myb include those for: acetylation, phosphorylation, SUMOylation, and ubiquitinylation. The presence of these PTM sites in addition to the deletion and mutation studies undertaken, strongly implicate post-translational modifications in the regulation of c-Myb.

Some of these PTMs could be subject to temporal fluctuations, for example during the cell cycle, and consequently lead to possible differential target gene regulation at different times in the progressing cell cycle. Post-translational modifications might directly influence c-Myb activity, conversely they might also do so indirectly by serving as anchoring points for other interacting proteins.

1.2.2.1. PTMs in the DBD region of c-Myb

Several serine residues in the DBD domain are known phosphorylation sites (specifically serine residues: 11, 12, and 116 (see below). All three of these modification sites have been implicated in down regulation of c-Myb dependent target genes – due to decreased ability of the disturbed (modified) DBD to interact with the MRE.

- S11 and S12 are phosphorylated by the casein kinase II and have been implicated in decreased DNA binding capacity [47]. This decrease however is a point of contention [5].
- S116 is a phosphorylation target for protein kinase A (PKA). When the serine at this residue is phosphorylated, c-Myb is no longer able to bind to and activate its target genes [3].
- A kinase that also seemed to affect the activity of c-Myb is the Pim-1 kinase. Pim-1 is also capable of phosphorylating specific DBD sites. This phosphorylation in cooperation with p100 has been proposed to increase the transactivational activity of c-Myb [41].

1.2.2.2. Motif in the TAD region of c-Myb

The central TAD region of c-Myb is known to contain a SUMO interacting motif (**SIM** – further explained in section 1.3.1), which is a non-covalent interaction site for SUMO. Mutations of this SIM domain have been shown to result in a large increase of c-Mybs transactivational potential [70].

1.2.2.3. PTMs in the CRD region of c-Myb

The importance of the CRD in relation to which target genes are regulated, at which time, and in what situations has been demonstrated in both deletion and domain swap mutations [45, 93]. The FAETL/LZ subdomain of the CRD has been implicated in c-Myb degradation via the 26S proteasome [16] The TP subdomain of the CRD has five lysine residues (K442, K445, K471, K480 and K485) targeted for acetylation by the acetyl transferases CBP and p300. These acetylations are thought to induce increased transactivation activity by the transcription factor [75, 84]. The EVES subdomain of the CRD is known for its post-translational modification sites.

Research undertaken in our own lab has shown that mutagenesis of the two lysine residues (K503 and K527) into arginine residues (**2KR mutant**) in the EVES domain of c-Myb results in an upregulation of c-Myb target genes. These two lysine residues have been shown to be SUMO conjugation sites (see subsection 1.2.1.3) [56].

The premise of this thesis is the assumption that these two lysine residues, when SUMO conjugated, interact with a powerful co-repressor. A further conjecture is that this co-repressor is the Activating transcription factor 7 – interacting protein (**ATF7IP**). These topics will be discussed in more detail in subchapter 1.3, 1.4 and subchapter 1.5.

In addition to the SUMOylation target lysine residues, the CRD also contains lysine residues targeted by the ubiquitinylation machinery. Poly-ubiquitinylation marks c-Myb for degradation via the 26S proteasome [7].

1.2.3. c-Myb protein-protein interactions

To understand the underlying mechanisms of c-Myb function, it is necessary to investigate the numerous interaction partners operating with this transcription factor. These partners affect all levels of c-Myb activity. While some partners regulate c-Myb directly (leading to either up- or down-regulation of the transcription factor), others are involved in the regulation and control of c-Mybs target genes. By cooperating with c-Myb a large network of combinatorial interaction layers emerge (reviewed by Ness et al. [60]).

Both the CREB-binding protein (**CBP**) and its homologue p300 are two of the most thoroughly described cooperative factors of c-MYB. As noted before (subsection 1.2.1.2), CBP and p300 are co-activators of c-Myb. The interaction between CBP/p300's KIX and the c-Myb's TAD domains is well established [94]. There is some evidence suggesting an additional point of interaction between CBP/p300's C/H2 and c-Myb's CRD domains [75].

The FAETL subdomain (located near the TP in c-Myb's CRD) and the C/H2 region of CBP/p300 have been shown to directly interact. The TP subdomain of the CRD has five lysine residues (K442 and K445 [75], K471, K480 and K485 [84]) targeted for acetylation by CBP/p300 (section 1.2.2). Sano *et al.* have argued that the acetylation of these residues could lead to an increase in binding affinity between c-Myb's TAD and CRD domains to CBP's/p300's KIX and C/H2 domains [75]. Upon binding of KIX at the TAD domain, the partially structured TAD domain is able to form an amphipathic helix, which is able to interact with a hydrophobic groove found in the KIX domain [94]. This leads to an increase of the transactivation activity by the transcription factor [75, 84].

The DBD of c-Myb also binds to the histone tails of H3 and H3.3, facilitating the acetylation of these tails [55] (see subsection 1.2.4).

Our laboratory has identified several protein interaction partners of c-Myb: Ubc9 [19], Mi-2α (CHD3) [71], FLASH and PIAS1 [2], as well as HIPK1 [51]. The chromatin remodeling factor Mi-2α (also known as CHD3) was originally identified as a NuRD co-repressor complex subunit, capable of binding both the DBD region as well as the FAETL subdomain of the CRD. In relation to c-Myb, Mi-2α acts as a coactivator [71]. HIPK1 is a nuclear kinase, found to interact with c-Myb in both its DBD and CRD. HIPK1 appears to phosphorylate c-Myb, thus modulating the transcription factor's activity and acting as a co-repressor [51]. FLASH is a multifunctional nuclear protein, shown to act as a coactivator of c-Myb function, directly binding to c-Mybs DBD. It has also been implicated as a PIAS1 interaction partner [2]. Ubc9 is associated with the CRD region of c-Myb and is a SUMO conjugase (E2 enzyme). PIAS1 interacts with the c-Myb DBD and is a SUMO ligase

(E3 enzyme), which cooperates with the E2 conjugases (such as Ubc9) in SUMOylation (see section 1.3.1). While these and other proteins have been shown to interact with c-Myb, many interactions remain to be investigated and interacting partners identified.

With this in mind, recent Yeast two Hybrid (**Y2H**) screenings in our laboratory have identified further c-Myb interaction partners. During these screenings, using full-length c-Myb as bait, 71 interacting protein candidates were found (Master thesis - Julie Emmert Olsen). One of the most interesting is ATF7IP - a large (136.4 kDa), nuclear protein, linked to both SUMO and chromatin [86, 35] (see subchapter 1.4).

1.2.4. c-Myb and epigenetic effects

Epigenetics (Epi being Greek for 'above') is the study of heritable changes in the expression patterns of a genome. While changes in chromatin structure result in different phenotypes, the underlying genotype remains unchanged. Chromatin structure can be influenced by chemical histone modifications (i.e. acetylations, methylations, phosphorylations, ubiquitylations) and DNA methylations. These chemical modifications result in tightly or less tightly packed DNA, contributing to expressed, un-expressed or down-regulated genes.

It has been demonstrated that the transcription factor c-Myb is both linked to several chromatin modulating proteins and the organization of chromatin [20, 55, 32, 91, 82]. Thus it has been shown that CBP/p300 not only activates c-Myb by binding to it and acetylating lysine residues in its CRD, but that c-Myb can also utilize the HAT activity of CBP/p300 to acetylate the tail of histones H3 and H3.3. As demonstrated by Mo *et al.*, the c-Myb DBD/SANT domain is capable of binding the N-terminal region of H3 histone tails. Mo *et al.*, further demonstrated that when c-Myb is simultaneously associated with p300 and H3 histone tails, H3 acetylation is promoted [55, 21]. Acetyl modifications on the histone tails are associated with the propagation of a more relaxed chromatin structure, facilitating the activation of gene expression.

As previously mentioned: ATF7IP has been identified as a novel interaction partner of c-Myb in our lab. Research conducted by others has linked ATF7IP to the

epigenetic players SETDB1 and MBD1 [23, 35, 86] as well as to histone expression levels [76]. These interactions re-enforce the hypothesis that c-Myb is an important regulator in chromatin compaction.

1.2.5. c-Myb targets

The c-Myb protein's highly conserved DBD recognizes and binds to the MRE in specific DNA sequences (see subsection 1.2.1.1) leading to the activation and expression of numerous specific target genes. It has been proposed that minor mutational changes of the DBD can corrupt the transcription factors specificity and hypothetically convert c-Myb into a transactivator for entirely different target genes (as reviewed by Zhou *et al*.) [93]. So far, more than 80 cellular targets of c-Myb regulation have been identified and validated to some extent, many more have been suggested yet still await further corroborating data [68].

The sheer number of c-Myb regulated target genes gives a certain indication as to the importance of this specific transcription factor. The identified c-Myb target genes are so numerous that they can be subdivided into three broad functional groups: housekeeping genes, genes involved in specific functions of differentiated cells, and genes linked to oncogenicity. This last group can be further organized into genes involved in: proliferation, survival, and differentiation (as reviewed by Ramsay *et al*. [68]).

As the v-Myb expressing virus causes leukaemia, initial studies investigating c-Myb were centered on c-Myb function in hematopoietic cells. Incidentally, active hematopoietic organs and immature progenitor cell-lines derived from leukaemia patients also exhibit the highest levels of c-Myb found. However, once differentiation of these cells is initiated, Myb levels were shown to decrease. This down-regulation of c-Myb upon differentiation highlights how high c-Myb levels and activity retain cells in their proliferative state [68, 93, 36]. Subsequent studies showed that precise levels of functioning c-Myb are a requirement in various stages of differentiation in hematopoietic cell lineages [73].

Additional studies have shown the necessity for c-Myb regulation in the development and homeostasis of colonic crypts, and in adult brain neurogenesis (as reviewed in Zhou and Ness [93] and Ramsay *et al* [68]).

1.2.6. The biological function of c-Myb

We have discussed how wild-type c-Myb is modified post-translationally, how it associates with protein interaction partners, as well as its role in chromatin organization and packaging. What remains to be elucidated is the biological function of c-Myb in normal cells, and how an alteration in the different molecular interactions can lead to alterations in c-Myb activity, and thereby to human disease.

The c-Myb transcription factor controls proliferation and differentiation of hematopoietic progenitors during blood cell development. During hematopoiesis the main function of c-Myb is to maintain proliferation of progenitor cells. When c-Myb is downregulated, cell differentiation progresses. Aberrations in the activity or function of c-Myb during this process, leads to a loss in blood cell development regulation and leukemogenesis [68].

However, over-expression and deregulation of *MYB* has been detected in various types of human cancers other than leukaemia [13], such as; breast- [38], colon- [85, 67], pancreatic- [88] and head and neck tumors [64]. Yet, as c-Myb is associated with proliferation, it is difficult to determine its actual role in these tumors, as pointed out by Zhou *et al* [93]: Increased levels of *MYB* gene expression in rapidly dividing cells would be expected when comparing them to normal resting cells.

With this in mind, the emergence of novel c-Myb post-translational modifications or interaction partners, especially ones that have strong links to activation or repression of transcriptional activity, could have major implications for human cancer biology.

1.3. SUMO

This section focuses on the Small Ubiquitin-like Modifier (**SUMO**), capable of associating in covalent and a non-covalent manner with a variety of proteins. We will discuss the process of SUMO conjugation and deconjugation (section 1.3.1), as well as SUMO's interaction with the c-Myb transcription factor and its network of interaction partners (section 1.3.3).

SUMO proteins are relatively small, weighing approximately 10 kDa and have a three-dimensional structure resembling that of ubiquitin. Their amino acid sequence however shares less than 20% sequence homology with ubiquitins [25]. SUMO proteins are expressed in all eukaryotic organisms. Four distinct ones (SUMO1 to SUMO4) are encoded by the human genome. Of these four SUMO variants SUMO1 – SUMO3 are found in all cells, while SUMO4 is tissue specific. SUMO2 and 3 share 97% sequence identity, while only 50% with SUMO1 [25].

SUMOylation is known to be highly dynamic. SUMOylation has a number of diverse outcomes for a target protein. These outcomes can be: change of localization, alteration of activity, stability, or changed interaction opportunities [72].

1.3.1. Non-covalent and covalent SUMO interactions

Non-covalent SUMO interaction occurs via a SUMO-interaction motif (**SIM**). SUMOylated proteins can bind to and associate with proteins containing the SIM motif. This motif has been characterized as a hydrophobic core flanked by acidic aa residues and occasionally Ser residues. The sequence of the hydrophobic core is: hxhh or hhxh (where h is either Val, Ile, Leu and x is representative of any amino acid residue) [25]. Non-covalent SUMO interactions will be further discussed in the ATF7IP (subchapter 1.4.1.2).

Covalent attachment of SUMO to a target protein happens via conjugation to the ε-amino groups of lysine side chains in the target protein. These conjugation sites are frequently found in the ΨKxE sequence motif. Here Ψ is a bulky alipathic aa, while x is any aa residue [25].

SUMO conjugation and deconjugation happens via the synergistic interplay of an enzyme cascade, very similar to the Ubiquitinylation machinery. The cascade consists of enzymes **E1-E3** (an activating enzyme, a SUMO conjugase and SUMO ligase) as well as a sentrin specific protease (**SENP**) (see figure 1.2: Mechanism of reversible target protein SUMOylation).

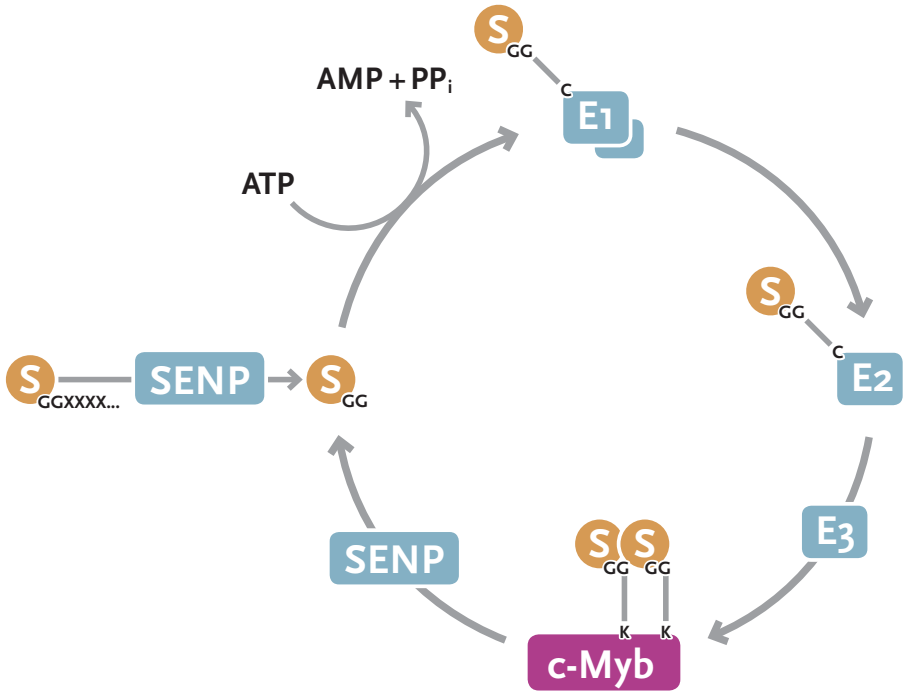

Figure 1.2: Mechanism of reversible target protein SUMOylation. Prior to the initial conjugation, immature SUMO has to be proteolytically cleaved. This maturation of SUMO is carried out by SENP. The mature peptide is subsequently activated by E1 heterodimer in an ATP dependent reaction. In the next step SUMO is transferred to E2 before finally being transferred from E2 to the target protein (in this case c-Myb), aided by E3 ligases. SUMOylated target proteins are SENP substrates – completing the conjugation/ deconjugation cycle (see text for further description). The figure is based on Geiss-Friedlander and Melchior review [25].

In the process of target protein SUMOylation, the first step is SUMO maturation. All SUMO proteins are initially expressed in pro-forms. The mature SUMO protein has two Gly-Gly residues marking the C-terminal of the mature protein. After these two amino acids the immature pro-forms have variable lengths of additional residues (spanning between 2 to 11 amino acids). The variable extension has to be cleaved off in order for SUMO to be conjugated to target proteins.

SENP is a family of sentrin specific proteases, needed in the maturation of SUMO. They are also involved in cleaving SUMO from the conjugated target proteins. This removal of SUMO by SENP ensures the reversibility of the modification.

E1 is an activating heterodimer (SAE1/SAE2), which in an ATP-dependent mechanism forms a thioester bond between the Gly residue on the C-terminus of the mature SUMO protein and a Cys residue in SAE1/SAE2. After the thioester bond formation, SUMO is transferred to the catalytic Cys residue of Ubc9 (E2 conjugating enzyme). The conjugation enzyme is then aided by the SUMO ligase (E3 enzymes like PIAS1 or PIASy) and an isopeptide bond is formed between the C-terminal Gly residue of SUMO and a Lys side chain of the target protein [25]. Subsequently a SENP protease can cleave SUMO from the target protein in an isopeptidase reaction, thus making the SUMO modification highly reversible.

1.3.2. The SUMO paradox

Although only a small fraction of a specific target protein is SUMOylated at any given time, the downstream effects can be dramatic. Different models have been proposed aiming to explain this paradox and it has been partially attributed to the very high turnover rate of SUMO modification. Meaning that, even though only a small subset is modified at any given time, if the pool of protein is observed over a short time span – each one of them might have become SUMOylated and deSUMOylated in quick progression [25].

In his review, Hay highlights SUMOylated transcription factors and how only a small proportion have the SUMO modification. Yet despite this small percentage, repression seems to be maximal and is relieved when the lysine residues used for SUMO conjugation are mutated [29].

1.3.3. SUMO and c-Myb

Research conducted in our laboratory has shown that of the three separate sites that c-Myb is contacted by SUMO, only one is non-covalent [70], with the other two being of a covalent nature [19].

While the SUMO conjugation of murine c-Myb was initially demonstrated by Bies *et al* [8], our laboratory has determined that in the human c-Myb transcription factor these SUMOylation sites are situated at lysine residues 503 and 527 (figure 1.3). In addition our lab showed that the SUMOylation occurs under more physiological

conditions than reported by Bies *et al*., that c-Myb is a good substrate for SUMO-1 conjugation, and that SUMOylation of these two sites is interdependent [19].

Figure 1.3: SUMOylated c-Myb CRD. Schematic based on research conducted in the Gabrielsen group. The c-Myb protein is a SUMOylation target. The conjugation acceptor sites are lysine residues 503 and 527 [19] (see text for more details).

The starting point for this thesis was the hypothesis that the SUMO conjugated to the CRD of c-Myb is involved in recruiting a negatively acting cofactor and that this cofactor is responsible for repression (see subchapter 1.5 Aims of study).

1.4. ATF7IP

The focus of this subchapter is to introduce the transcriptional cofactor ATF7IP, its molecular properties (section 1.4.1), PTMs (section 1.4.2) and protein-protein interactions (section 1.4.3).

ATF7IP (also known as MCAF1, AM, p621 or ATF-IP) was fist described in 2000 by De Graeve *et al.* who identified ATF7IP in a Y2H assay as an interaction partner of ATF7 and recognized it as the murine homologue of the human protein [22] previously identified by Gunther *et al*. as an Sp1 interaction partner [26]. Since then ATF7IP has been found to interact with several other components of the transcription machinery. These diverse interaction partners and their cellular functions strongly implicate ATF7IP as being involved in both activation (subsection 1.4.3.2) and repression (subsection 1.4.3.1) of gene expression, depending on the context and specific interaction partners.

ATF7IP is over-expressed in a number of human cancers [46]. Previously (subchapter 1.2) it was put forward that the emergence of novel c-Myb interaction partners with strong links to either repression or activation of transcriptional activity could have

major implications in human cancer biology. In this subchapter we introduce ATF7IP as one such possible candidate.

1.4.1. Molecular properties of ATF7IP

The *ATF7IP* gene is found on chromosome 12 (12p13.1) and codes for the large nuclear ATF7IP protein. ATF7IP spans 1270 amino acid residues and consists of two evolutionary conserved domains, **Domain 1** and **Domain 2**, flanking a very strong SUMO interaction motif (see figure 1.4). Not very much is known about these domains [86], other than that they are conserved from *Drosophila* to human and that they seem to be the main regions for interaction between ATF7IP and partner proteins (for further details see section 1.4.3).

ATF7IP does not contain a DNA binding domain. While reporting on the murine homologue of ATF7IP, mAM, De Graeve *et al.* noted an elevated amount of evenly distributed serine and threonine residues (see section 1.4.2), as well as weak ATPase activity and a potential nuclear localization signal [22].

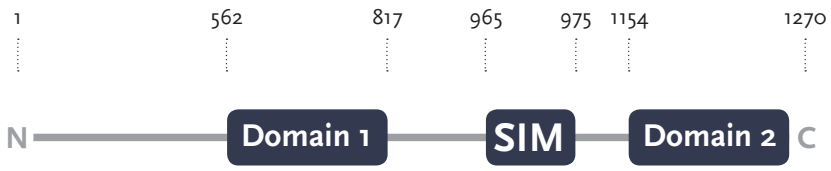

Figure 1.4: The structural and functional domains of ATF7IP. The ATF7IP protein is a nuclear protein spanning 1270 amino acid residues and weighing 136.4 kDa. The protein consists of a SIM domain (965 aa to 975 aa), flanked by two highly conserved regions; Domain 1 (562 aa-817 aa) and Domain 2 (1154 aa – 1270 aa). For further information see text.

1.4.2. ATF7IP and PTMs

As noted before, mAM contains an elevated amount of serine and threonine residues. Thus it comes as no surprise that ATF7IP is polyphosphorylated, showing phosphate clusters between 474 aa and 929 aa [33].

Although there have been no reports of human ATF7IP glycosylation, mAM has been found to be *O*-GlcNAc modified at threonine residues 902 and 903 [57]. As phosphorylation and *O*-GlcNAc modification are often reciprocal [15] and *O*-GlcNAc

is enriched on a number of proteins involved in eukaryotic gene transcription (such as Sp1 and RNAPII-CTD) [15], it seems likely that human ATF7IP would also contain this modification.

Additionally, ATF7IP has two acetylations on K332 and K938, as well as three ubiquitinylations in Domain 1 on Lysine residues K568 [87], K597 and K645 respectively. The Arginine residue at position 1087 is dimethylated [33]. ATF7IP does not appear to be a SUMOylation target [86].

1.4.3. ATF7IP and interacting proteins

To understand the implications that an interaction between ATF7IP and c-Myb might have on c-Myb target genes, it is important to know what other proteins ATF7IP interacts with, and how these influence transcriptional activation or repression. Although very little is known about the two domains of ATF7IP, all reported interactions with other proteins seem to happen via the binding to either one or both of these domains. Outlined in subsections 1.4.3.1, 1.4.3.2 and 1.4.3.3 are the interactions that have been reported so far. Subsections 1.4.3.4 and 1.4.3.5 contain models of ATF7IP dependant repression and activation.

1.4.3.1. Protein – Protein interactions with ATF7IP-Domain 1

Domain 1 of ATF7IP ranges from amino acid residues 562 to 817. Proteins that have been found to bind to this region of ATF7IP are the viral transcription factors Rta and Zta [10, 11], the general transcription factor TFIIE-α [46] and the H3K9 methyltransferase SETDB1 [35]. The general transcription factor TFIIE-β and the transcription factor Sp1 associate with both Domain 1 and Domain 2 of ATF7IP [46].

1.4.3.2. Protein – Protein interactions with ATF7IP-Domain 2

Domain 2 of ATF7IP ranges from 1154 to amino acid residue 1270 (the C terminal of the protein). This domain interacts with ERCC2/XPD and ERCC3/XBP (the helicases of transcription factor IIH), with MBD1 [35], with TFIIE-β, as well as with Sp1 [46] and Aire [90].

1.4.3.3. Protein – Protein interactions involving unknown region of ATF7IP

The murine homologue of ATF7IP reportedly interacts with subunits 3,4,7 and 8 of RNA polymerase II. The specific region of ATF7IP involved in this interaction has not been shown [22]. The interaction between ATF7IP and c-Myb (reported in this thesis and based on research by Julie Emmert Olsen for her master degree) is as of yet also not charted to a specific region of the ATF7IP transcription cofactor (this will be further discussed in chapter 4).

1.4.3.4. The strong SIM domain of ATF7IP

ATF7IP has a strong SUMO interaction motif. This SIM domain is 11 amino acid residues long and situated from 965 aa to 975 aa. The residues are: GVIDLTMDEE [86]. Uchimura *et al*. reported that SUMO2/3 has a five fold higher affinity for ATF7IP's SIM domain than SUMO1 [86]. Sekiyama et al. later corroborated this preference for SUMO2/3 [78]. Ichimura *et al.* reported that MBD1 interacts with ATF7IP-Domain 2 [35]; Uchimura *et al.* found that this interaction was enhanced by SUMOylation of MBD1 [86], inferring that MBD1 binds to Domain 2 of ATF7IP and that this interaction is enhanced by a SIM-SUMO interaction. This model will be further discussed in relation to c-Myb and ATF7IP interaction (section 1.4.4).

1.4.4. ATF7IP and interacting proteins in repression

ATF7IP is capable of binding a wide range of proteins and thus bridging between different interactants. Based on the studies discussed in subsections 1.4.3.1, 1.4.3.2, 1.4.3.3 and 1.4.3.4, a picture emerges of ATF7IP as a scaffold between MBD1 and SETDB1.

The model proposed is that ATF7IP is the protein bridging between DNA methylation and formation of heterochromatin. MBD1 binds to methylated CpGs and recruits ATF7IP, via which SETDB1 is recruited. SETDB1 has been shown to require ATF7IP as a cofactor, without ATF7IP the enzymatic activity of SETDB1 is greatly diminished [89]. SETDB1 is a selective histone methyltransferase, recognizing H3K9me2 and increasing the di-methylation to a tri-methylation state. HP1 is recruited to H3K9me3 and initiates the silencing of euchromatin by propagating facultative heterochromatin [77, 35, 86]. This concept is illustrated in figure 1.5.

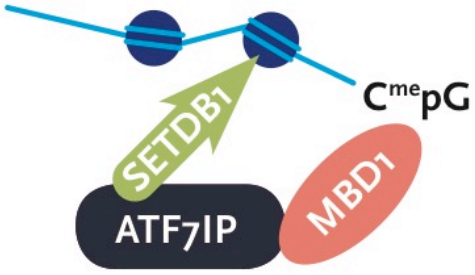

Figure 1.5: Schematic model of ATF7IP as a scaffold between MBD1 and SETDB1. In this model MBD1 binds to methylated CpGs and recruits ATF7IP, which in turn recruits SETDB1. SETDB1 trimethylates Lysine 9 on histone 3, leading to the recruitment of HP1 and thereby the propagation of heterochromatin.

1.4.5. ATF7IP and interacting proteins in activation

ATF7IP interacts with Sp1 via both Domain 1 and Domain 2, as well as with members of the general transcriptional apparatus: TFEII, TFHII and RNAPII. Liu *et al.* reported the involvement of ATF7IP in the maintenance of Cancer-associated Telomerase activity by bridging the gap between the transcription factor Sp1 and the transcriptionally active form of RNAPII [46]. Again ATF7IPs function is that of a scaffold or mediator–like protein. In this transcriptional activation model, ATF7IP facilitates the expression of Sp1 target genes by coupling Sp1 with the transcriptional apparatus. Illustrated in figure 1.6.

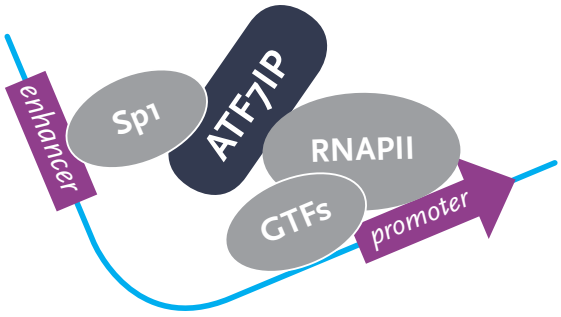

Figure 1.6: Schematic model of ATF7IP as a scaffold between Sp1 and the basal transcription machinery. In this model ATF7IP is recruited by Sp1, which in turn recruits the basal transcription machinery leading to the activation of Sp1 target genes.

Collectively, these models suggest that association with ATF7IP can either lead to repression via recruitment of epigenetic players or to activation by bridging transcription factor to the general transcription apparatus, promoting the initiation of gene expression. Applied on c-Myb this leads to two different models, which will be discussed in the Aim of the Study subchapter.

1.5. Aim of the Study

The c-Myb protein does not work alone. It is a hub in an intricate network of protein interactions. Research in the Gabrielsen group has identified several c-Myb interaction partners [19, 71, 2, 51], adding to the ever-increasing c-Myb web. During the course of these studies, the importance of SUMOylation and SUMO interaction in this network has become apparent [56, 70].

Recent Y2H screenings in our group identified the transcriptional cofactor ATF7IP as a putative novel c-Myb interaction partner (Master thesis - Julie Emmert Olsen). Depending on the context and its interaction partners, this transcriptional cofactor can be involved in either activation or repression of gene expression. ATF7IP is known to interact with the basal transcriptional apparatus [46], yet it also associates with MBD1 and SETDB1 in the propagation of compacted chromatin [23, 35, 86].

Based on the studies discussed previously, we would like to propose two possible models for how ATF7IP might affect c-Myb function:

1) **Model 1** - The Epigenetic Repressor Model (figure 1.7)
2) **Model 2** - The Mediator-like Activation Model (figure 1.8)

If Model 1 is operating it could explain some of the observations that have been made in relation to transcriptional silencing and SUMO involvement. As previously mentioned (section 1.3.2), SUMOylation of certain transcription factors leads to maximal transcriptional repression, this could happen via a protein such as ATF7IP. In this manner, the transcription factor would direct ATF7IP towards the DNA region in question. In its SUMOylated state, it would further recruit ATF7IP and the ATF7IP-associated histone methyl transferase would thereby initiate heterochromatin formation and transcriptional repression through epigenetic silencing. Model 1, The Epigenetic Repressor Model is illustrated in figure 1.7.

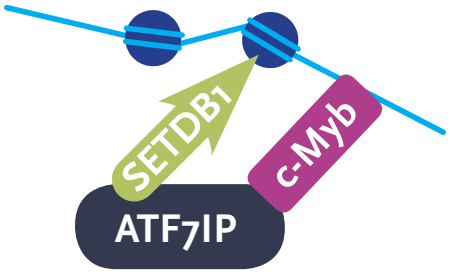

Figure 1.7: Schematic of Model 1. Illustration of the hypothesized c-Myb, ATF7IP and SETDB1 complex interaction. Research in other laboratories has characterized ATF7IP as a transcriptional coactivator or corepressor, based on its interaction partners. In this hypothetical model SUMOylated c-Myb would recruit ATF7IP, which in turn recruits SETDB1 leading to the formation of facultative heterochromatin and the silencing of c-Myb target genes (see text for more details).

Model 2 takes the mediator-like function that has been attributed to ATF7IP into consideration. ATF7IP has been implicated in activation of transcription by bridging the transcription factors bound at upstream enhancers to the general transcription factors (TFEII, TFHII) and the RNAPII associated with the core promoter. In this model we propose that the putative interaction of ATF7IP and c-Myb leads to an activation of c-Myb dependent transactivation. Model 2 The Mediator-like Activation Model is illustrated in figure 1.8.

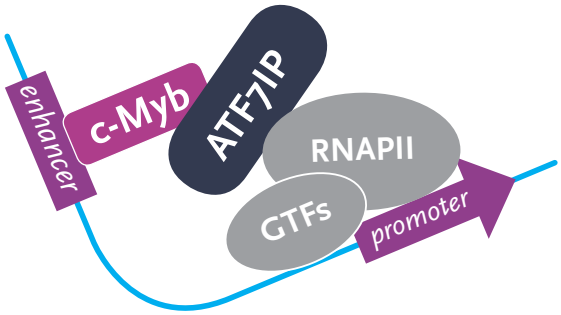

Figure 1.8: Schematic of Model 2. Illustration of the hypothesized c-Myb and ATF7IP mediator-like interaction complex. Research in other laboratories has characterized ATF7IP as a transcriptional coactivator or corepressor, based on its interaction partners. In this hypothetical model SUMOylated c-Myb would recruit ATF7IP, which in turn recruits the basal transcription machinery, leading to the activation of c-Myb target genes (see text for more details).

This thesis is divided into three main parts.

Part 1 is an investigation of the proposed interaction between c-Myb and ATF7IP. The validity of this interaction is addressed, as well as the role of SUMO-SIM in the association. GST-pulldown assays are used to determine whether ATF7IP and c-Myb do in fact interact.

If successful, functional reporter gene assays will then be utilized to investigate the effect this interaction has on c-Myb dependent transcription, addressing the questions in Parts 2 and 3.

Part 2 explores the functional implications that this hypothesized interaction might have on c-Myb target genes. Which of the hypothesized models, Model 1 or Model 2, is most plausible of the two?

Part 3 is a further exploration of the importance of the ATF7IP interaction partners, MBD1 and SETDB1, involved in the proposed Model 1.

2. Methods

This chapter describes the various laboratory techniques carried out in support of this thesis. For each technique a short introduction as well as a procedural overview are presented. When commercial kits are used, this is clearly indicated and listed in the appendix. The work for this thesis included the design of various expression constructs and mutants (see subchapter 2.1), cultivation and experimentation using mammalian cell lines (see subchapter 2.2), as well as interaction and functional studies (see subchapter 2.3).

2.1. Nucleic acid and Subcloning Techniques

Subcloning is the process of moving a DNA sequence from a parent to a destination plasmid using restriction (section 2.1.5) and ligation enzymes (section 2.1.8).

The recombinant plasmid with the desired DNA sequence (insert) is subsequently transformed into competent *E. coli* bacteria by transformation (e.g. heat shock) (see section 2.1.1), leading to the amplification of the plasmid. Thereafter, the plasmid DNA is extracted from the bacterial cells (see section 2.1.2). The concentration and purity of the extracted plasmid DNA is determined (section 2.1.4) and the constructs are verified using restriction digests (sections 2.1.5 and 2.1.6). The fragments separated using agarose gel electrophoresis can in turn be isolated from the gel (section 2.1.7) and be used for further experimentation. A subcloned DNA sequence can be subjected to mutagenesis (section 2.1.12), it can be sequenced (section 2.1.14) or it can be used for further experimentations and assays. If one should desire to use this DNA sequence at a later point, it can be stored in bacterial stem cultures (section 2.1.15).

2.1.1. Transformation of bacterial cells

Transformation is the introduction of naked, usually recombinant, DNA into bacterial cells across the cell membrane, to maintain and amplify said DNA. In some bacterial strains transformation occurs naturally, other bacterial strains have to be made competent prior to transformation.

There are different methods to induce competency. One is to heat shock competent cells, which are prepared using a calcium suspension solution. Another method is to induce competency by subjected the cells to high voltages, leading to electroporation, small pores opening in the cell membrane. To achieve the transformation, selection and amplification of the plasmid vector with a desired insert, the vector in question has to fulfil a number of pre-requisites:

- An origin of replication
- A polylinker (with unique cloning sites)
- Selectable markers (such as an antibiotic resistance gene)

During this work, heat shock competent *E. coli* DH5α cells where transformed with different DNA plasmids. During the work it is vital to maintain a disinfected environment, in our lab all bacterial work is therefore performed in a Class I microbiological safety cabinet.

Heat shock transformation procedure:

1. Thaw competent cells on ice.
2. Incubate 50 μL thawed competent cells with 1-5 μL (approximately 10 pg to 100 ng) plasmid DNA on ice for 20 minutes. During this step the naked DNA adheres to the cell membrane.
3. Heat-shock the transformation mixture at sub-lethal temperature, 42^0C for 90 seconds (depending on bacterial strain used). During this step the pores open, letting the free DNA pass the lipid-bilayer.
4. Place the transformation reaction on ice. This leads to the tightening of the pores.
5. After incubation the transformed cells are plated out on agar dishes, containing the appropriate antibiotic and/or selection marker (e.g. X-gal and IPTG for Blue/White selection) and, if the antibiotic in question is ampicillin, incubated at 37^0C for 12-16 hours.
6. When other antibiotics are used (e.g. kanamycin) an additional expression step will have to be included in the protocol. Add 800 μL LB-medium and incubate at 37^0C for 30 minutes. Then plate out on an agar dish containing the appropriate antibiotic. Incubate at 37^0C for 12-16 hours.

Following the incubation period the plates are checked for colonies and selectable markers are evaluated to determine the success of the experiment.

2.1.2. DNA extraction from bacterial cells

To extract plasmid DNA from the transformed bacteria, putative positive clones have to be determined and picked from the incubated agar dishes (section 2.1.1). The chosen clones are inoculated in a medium enriched with the appropriate antibiotic. The volume of the medium is dependent on whether a mini- or maxiprep is to be performed (depending on the amount of DNA required for further experiments). For both of these procedures our lab uses commercial kits.

Both kits make use of the principles of alkaline lysis and purification on anion-exchange columns. The bacterial cells from the cultures are pelleted, the supernatant is discarded and the pellet re-suspended in a buffer inhibiting nucleases. The cells are then lysed in an SDS/NaOH containing buffer, loosening cell walls and denaturing the chromosomal DNA releasing the plasmids. The alkaline solution is then neutralized with a KAc containing buffer. This neutralization renatures the plasmids and they remain soluble while most of the chromosomal DNA, bacterial proteins and potassium dodecyl sulfate is precipitated. After centrifugation the supernatant is loaded onto the column, the negatively charged plasmid DNA binds to the silica membrane and can be further washed with ethanolic buffer before it is eluted.

For minipreps the NucleoSpin®Plasmid and for maxipreps the NucleoBond®Xtra kits from Macherey-Nagel were used. The procedure was carried out in accordance with the manufacturers recommendations.

2.1.3. RNA extraction from mammalian cells

As RNA degradation is a serious problem, it is important to maintain a sterile and RNase free environment while working. All plastic and glassware should be sterile. RNA buffers and tools used should be kept separately to avoid contamination. Pipette tips with filters are to be used.

Extraction of total RNA from the transfected and harvested mammalian cells (subsections 2.2.5.3 and 2.2.4.4) was performed using a commercially available kit. The biological samples are first lysed and homogenized in a buffer, containing the chaotropic agent guanidine-isothiocyanate, immediately inactivating RNases. The total RNA binds to the silica membrane, impurities are washed away and isolated purified total RNA can be eluted.

The kit used was the RNeasy Mini Kit from Qiagen. The procedure was carried out in accordance with the manufacturers recommendations.

2.1.4. DNA/RNA concentration assessment

Nucleic acid concentrations were measured using the NanoDrop2000 UV-Vis spectrophotometer from Thermo Scientific, in accordance with the manufacturers recommendations. The NanoDrop2000 can be used to measure the UV-absorption at different wavelengths; the machine then calculates the nucleic acid concentration using a modified Beer-Lambert equation.

$$\mathbf{c = (A * \varepsilon)/b}$$

c = nucleic acid concentration in ng/ μL
A = absorbance in AU
ε = wavelength-dependent extinction coefficient in ng-cm/ μL
b= path length in cm

The extinction coefficients used are:

- dsDNA: 50 ng-cm/ μL
- ssDNA: 33 ng-cm/ μL
- RNA: 40 ng-cm/ μL

The NanoDrop2000 UV-Vis spectrophotometer can also be used to assess the purity of the nucleic acid solution. The 260nm/280nm ratio is a measurement of sample purity. DNA is generally accepted as pure DNA with a ratio of ~ 1.8. RNA is generally accepted as pure RNA with a ratio of ~ 2.0.

2.1.5. DNA restriction digest

Restriction endonucleases are enzymes that recognize and cleave DNA at specific sites in the nucleotide sequence, also referred to as restriction sites.

The plasmids used in molecular cloning procedures are usually laboratory engineered and contain an origin of replication, selectable markers and a multiple cloning site (**MCS**). The MCS is a short segment of DNA, which contains many (up to 20) unique restriction sites. The knowledge of these specific restriction sites and of the restriction site specificity of the different restriction enzymes makes these enzymes valuable tools. They are routinely used in subcloning and verification experiments.

Different restriction endonucleases are originally isolated from different organisms. As they originate from varied physiological environments, they have different requirements for achieving optimal conditions, such as buffer and temperature. These conditions can be looked up in the manufacturer's manual. When using enzymes that require different buffer systems, cleaving steps have to be carried out sequentially and the DNA has to be purified in between.

Alkaline phosphatases (e.g. SAP, CIP) are enzymes used to dephosphorylate the 5'-end of opened vectors, thereby hindering re-ligation without insert. Alkaline phosphatases are added to the restriction digest if the plasmid is cut with one enzyme, leaving complimentary overhangs.

When setting up restriction reactions for verification purposes a total amount of ~500 ng is used. When DNA is needed for further subcloning steps ~2 µg is recommended.

Restriction enzyme concentration is usually indicated in units/ µL. One Unit (**U**) refers to the amount of enzyme needed to digest 1 µg of λ-DNA within 1 hour in a 50 µL reaction volume at a specified temperature.

Setting up a restriction reaction procedure

1. Mix according to the table:

Reagent	Amount
H_2O	
Buffer 10x	2 – 5 µL
Plasmid DNA	500 ng - 2 µg
Enzyme 4000 – 10000 U/ mL	0.5 – 1 µL
SAP or CIP (when needed)	0.5 – 1 µL
Total volume	**20-50 µL**

2. Incubate for ~90 minutes at required temperature.

Inactivate the reaction either using heat shock (temperature depending on enzyme used) or by adding the DNA loading reagent.

2.1.6. DNA separation by agarose gel electrophoresis

Agarose gel electrophoresis is a standard method used to separate DNA molecules according to size. The negatively charged DNA molecules migrate through the gel towards the positively charged electrode (the anode). The migration front of the DNA through the gel can be observed by using dyes (e.g. bromophenol blue) in the gel-loading buffer (see appendix). The DNA itself is visualized under UV light using ethidium bromide (**EtBR**). EtBR intercalates into the structure of DNA molecules, resulting in a complex that brightly fluoresces under UV-light. To determine the sizes of the different DNA molecules they have to be judged relative to a DNA standard ladder applied on the same agarose gel. During this project the 1kb DNA ladder from Invitrogen was used.

Casting of an agarose gel procedure

The agarose percentage influences the migration speed and separation of the DNA molecules through the gel as it correlates with the pore size in the gel. A higher agarose percentage leads to slower migration rate. The different agarose gel percentages used in this thesis ranged from 0.7% to 1.5%.

1. Mix according to the table:

Reagent	Amount
Agarose powder	0.7 – 1.5 g
1xTAE buffer	100 mL
Total volume	**100 mL**

2. Boil solution to dissolve the agarose powder.
3. Let the solution cool to ~ 50^0C and add 1 drop of EtBr (final concentration of approximately 0.5 μg /mL).
4. Pour into gel tray and insert well comb.
5. Let the gel solidify.
6. Remove comb, place gel in the electrophoresis chamber and immerse it in running buffer (1xTAE).

Separating DNA on an agarose gel procedure

1. Mix according to the table:

Reagent	Amount
Restriction reaction	20 – 50 μL
4x Gel Loading buffer	5 – 12.5 μL
Total volume	**25 – 62.5 μL**

2. Spin the solution down quickly.
3. Apply the samples and the standard ladder to the wells.
4. Run the gel at 100 V for 40-60 minutes.
5. Visualize using the UV-doc station.

2.1.7. DNA purification from agarose gel

When carrying out a multistep cloning strategy, it is often necessary to separate DNA fragments, to isolate the wanted fragments.

The DNA is separated on an agarose gel; visualized using weak UV light and the area of the gel containing the wanted fragments is cut out using a clean scalpel. The gel containing the DNA is then solubilized in the appropriate volume of capture buffer. This capture buffer contains chaotropic salts, visual pH indicators and agents that imbue the silica membrane with positive charge. The chaotropic salts lower the agarose melting temperature and break the hydrogen bonds between water and DNA. The DNA is no longer soluble and binds to the positively charged silica membrane. The DNA associated to the membrane is washed with an ethanolic buffer, removing the chaotropic salts and other impurities. The DNA is again soluble and can be eluted from the column using water or an appropriate buffer.

During this project the NucleoSpin®ExtractII kit from Macherey-Nagel was used. The procedure was carried out in accordance with the manufacturers recommendations.

2.1.8. DNA ligation

Ligation is the process in which two DNA fragments with either blunt ends or sticky-ends are joined covalently together by enzymes called DNA ligases. DNA ligases form phosphodiester bonds between 5'phosphate and 3'hydroxyl groups on the termini of adjoining nucleotides, thereby closing nicks in ssDNA chains.

All ligation reactions for this thesis were performed using the T4 DNA ligase. This specific ligase joins cohesive and blunt ends in an ATP dependent reaction. To achieve optimal ligation it is important to not only use the enzyme specific physiological conditions, but also to consider the ratio between vectors and inserts. In this thesis ligations were always set up in three reactions: control (no insert), 1:5 and 1:10. The amount of required inserts were calculated using the following equation:

ng insert = ((ng vector * size (bp) insert)/size (bp) vector) * ratio

Setting up a ligation reaction procedure

1. Mix according to the table:

Reagent	Amount
H_2O	
T4 DNA Ligase Buffer 10x	2 µL
Vector	100 ng
Insert	Calculated in samples / none in control
T4 DNA Ligase 40 U/ µL	0.5 µL
Total volume	**20 µL**

2. Incubate at room temperature between 20 minutes and 2 hours.
3. Heat-inactivate ligase for 10 minutes at 65^0C.

The ligation reactions are subsequently transformed into competent DH5α cells and streaked onto antibiotic infused agar plates (see section 2.1.1). The control sample with no added insert can be used to assess the re-ligation frequency of the vector and thereby the relative amount of false positive clones.

2.1.9. Gateway recombination cloning

Gateway technology (Invitrogen) exploits the inherent ability of bacteriophage λ to integrate into and excise sequences from the bacterial *E. coli* genome. Using this technique simplifies subcloning by utilizing these site-specific recombinatorial abilities for rapid procedures, sidestepping traditional restriction and ligation steps. Gateway cloning relies on two recombination reactions, the BP (B for bacteria and P for phage) and the LR (L for left and R for right). These two reactions are catalysed using commercial enzyme mixtures, the BP Clonase™ and LR Clonase™ mix (Invitrogen kit). The site specificity in the Gateway system is imparted by the attachment (att) sites.

The first reaction is the BP reaction. The attB substrate, which can be a PCR product of the wanted insert flanked by specifically designed attachment bacteria sites, is recombined with an attP substrate. The attP substrate is the donor vector containing a ccDB gene between its att sites. During this recombination step the sequences flanked by the att sites are interchanged by recombination, thereby generating entry clones

(with attL sites) and by-products. The by-product contains the ccDB gene, while the entry clones contain the wanted insert.

The second reaction is the LR reaction. Here the entry clones (containing attL sites) from the BP reaction are mixed with destination vectors containing attR sites (again flanking a ccDB gene). As in the previous reaction, the sequences flanked by the att sites are interchanged during recombination and an expression clone containing the insert and by-product containing the ccDB gene are generated.

The ccDB gene interferes with the gene coding for DNA gyrase. DNA gyrase is a topoisomerase, relieving strain during replication, after helicase unwinds double stranded DNA. If DNA gyrase does not function, replication will not function and bacteria will not grow. Antibiotic selection markers are additionally employed for counter selection. This means that only the real recombinants allow functioning replication in the bacterial cell (see figure 2.1 for further details).

For this project the second reaction (LR reaction), was performed. The procedure was carried out in accordance with the manufacturers recommendations, with one alteration. Half the amount of reactants was used, with a total volume of 5 µL instead of 10 µL. This is enough for both transformation and back up, while being more economical.

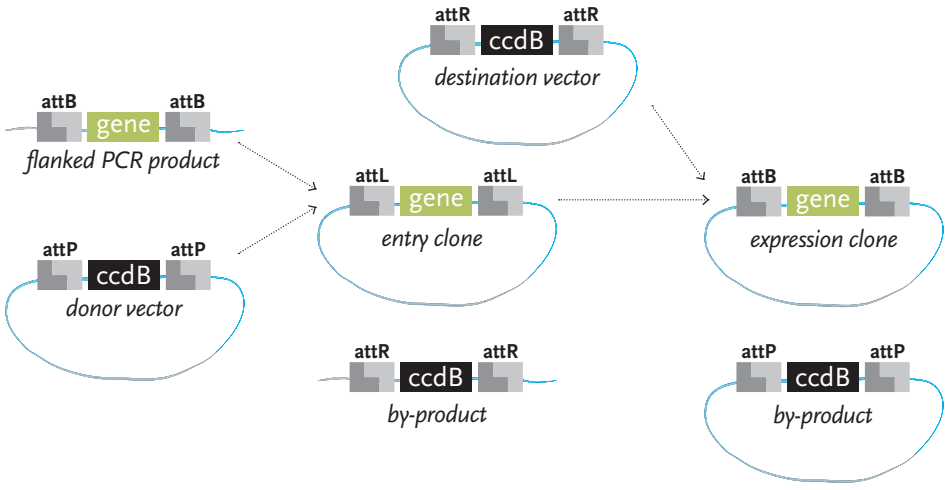

Figure 2.1: Schematic of gateway recombination cloning procedure. The diagram shows the BP and the LR reactions, from donor vector and flanked PCR product through to the subsequent expression clone. For further details see the text. The figure is based on the Invitrogen gateway user manual.

2.1.10. Polymerase chain reaction (PCR)

In PCR the enzymatic activity of DNA polymerase is exploited to amplify selected regions of DNA *in vitro*. This reaction requires a thermostable DNA polymerase, a DNA template (containing the target sequence), two "primers" (oligonucleotides complementary to the flanking sites of the target sequence) and the four deoxyribonucleotide triphosphates.

The process of PCR itself is divided into three consecutive repeating steps: denaturation, annealing and elongation.

1. Denaturation: During denaturing the PCR reaction mixture is heated to approximately 95^0C. The hydrogen bonds are broken and the dsDNA templates denature, generating ssDNA.
2. Annealing: The temperature of the reaction mixture is lowered, primer dependent. Primers anneal to complementary regions of the templates.
3. Elongation: During synthesis the temperature is raised to the optimum temperature of the DNA polymerase. The DNA polymerase extends the primers in 5'- 3' direction.

The DNA polymerases used in PCR are thermostable, to facilitate automation of the procedure and allow for multiple repeating cycles. The cycles are usually repeated approximately 30 times, leading to the exponential growth of the amplicon.

During this project the principle of PCR technology was applied for different methods: qRT-PCR (section 2.1.11), DNA mutagenesis (section 2.1.12) and cDNA synthesis (section 2.1.13).

2.1.11. quantitative real-time PCR (qRT-PCR)

There is a quantitative relationship between the amount of starting material (target sequence) and the amount of PCR product at any given cycle number.

Using real-time PCR it is possible to follow the progress of amplification, which is the on-going increase in numbers of specific amplicons, while the reaction is taking

place. This approach also permits estimation of the number of specific target sequences present in the reaction mixture before amplification is initiated.

The increase of amplicon numbers can be monitored in two main ways:

1. Using target specific probes (e.g. TaqMan). These target specific probes give rise to fluorescent signals in the presence of specific amplicons.
2. Using specific dyes (e.g. Sybr Green). These dyes fluoresce when binding to dsDNA.

The fluorescence is monitored and recorded cycle by cycle.

The threshold is defined and C_T is determined. The C_T is the fractional cycle number at which the fluorescence passes the fixed threshold. Once the C_T has been reached the amplification reaction can be described using the following equation:

$$\mathbf{T_n = T_0 * (E)^n}$$

T_n: the amount of target sequence at cycle n.
T_0: the initial amount of target sequence.
E: the efficiency of amplification.
n: cycle number

In the final stages of the PCR reaction the efficiency declines, until no more product accumulates.

The LC-96 Software is used to determine reaction efficiency (E), as well as the C_p values, the crossing points for *mim-1* and *hprt* mRNAs. ΔC is determined by subtracting the target C_p (*mim-1*) from the reference C_p (*hprt*). The relative level of *mim-1* mRNA is determined using E ^ (ΔC).

During this project qRT-PCR was utilized to quantify expression in the HD11 *mim-1* reporter gene assay (section 2.3.4). We used Agilent Brilliant III Ultra Fast SYBR

Green qPCR master mix to monitor amplicons in a LightCycler® 96 Real-Time PCR System (**LC-96**) from Roche.

Procedure for use of the LC-96

1. Centrifuge the 96 well sample dish at 3000 rpm, for 1 minute at room temperature.
2. Turn on the LC-96 and follow instructions on screen.
3. Press "Eject" to insert 96 well dish.
4. Press "NEW" and enter name and reaction volume.
5. Profile: make profile. Two-step cycle.

Cycles	Duration of cycles	Temperature
1	180 s	95^0C
45	5 s	95^0C
	10 s	60^0C

Meltingcurve:

	Duration	Temperature
None	5 s	95^0C
None	60 s	65^0C
Continuous	1 s	97^0C

6. When the programme is done, extract your data for analysis.

2.1.12. DNA mutagenesis

Site-directed mutagenesis is a method used to introduce specific changes into a DNA sequence *in vitro*. This reaction is based on the principles of PCR but has slightly altered requirements in order to introduce the mutation.

The DNA polymerase used for this experiment is PfuUltra™ from Stratagene; this polymerase has a very low error-rate. The two primers used for this reaction are complimentary to each other and complimentary to the template that is to be mutagenized, except for the nucleotide changes that are to be introduced into the sequence.

Prior to site-mutation the plasmid is prepared by subcloning the gene sequence that is to be mutagenized into an as small as possible vector. After plasmid preparation site-specific mutagenesis is carried out using a thermo cycler and the three consecutive repeating steps (denaturing, annealing and elongation) from the polymerase chain reaction (section 2.1.10).

1. Denaturation.
2. Annealing: The temperature of the reaction mixture is lowered. This temperature is primer dependent. The primers containing the point mutations are annealed to the target sequence.
3. Elongation: 68^0C (for PfuUltra™). PfuUltra™ extends and incorporates the mutagenic primers resulting in nicked circular strands.

After approximately 18 cycles the samples are taken out of the thermo cycler. The reactions now contain mutated linear DNA and non-mutated parental DNA templates.

Being cultivated in *E. coli* the parental templates are methylated and the mutated plasmids are not. Therefore, it is possible to selectively digest the un-mutated parental templates using the methyl sensitive DpnI restriction enzyme. This digestion leaves the mutated plasmids for subsequent transformation. The linear mutated strands are repaired once the plasmids are successfully transformed into the DH5α *E. coli* cells.

For this project site-specific mutagenesis was used to mutate the SIM motif of ATF7IP, abolishing ATF7IPs SUMO interaction. The procedure below is the result of numerous trials.

Site-specific mutagenesis procedure

1. Mix on ice, according to the table:

Reagent	Amount
H_2O	
PfuUltra™ Buffer x10	5 µL
Template	50 ng
Primer 1	125 ng
Primer 2	125 ng
dNTP 5 mM	1 µL
Glycerol	5 µL
PfuUltra™ Polymerase	1 U
Total volume	**50 µL**

2. Run following PCR program:

No	Process	Duration	Temperature
1	Denaturing	30 s	95^0C
2	Denaturing	30 s	95^0C
3	Annealing	60 s	55^0C
4	Synthesis	600 s	68^0C
5	Synthesis	600 s	68^0C
6	Cooling	∞	4^0C

Steps 2 to 4 are repeated 18 times.

Subsequently digestion with DpnI is carried out (see section 2.1.5) and *E. coli* are transformed using 8 µL plasmid and 90 µL bacterial cells (otherwise as seen in section 2.1.1).

During the work conducted in support of this thesis the site-specific mutagenesis procedure had to be modified several times. The procedure described here is the result of this optimization. For the standard procedure refer to the QuikChange Manual from Stratagene.

2.1.13. cDNA synthesis

First-strand or cDNA synthesis, is the process of generating complimentary DNA from total RNA using a reverse transcriptase. Mature mRNA has polyadenylated tails, poly-T oligonucleotide primers can prime these tails.

For this project cDNA was synthesized from mRNA using the commercially available kit AffinityScript QPCR cDNA Synthesis from Agilent.

First-strand cDNA synthesis procedure

1. Mix on ice, according to the table:

Reagent	Amount
RNase free H_2O	
1st Strand Mastermix (2x)	10 µL
Oligo(dT)primer 0.1 µg / µL	3 µL
AffinityScript RT/ RNase block enzyme mixture	1 µL
RNA	2 µg
Total volume	**20 µL**

For each sample there should also be a minus RT control. Use RNase free H_2O instead of the AffinityScript RT/ RNase block enzyme mixture.

2. Run following PCR program:

No	Process	Duration	Temperature
1	Annealing	5 min	25^0C
2	Synthesis	45 min	42^0C
3	Terminate	5 min	95^0C
4		∞	4^0C

After the program is finished, cDNA samples can be stored in the -20^0C freezer.

2.1.14. DNA sequencing

DNA sequencing was performed as an additional verification after subcloning using PCR. The ABI lab at the University of Oslo performed all of the DNA sequencing.

Preparing samples to be sent to ABI lab procedure

1. Mix according to the table:

Reagent	Amount
H_2O	
DNA Template	200 ng
Primer 5 μM	2 μL
Total Volume	**10 μg/ μL**

2.1.15. Plasmid Stem Culturing

DH5α *E. coli* cells can be stored in the -80^{0}C freezer with 15% glycerol for many years. With this procedure the cells are kept in a state of hibernation and can be thawed and re-cultured when required.

Procedure for cell hibernation

1. Mix according to the table:

Reagent	Amount
Cell suspension	1 mL
Autoclaved 50% Glycerol	430 μL
Total Volume	**~1.5 mL**

2. Store in cryogenic culture tubes at -80^{0}C.

2.2. Mammalian Cell Culturing

For this project a number of different mammalian expression systems were used, depending on the experiment performed. COS-1 cells were used for interaction studies, while CV-1, HD11 and HEK293-c1 cells were used for functional assays.

CV-1 cells are an adherent cell line derived from kidney fibroblast cells from an adult male African green monkey (*Cercopithecus aethiops*) [18]. COS-1 is an adherent cell line derived from the CV-1 cell line by transformation with a version of the SV40 virus, capable of expressing T antigen, making it suitable for transfections with vectors needing SV40 T antigen for overexpression [17]. The HEK293-c1 cell line is adherent and was derived from the human embryonic kidney cell line (HEK293 [31]). It has a stably integrated 5x Gal4 luciferase reporter [81]. The HD11 cell line is adherent and was derived from chicken (*Gallus gallus*) macrophage-like cells transformed with the AMV virus MC29. In this cell line v-Myb encoded by the AMV virus is defective and the *mim-1* gene is only expressed if the cells are transfected with c-Myb expression vectors [19, 37].

The sections in this subchapter will deal with the general protocols when working with mammalian cell lines. Specifications for the different cell lines are found in the corresponding subsections.

2.2.1. Routine Maintenance of Cells

When working with mammalian cell cultures it is important to maintain a sterile environment. Cells have to be protected against any possible contaminants (such as bacteria, fungi or other culture cells) by practicing sterile technique in a Class II microbiological safety cabinet. It is also important to know how to satisfy the needs for the specific cell line in question.

To maintain the cells they have to be fed and passaged according to their specific needs. All cell lines discussed in this thesis were grown in T-75 culture flasks in 12 mL of growth medium and subcultured three times per week. Cultured cells were kept at 37^0C in humidified air containing 5% CO_2.

During subcultivation adherent cells are loosened from the culture flask surface by enzymatic degradation. Trypsin degrades the cell adhesion and extracellular matrix components anchoring the cells to the flask surface.

Stocks of COS-1, CV-1, HEK293-c1 and HD11 cells are stored in cryotubes in a tank of liquid nitrogen. When cells are needed they can be taken up and cultured. Cell lines are normally subcultivated for up to 30 passages.

Procedure for routine cell maintenance

1. Pre-warm medium and trypsin at 37^0C. Do not pre-warm longer than 30 minutes – components in the serum have shorter half-life at higher temperatures.
2. Disinfect all utensils using 70% ethanol and set up working area in safety cabinet to minimize hand movements. Make sure that everything you need is ready and within reach.
3. Inspect the cells under a light microscope, note confluence.
4. Aspirate old medium from culture flask.
5. Wash cells with 10 mL Dulbecco's Phosphate Buffered Saline (1x**DPBS**). Do this carefully to not dislodge healthy adherent cells. Aspirate 1xDPBS.
6. Add 2.5 mL Trypsin-EDTA (0.05% Trypsin dissolved in EDTA) and incubate in the 37^0C cell incubator. Trypsination time is cell line dependent. Do not shake the bottle after trypsination as this might lead to clumping of loosened cells.
7. Add 9.5 mL of the fresh pre-warmed medium (or at least twice the volume of trypsin). Vigorously pipette up and down until the suspension is homogenous, breaking up any possible cell clumps.
8. Dilute the cells at a cell line and day specific ratio (see subsections 2.2.1.1 to 2.2.1.4).
9. Add pre-warmed fresh medium to achieve a total volume of 12 mL.
10. Incubate the cells at 37^0C in humidified air containing 5% CO_2 for either 48 or 72 hours depending on the ratio at which you have subcultivated.

2.2.1.1. COS-1

COS-1 cells are grown in Dulbecco's Modified Eagle's medium (**DMEM**) supplemented with 10% Foetal Calf Serum (**FCS**) and 1% Penicilin/Streptomycin (**PS**). When inspecting COS-1 cells under the microscope one can see that they grow in a monolayer and exhibit a fibroblastic morphology (meaning they have an elongated shape and grow attached or adherent to the culture dish). COS-1 cells are trypsinated for 4 minutes at 37^0C. They are subcultivated at a ratio of 1:3 or 1:6 and incubated for 48 or 72 hours respectively.

2.2.1.2. CV-1

CV-1 cells are grown in DMEM, supplemented with 10% FCS and 1% PS. CV-1 cells are trypsinated for 4 minutes at 37^0C. When inspecting CV-1 cells under the microscope one can see that they grow in a monolayer, have an elongated shape and are attached to the culturing dish. This cell line exhibits rapid growth, also explaining different split ratio than for COS-1 cells. They are subcultivated at a ratio of 1:5 or 1:10 and incubated for 48 or 72 hours respectively.

2.2.1.3. HEK293-c1

HEK293-c1 cells are grown in DMEM, supplemented with 10% FCS and 1% PS and 1 μg / mL medium Pyromycin. When inspecting HEK293-c1 cells under the microscope one can see that they grow in a monolayer, exhibiting a fibroblastic morphology. HEK293-c1 cells are trypsinated for 4 minutes at 37^0C. HEK293-c1 adhere very loosely – this should also be considered when washing with 1xDPBS. They are subcultivated at a ratio of 1:4 or 1:8 and incubated for 48 or 72 hours respectively.

2.2.1.4. HD11

HD11 cells are grown in Iscove's Modified Dulbecco's Medium (**IMDM**) supplemented with 8% FBS, 2% Chicken Serum and 1% PS. When inspecting HD11 cells under the microscope one can see a mixture of elongated and rotund cells. HD11 cells are trypsinated for 5 minutes at 37^0C. HD11 cells are very adherent. They are subcultivated at a ratio of 1:3 or 1:6 and incubated for 48 or 72 hours respectively.

2.2.2. Counting Cells

Cells are counted using a Countess™ automated cell counter from Invitrogen. Using this machine one can determine the cell concentration as well as the viability of the cells in question.

Counting cells procedure

1. Mix according to the table:

Reagent	Amount
Cell suspension	10 µL
Trypan Blue	10 µL
Total Volume	**20 µL**

2. Pipette 10 µL of suspension onto Countess™ cell counting chamber slide.
3. Focus using focus wheel until the live cells are white in the center.
4. Press count and the concentration for total and live cells will be displayed on the screen.

2.2.3. Transfecting Cells

Transfection is a hybrid term of transformation and infection and is the terminology used when referring to the non-viral introduction of nucleic acids into a eukaryotic cell. Viral gene transfer is usually called infection.

For this project transfections were performed using the lipid based non-liposomal TransIT® -LT1 Transfection Reagent from Mirus. The lipids in the reagent form a neutral complex around the negatively charged DNA allowing for transport across the cell membrane.

24 hours before transfection cells have to be seeded into appropriate cell culture dishes at a concentration depending on experiment and cell line, in a volume dependent on the culture dish. Cells are transfected with DNA amounts dependent on culture dish volume and experiment.

Seeding cells procedure

1. Split cells as outlined in section 2.2.1 steps 1-7.
2. Count cells as outlined in section 2.2.2.
3. Dilute cells to wanted volume and concentration (see subsections 2.2.3.1 – 2.2.3.4).
4. Transfer cells to culture dish required for the experiment and shake the dish in a back and forth and sideways motion (not circular motion).
5. Incubate cells for 24 hours at 37^0C in humidified air containing 5% CO_2.

Transfecting cells procedure

1. Inspect the seeded cells under a light microscope.
2. Pre-warm un-enriched growth medium at 37^0C and TransIT at room temperature for up to 30 minutes.
3. Disinfect all utensils using 70% ethanol and set up working area in safety cabinet to minimize hand movements.
4. Add un-enriched medium to DNA solution, volume dependent on culture dish and cell line (see tables in subsections 2.2.3.1 – 2.2.3.4). Pipette vigorously.
5. Add TransIT into the medium DNA suspension, use 2 μL TransIT per 1 μg DNA. Pipette vigorously and incubate on bench for 20 minutes.
6. Add mixtures drop by drop to the cells and gently shake the culture dish to distribute evenly.
7. Incubate cells for 24 hours at 37^0C in humidified air containing 5% CO_2.
8. After 24 hours of incubation cells are inspected under the microscope and the cell lysates are collected in correlation with the down-stream application they are intended for (see sections 2.3.1 – 2.3.6).

2.2.3.1. COS-1

COS-1 seeding and transfection for GST-pulldown analysis and general western blot analysis.

COS-1 cells are seeded in accordance with specifications below:

Culture dish	Volume per well	Cells seeded per well
15 cm dish	30 mL	2.5×10^6
10 cm dish	10 mL	1×10^6
6 well dish	3 mL	2×10^5

COS-1 cells are transfected in accordance with specifications below:

Culture dish	Medium per well	DNA amount	TransIT
15 cm dish	1 mL	12.5 μg	25 μL
10 cm dish	1 mL	5 μg	10 μL
6 well dish	250 μL	1 μg	2 μL

2.2.3.2. CV-1

CV-1 seeding and transfection for transient reporter gene assay, accompanying western blot analysis, general western blot analysis and protein phosphatase assay.

CV-1 cells are seeded in accordance with specifications below:

Culture dish	Volume per well	Cells seeded per well
6 well dish	2 mL	1.2×10^5
24 well dish	500 μL	0.2×10^5

CV-1 cells are transfected in accordance with specifications below:

Culture dish	Medium per well	DNA amount	TransIT
6 well dish	150 μL	1 μg	2 μL
24 well dish	50 μL	≤ 1 μg	≤ 2 μL

2.2.3.3. HEK293-c1

HEK293-c1seeding and transfection for interactants in stably integrated luciferase reporter gene assay, accompanying western blot analysis and general western blot analysis.

HEK293-c1 cells are seeded in accordance with specifications below:

Culture dish	Volume per well	Cells seeded per well
6 well dish	2 mL	1.2×10^5
24 well dish	500 µL	0.34×10^5

HEK293-c1 cells are transfected in accordance with specifications below:

Culture dish	Medium per well	DNA amount	TransIT
6 well dish	150 µL	1 µg	2 µL
24 well dish	50 µL	≤ 1 µg	≤ 2 µL

2.2.3.4. HD11

HD11 seeding and transfection for *mim-1* reporter gene assay and accompanying western blot analysis.

HD11 cells are seeded in accordance with specifications below:

Culture dish	Volume per well	Cells seeded per well
6 well dish	2 mL	5×10^5

HD11 cells are transfected in accordance with specifications below:

Culture dish	Medium per well	DNA amount	TransIT
6 well dish	150 µL	2 µg	4 µL

2.3. Protein Techniques

As proteins are rapidly degraded it is important to always work on ice, spin cold and to include the appropriate protease inhibitors when preparing the cell lysates.

2.3.1. GST-protein purification and GST-pulldown

Glutathione S-transferase (GST) has a high affinity for glutathione, as it is the enzyme conjugating glutathione to substrates. This affinity can be exploited to experimentally test protein-protein interactions *in vitro*.

The DNA sequence encoding the protein that is to be tested is subcloned in frame with a GST-coding sequence into an expression vector. Cells are transformed, lysed and the cell lysates containing the GST-protein fusions are extracted. These GST-protein fusions can be purified from the crude cell lysate by letting them bind to glutathione-covered sepharose beads (GS-beads). Subsequently, the GS-beads with the attached GST-proteins can be used to pulldown interacting proteins expressed in mammalian cells. After pulldown the binding between the GS beads and the proteins to be analysed is abolished using 3x SDS gel loading buffer (**GLB**). The samples can then be applied to an SDS-PA gel and analysed by western blotting.

For this project GS beads from GE healthcare were used for GST-pulldown experiments. The GST-fusion proteins were mixed with lysates from transiently transfected COS-1 cells, which had been seeded out on either 10 or 15 cm cell culture dishes (section 2.2.3 and subsection 2.2.3.1).

Preparing buffers and defrosting GST-proteins procedure

1. To make a 0.2 M NEM solution, 0.125 g NEM powder are dissolved in 5 mL dH_2O. N-ethylmalemide (**NEM**) is a deSUMOylation inhibitor and only required for experiments in which SUMO conjugation is thought to be important. This solution is prepared fresh upon use and is highly toxic!
2. Take 1 M DTT solution from freezer and use as 1 mM final concentration.

3. To prepare protease inhibitor take 1 Protease Inhibitor Complete tablet from Roche and dissolve in 500 μL dH_20 by rotating on the rotator in the 4^0C room, this makes 100x stock solution.
4. Take GST-proteins out of -80^0C freezer and thaw on ice.
5. Use the above solutions to finish the binding buffer (**BB**) and the potassium acetate interaction/lysis buffer (**KAc**). Per pulldown 2 mL BB and 1.5 mL KAc are needed. See appendix for KAc and BB recipes as well as for complete KAc and complete BB.

Purification of GST fusion proteins procedure

The beads are stored in a 20% ethanol solution, which has to be washed away prior to use.

1. Prepare 40 μL of 50% mix per pulldown. Take out 1.33 x the volume of 100% glutathione needed (meaning 1.33 x 20μL per pulldown) and transfer to a 50 mL falcon tube.
2. Wash by mixing with approximately 3 mL cold BB per 400 μL beads.
3. Sediment the beads by centrifuging at 500 x g for 5 minutes at 4^0C.
4. Carefully aspirate the supernatant. The beads will remain as a gel-like mass at the bottom of the tube.
5. Add the required amount of cold Complete BB to the washed beads. For one pull-down you will need 40 μL of the 50% mix – meaning 20 μL washed beads and 20 μL complete BB. The 50% mix is now ready to use.

Binding GST-fusion protein to glutathione sepharose procedure

1. Mix on ice according to the table:

Reagent	Amount
Complete BB	500 µL
50 % mix	40 µL
GST-fusion protein	X amount (usually 0.5 – 200 µL)

2. Incubate the samples for one hour in the 4^0C room, on the rotator.
   → This incubation time can be used to prepare cell lysates.
3. After the hour-long incubation and before pulldown, wash the GST-fusion proteins fused to the GS beads 3 times with 500 µL BB. Centrifuge at 3000 x g for 1 minute at 4^0C.

Preparation of COS-1 cell lysate procedure

During the preparation of the COS-1 cell lysate make sure to work on ice to counteract protein degradation.

1. Aspirate the medium.
2. Scrape the cells 2 x in PBS (use 2x 10 mL per 15 cm dish and 2x 5 mL per 10 cm dish) transfer the PBS with the scraped cells to a 50 mL falcon tube.
3. Centrifuge at 500 x g for 5 minutes at 4^0C.
4. Aspirate the supernatant retaining only the pelleted cells at the bottom of the falcon tube.
5. Dissolve the pellet in the remaining supernatant (approximately 500 µL) and transfer to a microcentrifuge tube.
6. Spin down the microcentrifuge tube at 500x g for 5 minutes at 4^0C and remove the supernatant.
7. Add 315 µL KAc per pulldown and incubate for 30 minutes on a rotator in the 4^0C room. The 30 minutes incubation time can be used to wash the GST – fusion proteins.
8. After the 30 minutes incubation time centrifuge the lysates for 10 minutes at 4^0C at maximum speed.
9. The supernatant is transferred to new microcentrifuge tubes. This is the ready to use cell lysate.

Pulldown of interacting proteins procedure

1. Transfer 5% input (15 μL) from COS-1 lysates into new microcentrifuge tubes and add 10 μL 3 X SDS PAGE GLB.
2. Transfer 300 μL COS-1 lysate to the beads with the Glutathione - GST protein and incubate for 1 hour on a rotator in a 4^0C room.
3. After the hour-long incubation time wash the samples twice with KAc. Centrifuge at 3000x g, for 1 minute at 4^0C.
4. After the last washing step add 20 μL 3 X SDS PAGE GLB to each sample.
5. Denature all samples at 95^0C for 5 minutes. Thereafter, they can either be stored in a – 80^0C freezer or applied on gel for analysis.

For this project western analysis of GST-pulldown assays was performed using Criterion XT Precast, 4-12% Bis- Tris, 12+2 well comb Gels from BioRad.

2.3.2. Luciferase Reporter Gene Assay

Using the reporter gene assay method it is possible to quantify gene expression. With this method one can determine how a protein (the effector) affects the transcriptional activity of a reporter gene. The reporter gene should code for an easily quantifiable product. In the luciferase assays used for this project, the reporter gene codes for the luciferase enzyme. This enzyme oxidizes luciferin substrate generating a light reaction. The binding of the effector protein to the regulatory elements can lead to an increase or decrease in degree of reporter gene transcription – and thus to an increase or decrease in luminescence. Using a luminometer, the light production is readily measurable. Measuring the light production measures the transcriptional activity of the effector, making activity increase or decrease quantifiable.

During this project both transiently transfected (natural and synthetic) and stably integrated (synthetic) reporter genes were used (further discussed in subsections 2.3.2.1, 2.3.2.2 and section 4.3.2) to evaluate changes in c-Myb's transactivation activity. The Luciferase Assay System Kit from Promega was used and the assay was conducted in triplicates. The data from three different independent experiments was normalised. The luminometer used for this project is the VICTOR2™ multilabel

counter from PerkinElmer Life Sciences. This machine utilizes a pump that injects the luciferin substrate into each well just prior to measurement.

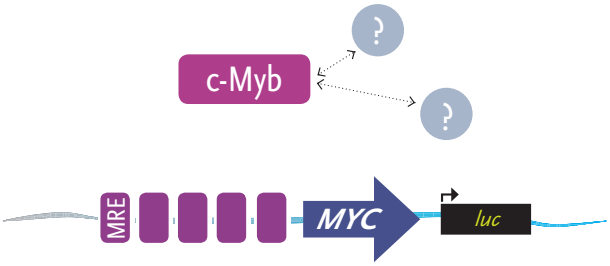

Figure 2.2: Schematic of a transient synthetic reporter construct. This specific reporter construct has five Myb responsive elements (MREs). When c-Myb interacts with the MREs, luciferase expression is initiated. The more luciferase is expressed the more luciferin can be catalysed and the measurable light emission in the system increases.

Lysate collection prior to luciferase measurements procedure

1. Mix or thaw the luciferase substrate and dilute the passive lysis buffer.
2. Inspect cells under light microscope and determine whether cells look healthy.
3. Aspirate cell medium.
4. Wash the cells with 1xDPBS (wash x 2 if using CV-1 cells and x1 if using HEK293-c1 cells).
5. Add 100 µL passive lysis buffer per well and incubate on oscillator for 15 minutes at room temperature.
6. Transfer the lysates to new microcentrifuge tubes and centrifuge at maximum speed for two minutes.
7. Transfer 20 µL lysate into 96 well dish and measure the light emission with the luminometer. For this project the luminometer was programmed with the main parameters shown below:

Action	Variable
Substrate injection volume	20 µL
Shaking duration	3 seconds
Shaking speed	Fast
Measurement time	1 second
Emission aperture	Normal

8. When the program is done, extract your data for analysis.

Lysate collection for western blot analysis procedure

1. Inspect cells under light microscope.
2. Aspirate cell medium.
3. Wash the cells with 1xDPBS (wash x2 if using CV-1 cells and x1 if using HEK293-c1 cells).
4. Add 100 μL complete 3xSDS GLB per well and incubate on oscillator for 5 minutes at room temperature.
5. Collect the lysates (each triplicate into one microcentrifuge tube).
6. Centrifuge the samples at 3000 rpm for 2 minutes.
7. Sonicate the samples with the following settings: 7s on, 15s off, high intensity, 10 cycles, at 20^0C.
8. Denature all samples at 95^0C for 5 minutes. After boiling they can either be stored in a – 80^0C freezer or applied to gel for analysis.

During this project western analysis for luciferase assays was performed using large 10% SDS-PA gels.

2.3.2.1. Luciferase Assays using Transiently Transfected Reporters

In the transiently transfected luciferase assays, reporter plasmids (with both synthetic and natural regulatory elements) were co-transfected with plasmids encoding effectors and co-factors into CV-1 cells seeded into 24 well culture dishes. For seeding and transfection see section 2.3.3 and subsection 2.2.3.2.

Transiently transfected reporter plasmids are not fully chromatinized, exhibiting only intermediate levels of nucleosomal assembly [30]. For this project all transfected c-Myb expressing plasmids in the transient assays encoded the full-length c-Myb versions (with intact DBD region).

2.3.2.2. Luciferase Assays using Stably Integrated Reporters

In the stably integrated luciferase assays, HEK293-c1 cells (seeded into 24 well culture dishes) were co-transfected with plasmids encoding effectors and co-factors. For seeding and transfection see section 2.3.3 and subsection 2.2.3.2.

In the HEK293-c1 cells the reporter gene is stably integrated into the genome and preceded by three Gal4 responsive elements [81]. This means that effectors used for this system require a Gal4 binding domain.

During this project the HEK293-c1 system was used with both GBD-VP16 and GBD-hcM(194-640). The latter is a Gal4 binding domain and c-Myb fusion protein in which the natural DNA binding domain of c-Myb has been removed.

2.3.3. HD11 mim-1 Reporter Gene Assay

The HD11 *mim-1* system, like the luciferase systems, is a reporter gene assay. HD11 cells are chicken macrophages containing the *mim-1* gene in their genome. This gene however, is not expressed unless plasmids encoding c-Myb are transfected into the cells [19, 37].

When c-Myb is ectopically expressed in the HD11 cells (for seeding and transfection see section 2.3.3 and subsection 2.2.3.4), transcription of the *mim-1* gene is initiated resulting in *mim-1* mRNA. The transcription levels of this reporter can be determined and quantified by first reverse transcribing the mature mRNA into cDNA (section 2.1.13) and then using this cDNA in quantitative real-time PCR analysis (section 2.1.11).

The HD11 *mim-1* system is both a natural reporter and fully chromatinized as it is naturally occurring in the cellular genome.

During this project the HD11 *mim-1* reporter gene assay was used to determine the expression levels of c-Myb target gene *mim-1* using different co-transfection parameters. The plasmids used for qRT-PCR are listed in the appendix.

Lysate collection for qRT-PCR procedure

1. Inspect cells under light microscope.
2. Aspirate cell medium.
3. Wash the cells twice with 1xDPBS.
4. Trypsinate cells using 500 μL Trypsin. Incubate for approximately 15-20 minutes in the 37^0C incubator (or until the cells loosen).
5. Add 3 mL pre-warmed medium per well and pipette up and down, further loosening the cells.
6. Transfer triplicates to 15 mL tubes.
7. Isolate total RNA as described in section 2.1.3.
8. Synthesize cDNA from mature mRNA as described in section 2.1.13.
9. Quantify *mim-1*, *hprt* and *myb* expression using qRT-PCR as described in section 2.1.11.

Lysate collection for western blot analysis procedure

1. Steps 1-6 as above. After step 6 transfer 600 μL from the cell suspension into a separate microcentrifuge tube.
2. Centrifuge the samples at 3000 rpm for 2 minutes.
3. Aspirate excess medium.
4. Add 100 μL 3xSDS GLB.
5. Sonicate the samples with the following settings: 7 s on, 15 s off, high intensity, 10 cycles, at 20^0C.
6. Denature all samples at 95^0C for 5 minutes. After boiling they can either be stored in a – 80^0C freezer or applied to gel for analysis.

2.3.4. Protein Phosphatase treatment

Lambda Protein Phosphatase (**λ-PPase**) is a phosphatase, which dephosphorylates serine, threonine and tyrosine residues. λ-PPase was first isolated from bacteriophage lambda infected *E. coli* and its function is Mn^{2+}-dependent.

Cell lysates that are to be treated with λ-PPase require a buffer that both preserves the protein and allows enzymatic activity, for this the PTP buffer is used (see appendix). This buffer is void of salts and detergents. Before use the PTP buffer has to be enriched with protease inhibitor, thereby inhibiting protein degradation. Since phosphate is a negatively charged group, dephosporylation will result in an electromobility shift, which can be observed when running a treated sample next to an un-treated control.

During this project λ-PPase treatment was performed on ATF7IP proteins ectopically expressed in CV-1 cells, which had been seeded into 6 well culture dishes. For seeding and transfection see section 2.3.3 and subsection 2.2.3.2.

Lysate collection in λ-PPase treatment procedure

1. After transfection of CV-1 cells and 24 h incubation, cells are inspected. The confluency level should be approximately 80-90%.
2. Aspirate the medium.
3. Wash the cells twice with 2 mL room temperature 1xDPBS.
4. Put culture dishes on ice and use 500 μL cold 1xPBS to scrape the cells.
5. Transfer the cell suspensions from each triplicate to microcentrifuge tubes and centrifuge the samples at 1000 x g for 5 minutes at 40C.
6. Aspirate the PBS from the pellet and re-suspend in 200 μL PTP-buffer containing PMSF (1 mM), Leupeptin (10 μg/ mL) and Aprotinin (10 μg/ mL).
7. Sonicate the samples with the following settings: 7 s on, 15 s off, high intensity, 10 cycles, at 20^0C.
8. After sonication freeze the samples overnight (or for at least an hour) in the -80^oC freezer.

Treatment of lysates with λ-PPase procedure

1. Mix the samples as indicated in table below:

Reagent	Sample	Control
Cell lysate	33 μL	33 μL
10x λ-PPase NEB Buffer	4 μL	4 μL
250mM $MnCl_2$	4 μL	4 μL
dH_2O	-	1 μL
λ-PPase, 400,000 units/ml	1 μL	-
Total Volume	**42 μL**	**42 μL**

2. Incubate the samples for 15 minutes at 30^oC.
3. Add 20 μL complete 3xSDS GLB per sample.
9. Denature all samples at 95^0C for 5 minutes. After boiling they can either be stored in a -80^0C freezer or applied to gel for analysis.

2.3.5. SDS-PAGE

Proteins with varying molecular mass can be separated independent of charge and three-dimensional structure using sodium dodecyl sulfate polyacrylamide gel electrophoresis (**SDS-PAGE**) under reducing conditions.

SDS is anionic and disrupts non-covalent interactions, while the reducing agent (either β-mercaptoethanol or dithiothreitol) is used to reduce disulphide bonds. SDS molecules associate with the amino acid residues of proteins in a 1:2 ratio, thereby binding in amounts roughly proportional to the molecular weight of the protein. The binding of the SDS molecules leads to a net negative charge that is so large - the original charge of the protein becomes irrelevant.

Smaller polypeptides migrate through the gel faster than larger polypeptides. Due to an almost equal mass to charge ratio – the speed of movement through the gel is usually almost exclusively determined by the mass of the protein. An exception that should be noted are proteins that have branched covalently attached PTMs, for example: c-Myb and its SUMO conjugates. In this case the branching of the SUMO residues leads to migratory retardation through the gel. Meaning that the SUMO

modified c-Myb protein travels at a slower speed than the combined molecular weight of c-Myb and SUMO would suggest.

During this project protein separation from GST-pulldown assays was performed using Criterion XT Precast, 4-12% Bis- Tris, 12+2 well comb Gels from BioRad. All other experiments were conducted using large SDS-PA gels made in the lab.

Unpolymerized acrylamide is a neurotoxin; utmost care should be taken in handling. Ammonium persulfate (**APS**) initiates polymerization catalysed by TEMED.

Casting large SDS-PA gels procedure

This procedure is for large discontinuous gels with glass plates that are approximately 20 cm high and 20 cm wide. As water or dust can lead to uneven polymerization it is very important to thoroughly clean all utensils before attempting to cast the gel.

1. Assemble the glass plates. They are held apart by spacers and tightened by clamps. The spacers need to be matched to the comb to be used in step 7.
2. Use 1% agarose gel and a transfer pipette and apply the agarose gel on the outside of the spacers between the two glass plates. This is to make sure the polyacrylamide gel does not leak.
3. Mix the separating gel solution (see appendix) and pour it between the two glass plates until it is approximately 5 cm from the top.
4. Apply dH_2O to the top to even the gel front and to exclude air bubbles, let the gel polymerize (for between 20 minutes to 2 hours).
5. Remove the water from the gel.
6. Mix the stacking gel (see appendix) and pour it between the two glass plates on top of the separating gel.
7. Insert the comb carefully from one side – pushing out any potential air bubbles. Wait and let the gel polymerize.
8. After polymerization, remove the comb and wash away any remaining buffer using laboratory grade water. Finally, remove the clamps and the bottom spacer.

Mounting large SDS-PA gels procedure

1. Mount the two glass plates containing the gel in the electrophoresis chamber. Clamp into place and fill with electrophoresis buffer until the wells are covered.
2. Fill electrophoresis buffer into the bottom of the electrophoresis chamber and remove any air bubbles that might be trapped between the two glass plates under the gel.
3. Apply the samples to the gel (for sample preparation, see the various experimental protocols).
4. Run the large homemade gel at constant current (7 mA) over night. By watching the dye front and the standard ladder it is possible to monitor the migration path. (The commercially available BioRad gels were run at constant voltage (200 V) for approximately 1 hour).

During this project all SDS-PAGE protein separations were detected using western blot analysis (see section 2.3.6).

2.3.6. Semi-dry Western blotting

After separating proteins based on their molecular weight (SDS-PAGE) it is possible to transfer these proteins onto a membrane. This is achieved by passing an electrical current through the gel to move the proteins from the gel towards the anode and onto the membrane. In semi-dry western blotting the current is carried through filter papers that have been immersed in anode and cathode buffer respectively.

Once transferred the proteins can be probed and detected using protein specific antibodies. This method is referred to as either western blotting or immunostaining.

During this project polyvinylidene difluoride (PVDF) membrane and Whatman filter paper from GE Healthcare were used when transferring proteins onto membrane. For detection, secondary antibodies conjugated to horseradish peroxidase (HRP) were used. In the presence of the required substrate (SuperSignal West Dura Extend Duration Substrate from ThermoScientific) HRP catalyses a chemiluminescent reaction, this reaction releases light which is detected and recorded using a CCD

camera (during this thesis the Kodak Image Station 4000R Pro was used). The different antibodies are noted in the results section and listed in the appendix.

Protein transfer onto membrane procedure

1. Separate the proteins by SDS-PAGE as outlined in section 2.3.5.
2. Cut the membrane and 6 pieces of Whatman filter paper to the required size.
3. Activate the membrane in methanol for 2 minutes then move it to the anode buffer.
4. Soak 3 filter papers in the anode (+) buffer and 3 filter papers in the cathode (-) buffer.
5. After SDS-PAGE has run gently remove the gel from the glass plates and assemble the blotting stack from bottom (anode) to top (cathode).
   → 3 filter papers soaked in anode buffer
   → activated membrane
   → polyacrylamide gel containing separated proteins
   → 3 filter papers soaked in cathode buffer
   Remove air bubbles.
6. Transfer proteins to membrane at constant current (140 mA) for 1 hour and 5 minutes.
7. After protein transfer has run, carefully lift the corner of the stack to assess by looking at the molecular weight standard whether transfer has been successful, in which case the membrane can be removed and fixed in methanol for 2 minutes.

Blocking and incubating with antibody procedure

1. Block the membrane using 1xTBS-T with 5% milk, by incubating for 30 minutes on oscillator.
2. Immerse the membrane in primary antibody in 1xTBS-T with 5% milk. The amount of antibody used has to be determined experimentally (see results and appendix). Incubate in the 4^0C room on the oscillator over night.
3. Wash the membrane 3 x 20 minutes using in 1xTBS-T with 5% milk.
4. Immerse the membrane in secondary antibody in 1xTBS-T with 5% milk. The amount of antibody used has to be determined experimentally (see appendix). Incubate on the oscillator at room temperature for one hour.
5. Rinse membrane six times with 1xTBS-T.
6. Wash the membrane for an additional 20 minutes in 1xTBS-T.
7. Take the membrane to the CCD camera, incubate the membrane in substrate for 1 minute and subsequently image the blot.

When needing to detect more then one specific protein it is necessary to strip off antibodies from the previous incubation and detection round. During this project membranes were stripped using the Restore Western Blot Stripping Buffer from ThermoScientific. For GST-pulldown assays it was necessary to dye the membrane, this was done by incubating the membrane for five minutes in 1x Ponceau red stain before drying and scanning.

3. Results

The main objectives of this thesis are to confirm and characterize the interaction between c-Myb and ATF7IP and to address the functional implications of this interaction. The results are divided into three sections, focusing on development of tools (subchapter 3.1), interaction studies (subchapter 3.2) and functional studies (subchapters 3.3, 3.4, 3.5, 3.6, 3.7 and 3.8). For both the interaction and functional studies a number of questions are posed and experiments aiming to answer these questions are presented.

3.1. Development of tools

3.1.1. Generating plasmids for expression of ATF7IP and its partners

Prior to protein-protein interaction and functional studies a number of plasmids had to be generated. The construction of these plasmids is described in this section, while the specific methods used are described in chapter 2. Particular thanks goes to Dr. Mitsuyoshi Nakao at Kumamoto University in Japan for gifting the FLAG-tagged full-length human ATF7IP expressing plasmid pcDNA3-FG-MCAF [23]. To avoid confusion this plasmid will henceforth be referred to as pcDNA3-FG-ATF7IP in this thesis. The plasmids available in the laboratory will not be described here (see appendix for list of all plasmids used).

3.1.1.1. Subcloning of the 3FLAG-tagged ATF7IP construct

Before studying the binding between full-length ATF7IP and human c-Myb, ATF7IP cDNA had to be subcloned into a mammalian expression vector in frame with 3FLAG: expressing an N-terminally 3FLAG tagged ATF7IP protein. This was found necessary in order to be able to detect ATF7IP in a robust manner (see figures 3.9, 3.10 and 3.11). Initially, ATF7IP cDNA was subcloned into frame with the myc tag. However, this was found to be inadequate for the detection of ATF7IP in western blot analysis.

The gift plasmid pcDNA3-FG-ATF7IP was opened with XhoI, excising the ATF7IP insert. The pCIneo-myc vector was opened with SalI and treated with SAP to prevent re-ligation. As XhoI and SalI have compatible overhangs it was possible to ligate the

ATF7IP insert into the pCIneo vector generating pCIneo-myc-ATF7IP (the orientation of the insert had to be checked by verification restriction digest). This pCIneo-myc-ATF7IP vector was used for mutagenesis of the ATF7IP SIM domain (subsection 3.1.1.2).

After initial expression and unsuccessful detection experiments, it was decided to further subclone ATF7IP into a 3FLAG expression vector. The pCIneo-myc-ATF7IP plasmid was opened using XhoI (using an XhoI restriction site found in pCIneo-myc) and NotI restriction enzymes. The 3849 bp long insert was isolated using gel electrophoresis and gel band purification. The plasmid, pCIneo-3FG-hcM, was also digested with XhoI and NotI (removing the c-Myb coding sequence from the plasmid) and ATF7IP was ligated in frame with the 3FLAG coding sequence, generating pCIneo-3FG-ATF7IP.

The plasmid was verified by both restriction verification and sequencing analysis. Expression analysis using the construct resulted in successful detection of ATF7IP (see figure 3.3).

3.1.1.2. Mutagenizing the ATF7IP construct

As the initial hypothesis was that the strong SIM domain of ATF7IP plays an important part in the c-Myb – ATF7IP interaction, one of the initial steps was to generate an ATF7IP SIM mutant.

To mutagenize the SUMO interaction motif of ATF7IP, the sequence encoding the region harbouring the SIM domain had to first be subcloned into a smaller temporary vector. The Bluescript SKII+ (pBS) vector was chosen; it is both small and contains sequences that can be used for Blue/White colour selection making it an optimal cloning vector. Generating pCIneo-3FG-ATF7IP-SIM-AADA (the SIM mutant) took place in 4 steps: subcloning, mutagenesis, backcloning and an additional subcloning step.

1. pBS was digested with EcoRI and NotI restriction enzymes. pCIneo-myc-ATF7IP was also digested with EcoRI and NotI, and a 1376 bp long sequence containing the

SIM region was isolated. Ligating the insert into the vector generated the pBS-ATF7IP-EcoNot plasmid.

2. To generate pBS-ATF7IP-EcoNot SIM-AADA from pBS-ATF7IP-EcoNot, the latter was subjected to mutagenesis, introducing the SIM mutation. The four amino acids VIDL (residues 966 - 969) were mutated into AADA (using the QuikChange method and the primers M167 and M168, see appendix). This mutation should destroy the SIM in human ATF7IP while also introducing a unique SacII restriction site into the nucleotide sequence for verification purposes.

3. In the initial backloning step pBS-ATF7IP-EcoNot SIM-AADA was digested with PpuMI and a 639 bp SIM-AADA sequence fragment was isolated. The pCIneo-myc-ATF7IP vector was also treated using the PpuMI restriction enzyme and a 8722 bp fragment was isolated and SAP treated. Subsequently the 639 bp long fragment was ligated into the 8722 bp long fragment and pCIneo-myc-ATF7IP-SIM-AADA was generated.

As it became apparent that detection of the single myc tag was not successful, ATF7IP-SIM-AADA was subcloned in frame with a 3FLAG tag as described in subsection 3.1.1.1 and pCIneo-3FG-ATF7IP-SIM-AADA was generated.

The plasmid was verified by both restriction verification and sequencing. Expression of the construct resulted in successful detection of ATF7IP (see figures 3.9 B, 3.10 and 3.11).

3.1.1.3. Subcloning of the HA tagged hMBD1 construct

As discussed in the Introduction, MBD1 is one of the key partners of ATF7IP. To express and detect hMBD1 in experiments, we subcloned its coding sequence into an expression vector in frame with the HA-tag.

The full-length cDNA encoding human hMBD1 was purchased from SourceBioscience in a pOTB7 vector (pOTB7-MBD1). It was decided to HA tag hMBD1 since it contained restriction sites well positioned for subcloning. The

subcloning resulting in the pCIneo-HA-hMBD1 plasmid was conducted in 2 consecutive steps.

1. The purchased pOTB7-MBD1 plasmid was digested with NcoI and a 2438 bp long fragment was isolated. The pGEX-KG plasmid, used for its suitable combination of recognition sites, was also digested with NcoI and treated with SAP. The 2438 bp long insert was ligated into the vector and pGEX-KG-hMBD1 was generated.

2. pGEX-KG-hMBD1 was digested with SalI and SmaI restriction enzymes and a 2485 bp long fragment isolated. pCIneo-HA was digested with XhoI and SmaI. As XhoI and SalI have compatible overhangs, it was possible to ligate the hMBD1 insert into the opened vector, generating pCIneo-HA-hMBD1.

The hMBD1 coding sequence was verified by sequencing, the subcloning steps by restriction verifications. Expression of the construct resulted in successful detection of MBD1 (see subsection 3.1.2.4).

3.1.1.4. Gateway cloning of SETDB1 into an expression vector

SETDB1 is another key partner of ATF7IP. To express hSETDB1 in our mammalian cell lines for the various experiments we subcloned its coding sequence into a mammalian expression vector.

The full-length cDNA encoding human SETDB1 was purchased from SourceBioscience in a pOTB7 vector (pOTB7-SETDB1). The pOTB7 vector is a Gateway entry clone. Using the pCIneo-RfA destination vector and pOTB7-hSETDB1 entry clone in a LR reaction generated the pCIneo-hSETDB1 expression vector.

The hSETDB1 coding sequence was verified by sequencing, the gateway-cloning step by additional restriction verification. Expression of the construct resulted in successful detection of hSETDB1 using an anti-SETDB1 antibody (see figure 3.5).

3.1.2. Protein expression and Antibody detection

This section is a collection of the initial expression and detection studies of the constructed plasmids (subsections 3.1.2.1 and 3.1.2.2), a first foray into the migration pattern of ATF7IP (subsection 3.1.2.3), as well as initial dosage response tests for the later functional assays (subsections 3.1.3.4 and 3.1.3.5).

3.1.2.1. Detecting 3FLAG-tagged COS-1 cell lysates

In order to carry out interaction or function studies using ATF7IP, it is important to have a method for detecting the protein.

In initial expression and detection experiments we transfected pcDNA3-FG-ATF7IP, pCIneo-3FG-ATF7IP-CTD, pCIneo-3FG-hcM and pCIneo-3FG-hcM-SUMO1 plasmids into COS-1 cells. The results are shown in figure 3.1.

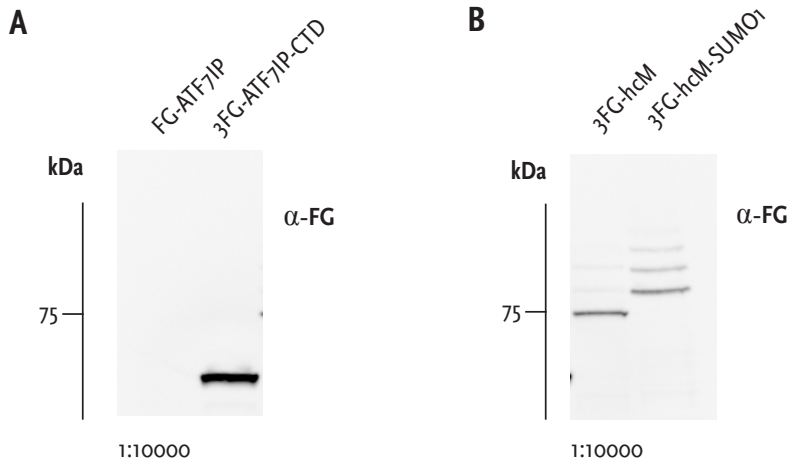

Figure 3.1: Testing antibody concentration and detection for 3FLAG-tagged lysates. COS-1 cells were seeded into four wells of a six well dish ($2x10^5$ cells per well in 3 mL medium per well). After 24 hours cells were transfected with 1 μg plasmid DNA each (pcDNA3-FG-ATF7IP, pCIneo-3FG-ATF7IP-CTD, pCIneo-3FG-hcM and pCIneo-3FG-hcM-SUMO1 respectively). After 24 hours cells were lysed and samples were separated using a CriterionXT 4-12% BisTris, 12+2 well gel from Biorad. After gel separation and blotting, the membranes were incubated with primary anti-FLAG antibody (diluted 1:10000) and secondary anti-mouse-HRP antibody (diluted 1:10000).

As can be seen from figure 3.1 A and B, using anti-FLAG at a 1:10000 dilution works well for the 3FLAG-tagged proteins (3FG-ATF7IP-CTD, 3FG-hcM and 3FG-hcM-SUMO1), the FLAG-tagged full-length ATF7IP protein however, is not detectable. This does not necessarily mean that the full-length FG-ATF7IP protein is not expressed. The 3FLAG tag is an improvement of the original single FLAG, it uses

three consecutive FLAG epitopes, making it ideal in low-level expression cases. Based on these blots, further subcloning of ATF7IP in frame with 3FLAG became necessary (subsection 3.1.1.1).

In Figure 3.1 B one can also see that the 3FG-hcM-SUMO1 fusion construct exhibits a 2nd and 3rd band representing a significant fraction (this phenomenon is further explained in section 3.2.1).

3.1.2.2. Detecting ectopic and endogenous ATF7IP in HEK293-c1 cell lysates

Using anti-FLAG antibody we were able to detect 3FG-ATF7IP (see figures 3.2 A and figure 3.3). Yet as the blots had to be exposed for 40-50 minutes during image capture, suggesting quite low expression levels, the question arose as to whether the amount of ectopically expressed ATF7IP might be too low?

To determine the levels of endogenous versus ectopic ATF7IP, an anti-ATF7IP primary antibody was purchased from Bethyl Laboratories and tested in lysates from transfected HEK293-c1 cells. The results are shown in figure 3.2.

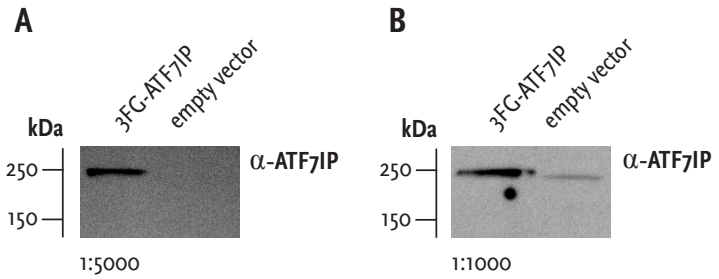

Figure 3.2: Testing antibody concentration and detection of 3FG-ATF7IP. **A and B:** HEK293-c1 cells were seeded into a 6 well dish ($1.2x10^5$ cells/well in 2 mL medium per well). After 24 hours cells were transfected with 1μg plasmid DNA each (two with pCIneo-3FG-ATF7IP and two with empty vector pCIneo). Cells were lysed after 24 hours and western lysates prepared. Samples were separated using a large 10% SDS-PA gel. After gel separation and blotting, the membranes were incubated with primary anti-ATF7IP antibody (over a dilution range) and secondary anti-rabbit-HRP antibody (diluted 1:10000).

From the results of expression and detection (figure 3.2), there is a clear difference between the samples that were transfected with pCIneo-3FG-ATF7IP and those that were transfected with empty vector. When using the 1 to 5000 antibody dilution, a band is visible at 250 kDa. No other bands are detected on the membrane (figure 3.2

A). Using the more concentrated antibody dilution (1 to 1000), both ectopic and endogenous ATF7IP can be seen (figure 3.2 B).

We conclude that the anti-ATF7IP antibody is well-suited for detection of ectopic, as well as endogenous ATF7IP.

3.1.2.3. Detecting 3FG-ATF7IP in CV-1 cell lysate after Phosphatase treatment

ATF7IP has a molecular weight of 136.4 kDa, yet it is usually detected as two strong bands: one migrating at 250 kDa and the other at 150 kDa, with a number of additional weaker bands.

To determine whether this migration shift could be partially due to poly-phosphorylation of ATF7IP, a λ protein phosphatase (**λ-PPase**) was used to strip the protein of phosphate groups. In figure 3.3 a phosphatase treated sample (left) is shown next to a control sample (right). GAPDH is used as a loading control.

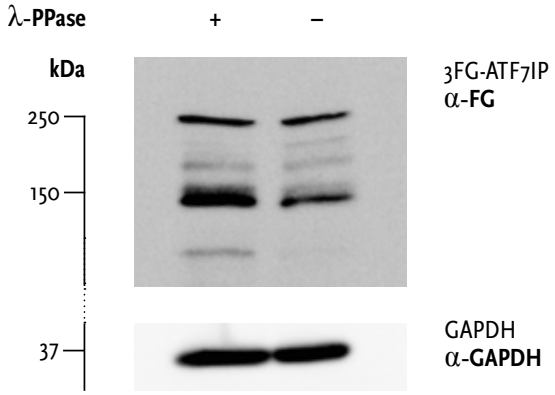

Figure 3.3: Detection of 3FG-ATF7IP after phosphatase treatment. CV-1 cells were seeded into six wells of a 6 well dish ($1.2x10^5$ cells/well in 2 mL medium per well). After 24 h cells were transfected with 1 μg pCIneo-3FG-ATF7IP per well. Cells were lysed after 24 h and lysates collected for phosphatase treatment. The lysates were prepared for λPPase treatment. A λPPase positive and a control sample were separated using a large 10% SDS-PA gel. After gel separation and blotting, the upper part of the membrane was incubated with primary anti-FLAG antibody (diluted 1:10000) and secondary anti-mouse-HRP antibody (diluted 1:10000). The lower part of the membrane was incubated with primary anti-GAPDH antibody (diluted 1: 4000) and secondary anti-mouse-HRP antibody (diluted 1:10000).

From the results (figure 3.3) we see that the lane containing the λ-PPase treated sample, the fraction of 3FG-ATF7IP seen at 250 kDa does not disappear, nor decrease

after phosphatase treatment. One of the weaker bands (under 250 but above 150 kDa) diminishes and the 150 kDa band increases in strength. The loading control appears even. These results indicate that although there seems to be some phosphorylation sensitive to λ-PPase (seen by the disappearance of the second band from the top in the λ-PPase treated sample), the band at 250 kDa does not appear to be caused by this post-translational modification. This conclusion assumes that the conditions used for dephosphorylation lead to full removal of phosphate groups. Although we lack a good positive control here, the conditions used were identical to conditions previously used in the lab where full shifts were observed. This migration paradox will be further discussed in section 4.2.4.

3.1.2.4. Detecting HA- hMBD1 in COS-1 cell lysate

To ectopically express hMBD1 we subcloned its cDNA into an expression vector, in frame with the HA-tag (see subsection 3.1.1.3). COS-1 cells were transfected with the pCIneo-HA-hMBD1 plasmid, the proteins were detected using an anti-HA primary antibody. The results of expression and detection are shown in figure 3.4.

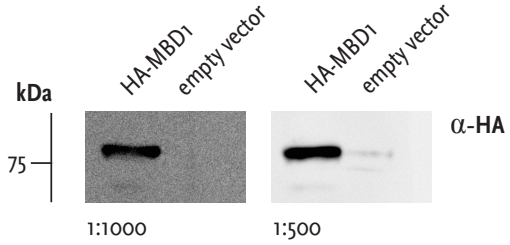

Figure 3.4: Testing antibody concentration and detection for HA-tagged human MBD1. COS-1 cells were seeded into six wells of a 6 well dish ($2x10^5$ cells/well in 3 mL medium per well). After 24 h cells were transfected with 1 μg plasmid DNA each (pCIneo-HA-hMBD1 and pCIneo). Cells were lysed after 24 h and western lysates prepared. Samples were separated using a large 10% SDS-PA gel. After gel separation and blotting, the membranes were incubated with primary anti-HA antibody (diluted 1:1000, 1:500) and secondary anti-rabbit-HRP antibody (diluted 1:10000).

The anti-HA primary antibody works very well in the detection of HA-hMBD1 lysate from COS-1 cells. Only minor levels of unspecific binding are detected in the pCIneo transfected control lysate, when using a 1:500 dilution. For subsequent experiments the 1:500 dilution was used.

3.1.2.5. Detecting hSETDB1 in COS-1 cell lysate

To ectopically express hSETDB1 we transfected the pCIneo-hSETDB1 plasmid (generated in subsection 3.1.1.4) into COS-1 cells. For detection an anti-SETDB1 primary antibody (see appendix) was used. The results are shown in figure 3.5.

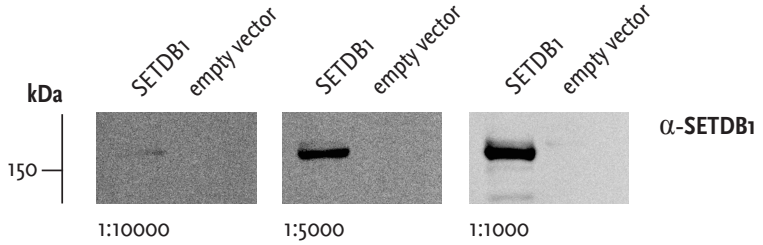

Figure 3.5: Testing antibody concentration and detection for human SETDB1. COS-1 cells were seeded into six wells of a 6 well dish ($2x10^5$ cells/well in 3 mL medium per well). After 24 h cells were transfected with 1 μg plasmid DNA each (pCIneo-hSETDB1 and pCIneo). Cells were lysed after 24 h and western lysates prepared. Samples were separated using a large 10% SDS-PA gel. After gel separation and blotting, the membranes were incubated with primary anti-SETDB1 antibody (diluted 1:10000, 1:5000, 1:1000) and secondary anti-rabbit-HRP antibody (diluted 1:10000).

Based on the western results, the anti-SETDB1 primary antibody works very well in the detection of hSETDB1 lysate from COS-1 cells. The 1:1000 dilution was used for subsequent experiments.

3.1.3. Dosage Response for Luciferase Assays

To determine the functional implications of ATF7IP on its interaction partner, c-Myb, a number of luciferase assays were performed. Before adding ATF7IP to these assays, the dosages of c-Myb and other interactants had to be determined to find input amounts leading to a reasonable response.

3.1.3.1. *c-Myb dosage in transient reporter models*

CV-1 cells were co-transfected with a luciferase reporter driven by a synthetic Myb responsive promoter in transient transfections and with plasmids encoding either c-Myb or c-Myb-2KR, in different amounts. The results of the dosage response are shown in figure 3.6.

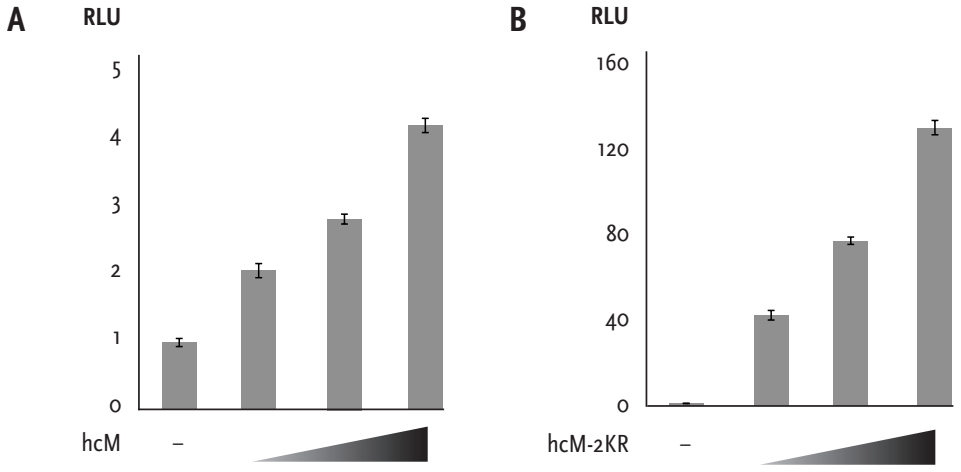

Figure 3.6 (A and B): c-Myb dosage response in transient synthetic pGL4x-5xMRE(GG)-myc reporter assay. CV-1 cells were seeded into 21 wells of a 24 well dish ($0.2x10^5$ cells/well in 0.5 mL medium per well). After 24h cells were transfected with 0.5μg plasmid DNA per well. Using 0.1 μg pGL4x-5xMRE(GG)-myc and increasing amounts of either pCIneo-hcM-HA or pCIneo-hcM-HA-2KR (0.05 μg , 0.1 μg or 0.2 μg). Cells were lysed with passive lysis buffer after 24 h and lysates collected for luciferase analysis. Values are given as relative luciferase units (RLU) they represent the mean RLU ± SEM Values are calculated from three independent experiments carried out in triplicates.

Based on these results, it was determined that 0.2 μg of the c-Myb effector should be used in subsequent luciferase assays.

3.1.3.2. hSUMO1-Q94P and hSUMO2-Q90P dosage response in transient reporter models

One of the concerns that needed to be addressed for this study was the low steady-state level of SUMOylation of c-Myb at any given time (see section 1.3.2). This concern becomes especially critical when the cofactors studied (ATF7IP) in relation to c-Myb are hypothesized to depend on a SUMO-SIM interaction. Could it be that the fraction of SUMOylated proteins is too small to be measured efficiently in a functional assay? To circumvent this problem, SENP resistant SUMO1 and SUMO2 mutants (pCIneo-hSUMO1-Q94P and pCIneo-hSUMO2-Q90P respectively) were designed and cloned by Marit Ledsaak. These mutants should enhance natural SUMOylation levels by being SENP resistant – meaning SENP is unable to deconjugate the SUMO peptides once attached.

These SENP resistant SUMO mutants can also be used to determine whether SUMO1 and SUMO2 have different effects on c-Myb activity since c-Myb may be "loaded" with one or the other.

The hSUMO1-Q94P and hSUMO2-Q90P dosage response experiments were performed using two different transient synthetic reporters pGL4x-5xMRE(GG)-myc-enhancer and pGL4x-5xMRE(GG)-myc (constructs by Marit Ledsaak). As it is difficult to measure repressive effects in luciferase assays we hoped that the pGL4x-5xMRE(GG)-myc-enhancer reporter would lead to an increased level of activation when using only the reporter and c-Myb effector, which would have given more space for repressional effects. As this was not the case (see figure 3.7 A and B) it was determined to continue experimentation with the pGL4x-5xMRE(GG)-myc reporter (see figure 3.7 B and C) .

To determine the effects that SENP resistant SUMO1 and SUMO2 have on c-Myb, western blot analysis was performed for the pGL4x-5xMRE(GG)-myc reporter assay (figure 3.7 B).

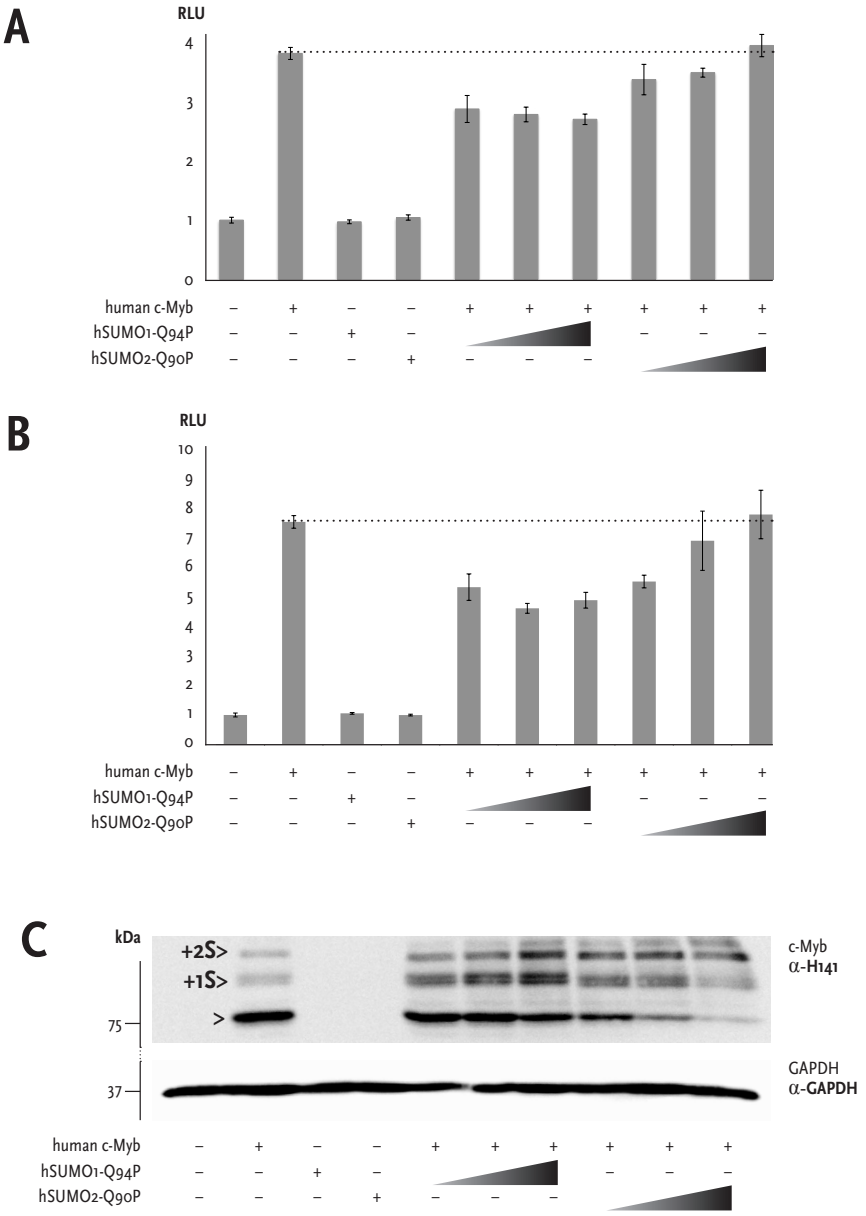

Figure 3.7 (A - C): Testing the effect SUMO1 vs. SUMO2 on c-Myb by using increasing amounts of SENP resistant hSUMO1-Q94P and hSUMO2-Q90P. CV-1 cells were seeded into 24 well dishes ($0.2x10^5$ cells/well in 0.5 mL medium per well). After 24 h cells were transfected with 0.5 µg plasmid DNA per well. Using 0.1 µg pGL4x-5xMRE(GG)-myc-enhancer **(A)** 0.1 µg pGL4x-5xMRE(GG)-myc or **(B)** as reporter, 0.2 µg pCIneo-hcM-HA as effector, 0.05 µg pCMVB-T7-PIASy and increasing amounts of either pCIneo-hSUMO1-Q94P or pCIneo-hSUMO2-Q90P (0.05 µg , 0.1 µg or 0.2 µg). After 24 hours cells were lysed with passive lysis buffer for luciferase assay and in 3xSDS GLB for western blot analysis. Values are given as relative luciferase units (RLU) they represent the mean RLU ± SEM Values are calculated from three independent experiments carried out in triplicates. **(C)** For the western blot analysis c-Myb was detected using primary anti-hcM antibody (H141) and secondary antibody anti-rabbit-HRP, the loading control GAPDH was detected using primary antibody anti-GAPDH and secondary antibody anti-mouse-HRP. The arrow denotes c-Myb, the +1 arrow denotes the fraction of c-Myb proteins with one SUMO modification, while the +2 arrow denotes the fraction of c-Myb proteins that are SUMO conjugated at two sites. The dotted line corresponds to the level of c-Myb activity before SUMO mutant are loaded.

As seen in both reporter assays (figure 3.7 A and B), there is an observable difference on activational levels by c-Myb depending on whether it is SUMOylated by SUMO1 or SUMO2. Increasing levels of SUMO1 appears to lead to increased repression, while SUMO2 seems to be repressive in smaller doses. Upon increase of the dose this repression appears to weaken.

In the western blot (figure 3.7 C) SENP resistant SUMO mutants lead to a clear increase of c-Myb SUMOylation as expected (see arrows on figure 3.7 C). However, there is a significant difference in c-Myb levels when comparing the additions of hSUMO1-Q94P and hSUMO2-Q90P. While increasing levels of hSUMO1-Q94P appears to increase the total amount of c-Myb (summing up all bands), it appears that increasing levels of SENP resistant SUMO2 conjugation leads to a decreased total amount of c-Myb suggesting an increase of c-Myb degradation. This result seems counterintuitive compared to the functional measurements, in which c-Myb activity was less repressed by SUMO2 than by SUMO1. On the other hand, it is consistent with poly-SUMO2 being linked to degradation through the SUMO-targeted ubiquitin ligases (**STUbLs**) [83, 65]. It is also noteworthy that the correlation between levels of SUMOylation and activity is not a simple one. We know that reducing SUMO-levels from the wild type situation causes a major increase in activity. Here we see a major increase in levels of SUMOylation, but the further reduction in c-Myb activity is rather modest.

Subsequent luciferase assays with SUMO-QP mutants will be performed using 0.2µg pCIneo-hSUMO1-Q94P and pCIneo-hSUMO2-Q90P respectively.

3.2. Validation of the interaction between c-Myb and ATF7IP.

As there is a certain degree of false positives in using Y2H screenings, the first step in this study was to confirm or refute the proposed ATF7IP – c-Myb interaction. In order to achieve this, a number of GST-pulldown assays were performed. These pulldowns addressed whether ATF7IP and c-Myb in fact interact and the role of SUMO-SIM in this interaction. With the GST-pulldowns we also tried to explore whether we could confirm the SUMO2/3 preference of ATF7IP over SUMO1 reported by Sekiyama *et al*. [78] Additionally, we aimed to determine whether this reported SUMO preference would influence the binding affinity between ATF7IP and c-Myb depending on SUMO1 or SUMO2 conjugation of c-Myb.

3.2.1. Do c-Myb and ATF7IP interact, if so is this interaction SUMO dependent?

To validate the interaction between human c-Myb and ATF7IP, a GST-pulldown assay was performed in lysates of COS-1 cells transfected with plasmids encoding c-Myb in different formats. A GST-fused C-terminal region of ATF7IP was used (GST-ATF7IP-CTD). This C-terminal region spans amino acid residues 896 to 1270 of human ATF7IP. Contained within this region are both the SIM domain and Domain 2 of ATF7IP (see section 1.4.1).

Four different c-Myb protein variants were tested:

1. Wild-type c-Myb protein (3FG-hcM).
2. A mutant version of c-Myb (3FG-hcM-2KR), in which two lysine residues conjugatable by SUMO are mutated into arginine residues (see figure 1.3, section 1.3.3).
3. Two fusion constructs meant to increase the overall level of SUMOylation (3FG-hcM-Ubc9) or mimic fully SUMOylatedc-Myb (3fg-hcM-SUMO1).

As it is hypothesized that the ATF7IP interaction with c-Myb is either dependent on or enhanced by the SUMO conjugations on c-Myb, the deSUMOylation inhibitor NEM is added to the KAc interaction buffer. The results of the pulldown are shown in figure 3.8.

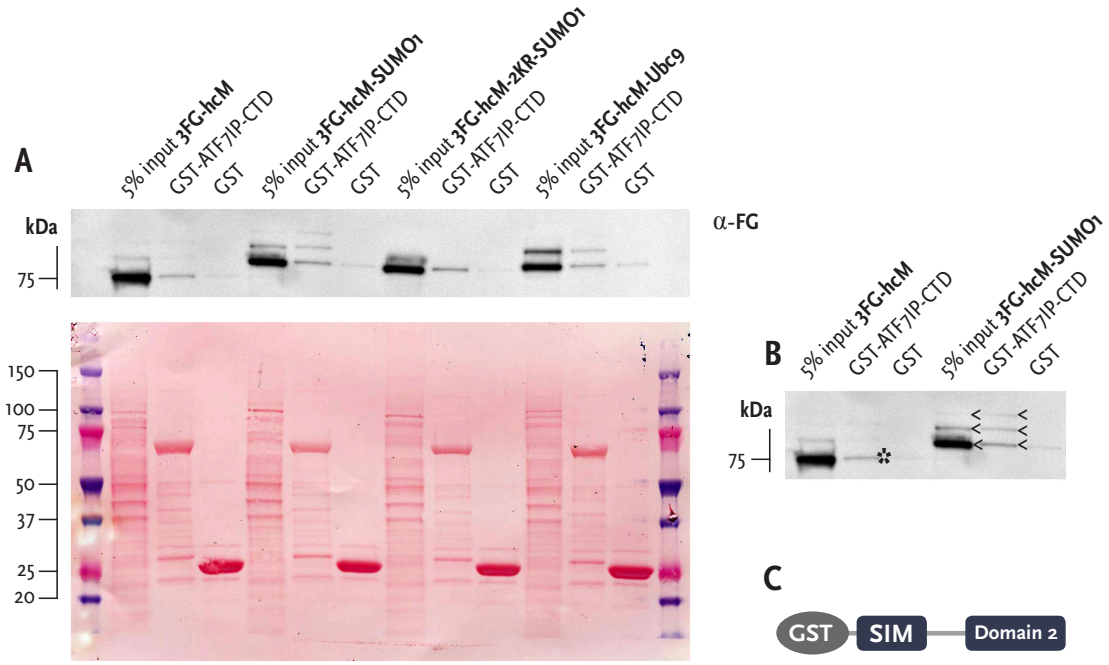

Figure 3.8 A - C: GST-pulldown using GST-ATF7IP-CTD with 3xFG-hcM, 3xFG-hcM-SUMO1, 3xFG-hcM-2KR-SUMO1 and 3xFG-hcM-Ubc9. (A) Four 15 cm plates containing $2.5x10^6$ COS-1 cells in 30 mL medium were seeded. 24 hours after seeding each plate was transfected using 12.5 μg plasmid DNA (pCIneoB-3FG-hcM, pCIneoB-3FG-hcM-SUMO1, pCIneoB-3FG-hcM-2KR-SUMO1 or pCIneoB-3FG-hcM-Ubc9). 24 hours after transfection, cells were harvested and lysed in NEM containing KAc interaction buffer. Pulldown was performed with 5 μL GST-ATF7IP-CTD from BL21(DE3)LysS cell lysate, 5 μL GST control (proteins expressed by Julie Emmert Olsen) and 300 μL COS-1 cell lysate. Samples were separated on a Criterion XT BisTris 4%-12% gel. After gel separation and blotting the membrane was incubated with primary anti-FLAG antibody and secondary anti-mouse-HRP antibody. The PVDF-membrane was subsequently dyed with Ponceau red. **(B)** Outtake from figure 3.8 A. The star indicates 3FLAG-tagged human c-Myb, without SUMO modifications. The arrow-heads point at the 3FLAG-tagged human c-Myb-SUMO1 input (5%) and how much of the total is retained by GST-ATF7IP-CTD. **(C)** Schematic illustration of GST-ATF7IP-CTD.

We observed a clear interaction between the unSUMOylated form of c-Myb (indicated by a star) and GST-ATF7IP-CTD, not observed with the GST control. When comparing the 5% input of the 3FG-hcM-SUMO1 lysate with the relative amounts of retained protein (indicated by arrows), one can see that the interaction intensifies as SUMOylation of c-Myb increases, suggesting a preference of the ATF7IP SIM for polySUMO over monoSUMO. Based on the pulldown assay (figure 3.8) we conclude that there is an interaction between ATF7IP and c-Myb and that this interaction becomes stronger in the presence of SUMO conjugated to c-Myb.

Additional information that can be drawn from this pulldown assay, is that SUMO modification resembles a positive feedback loop. This idea has been touched upon

previously in subsection 3.1.2.1 figure 3.1B where antibodies were tested on 3FG-hcM and 3FG-hcM-SUMO1 lysates. In figure 3.8 we observe that when comparing 3FG-hcM and its SUMOylation states with 3FG-hcM-SUMO1, the latter has more SUMO conjugated at its conjugation sites. As mentioned in subsection 3.1.2.1 this could be due to SUMO attracting the SUMOylation machinery, thereby leading to more efficient SUMOylation. When Ubc9 (a SUMO conjugase, E2 enzyme) is fused to c-Mybs C-terminal (3FG-hcM-Ubc9), SUMOylation is also increased, as would be expected.

Taken together these results suggest that c-Myb and ATF7IP do interact, that the interaction is enhanced by SUMO conjugated to c-Myb and that ATF7IP might favour polySUMO over monoSUMO modifications.

3.2.2. Does ATF7IP preferentially interact with SUMO1 or SUMO2-conjugated substrates.

To confirm previous reports stating that the SIM of ATF7IP preferentially interacts with SUMO2/3 over SUMO1 [78] and to test whether mutating the SIM domain of ATF7IP would destroy the reported interaction between ATF7IP and SUMO, we performed GST-pulldown assays in lysates of COS-1 cells transfected with plasmids encoding ATF7IP wild-type and the ATF7IP SIM mutant. The GST-fusion proteins used were: SUMO1, SUMO2 or 3xSUMO1 fused to GST (figure 3.9 A and B).

From the pulldown assay using full-length 3FG-ATF7IP lysate (figure 3.9 A), we observed a clear preference for binding of ATF7IP to SUMO2 over SUMO1 and polySUMO over monoSUMO. This polySUMO preference of ATF7IP corroborates results discussed in section 3.2.1. The full-length 3FG-ATF7IP-SIM-AADA was expected to have lost all SUMO-binding. However, the mutant proteins in the lysate exhibited stickiness, binding equally well to the GST control, GST-SUMO1, GST-3xSUMO1 and GST-SUMO2 (figure 3.9 B). The binding detected in the sample lanes was not more intense than the control. One can thus conclude that when the reported SIM domain of ATF7IP is mutated, the protein no longer interacts with either SUMO1 or SUMO2.

As there is an interaction between ATF7IP and unSUMOylated c-Myb, and as the interaction increases in direct correlation to increased SUMOylation levels of c-Myb, a GST-pulldown assay was designed to determine whether the interaction between ATF7IP and c-Myb differs depending on c-Myb being conjugated by SUMO1 or by SUMO2. To determine this a GST-pulldown assay was designed using the SENP resistant SUMO1 and SUMO2 mutants discussed in subsection 3.1.3.2. COS-1 cells were co-transfected with pCIneo-3FG-hcM, and either pCIneo-hSUMO1-Q94P or pCIneo-hSUMO2-Q90P, as well as with the SUMO ligase expressing pCMVB-T7-PIASy. The idea is that overexpression of either of the SENP resistant SUMO mutants in the cells would result in 3FG-hcM proteins mainly modified by SUMO1 or SUMO2. We used the GST-ATF7IP-CTD fusion protein from section 3.2.1 for the pulldown analysis in figure 3.9 C).

Comparing the 5% inputs of both lysates with the amount of modified c-Myb pulled down by the GST-fusion protein (figure 3.9 C), one clearly sees that the input of the SUMO1-modified c-Myb was much higher than that of the SUMO2-modified c-Myb, consistent with the stabilizing and destabilizing effect observed earlier (figure 3.9 A). Further comparing the input with the relative retention we conclude that SUMO2-modified c-Myb has a higher affinity for ATF7IP than SUMO1-modified c-Myb.

While speculative, it appears that c-Myb (figure 3.9 C) has modifications in addition to SUMOylations (3^{rd} and 4^{th} band over unmodified c-Myb). The interaction levels weaken with these extra modifications. Based on this assay, it is not possible to determine which of the c-Myb modifications discussed in (section 1.2.2) are the ones seen in this western blot. We know from other studies in the lab that SUMOylation of c-Myb facilitates additional phosphorylation leading to slower migrating bands (Matre *et al*., manuscript submitted).

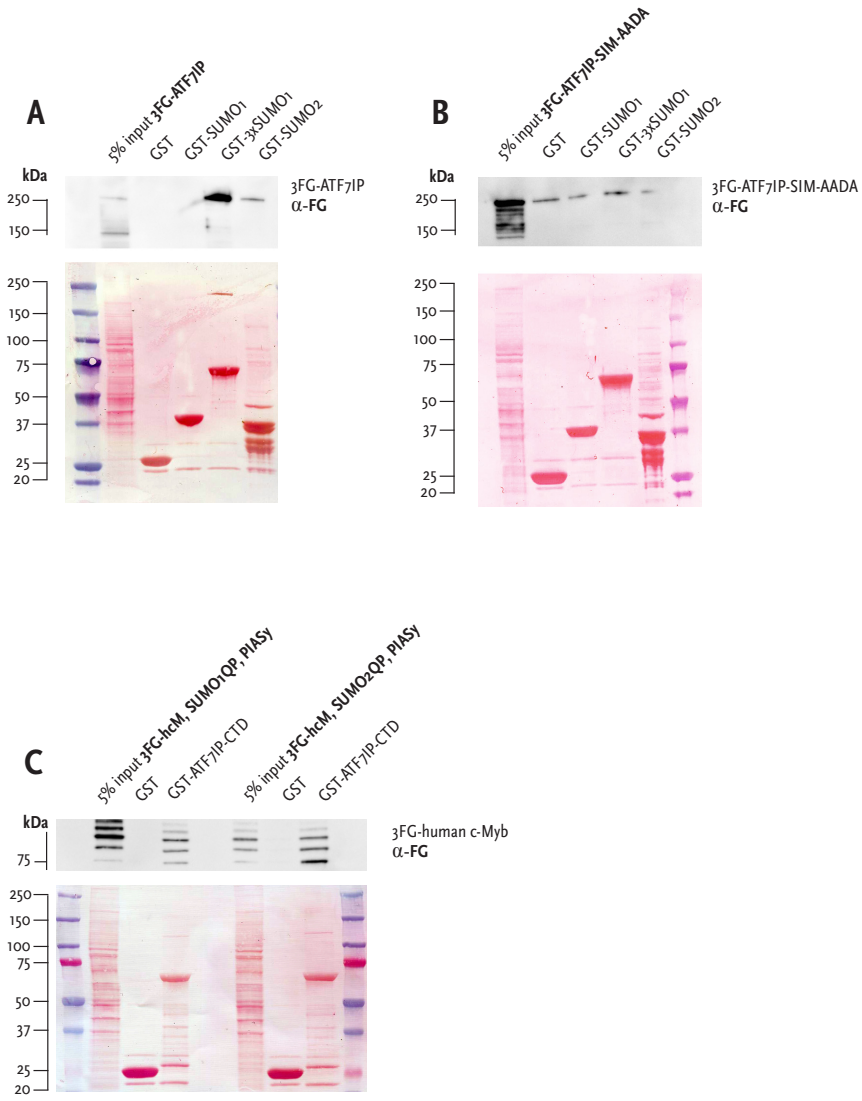

Figure 3.9: A and B) GST-pulldown using GST fused to SUMO1, 3xSUMO1 and SUMO2 with (A) 3FG-ATF7IP and (B) 3FG-ATF7IP-SIM-AADA. Four 15 cm plates containing $2.5x10^6$ COS-1 cells in 30 mL medium each were seeded. After 24 hours each plate was transfected using 12.5 µg plasmid DNA (pCIneo-3FG-ATF7IP or pCIneo-3FG-ATF7IP-SIM-AADA). 24 hours after transfection, cells were harvested and lysed in KAc interaction buffer. Pulldown was performed with 5 µL GST control, 10 µL GST-SUMO1, 20 µL GST-3xSUMO1, 20 µL GST-SUMO2 and 300 µL COS-1 cell lysate. Samples separated on a Criterion XT BisTris 4%-12% gel. After gel separation and blotting the membrane was incubated with primary anti-FLAG antibody and secondary anti-mouse-HRP antibody. The PVDF-membrane was dyed using Ponceau red. **(C) GST-pulldown using GST-ATF7IP-CTD with c-Myb conjugated by SUMO1 and c-Myb conjugated by SUMO2** Four 15 cm plates containing $2.5x10^6$ COS-1 cells in 30 mL medium each were seeded. 24 hours after seeding each plate was transfected using 11.25 µg plasmid DNA (5 µg pCIneo-3FG-hcM, 5 µg of either pCIneo-hSUMO1-Q94P or pCIneo-hSUMO2-Q90P and 1.25 µg pCMVB-T7-PIASy). 24 hours after transfection, cells were harvested and lysed in KAc interaction buffer. Pulldown was performed with 5 µL GST-ATF7IP-CTD, 5 µL GST control and 300 µL COS-1 cell lysate. Samples were separated on a Criterion XT BisTris 4%-12% gel. After gel separation and blotting the membrane was incubated with primary anti-FLAG antibody and secondary anti-mouse-HRP antibody. The PVDF-membrane was dyed using Ponceau red.

3.3. What are the functional implications of the c-Myb – ATF7IP interaction? Is there a functional difference between ATF7IP wild-type and an ATF7IP SIM mutant?

To address the implications of the interaction between c-Myb and ATF7IP, a number of different functional assays were designed. As c-Myb has been shown to be involved in chromatin dependent regulation [55] and as ATF7IP has strong links to both the epigenetic "reader" MBD1 and "writer" SETDB1 [35, 86], the choice of assay system becomes very important. We used both a luciferase reporter driven by a natural Myb responsive promoter in transient transfections and a synthetic, stably integrated luciferase gene reporter. Using these two different assays we hoped to gain insight into possible chromatin specific contributions.

3.3.1. Luciferase Assays in CV-1 cells using transiently transfected reporters

Our initial hypothesis was that the interaction between ATF7IP and c-Myb would lead to a repression of c-Myb target genes. A repression we thought would be alleviated using the ATF7IP SIM mutant.

To monitor the assumed repression, we transiently transfected CV-1 cells with the reporter plasmid where the luciferase gene is driven by the natural Myb responsive MYADM promoter (pGL3-MYADM) and plasmids encoding either the c-Myb or the c-Myb-2KR effector, ATF7IP (both wild type and mutant) and p300. Three different luciferase reporter gene assay co-transfection set-ups were designed. The results are shown in figure 3.10. No repression was observed.

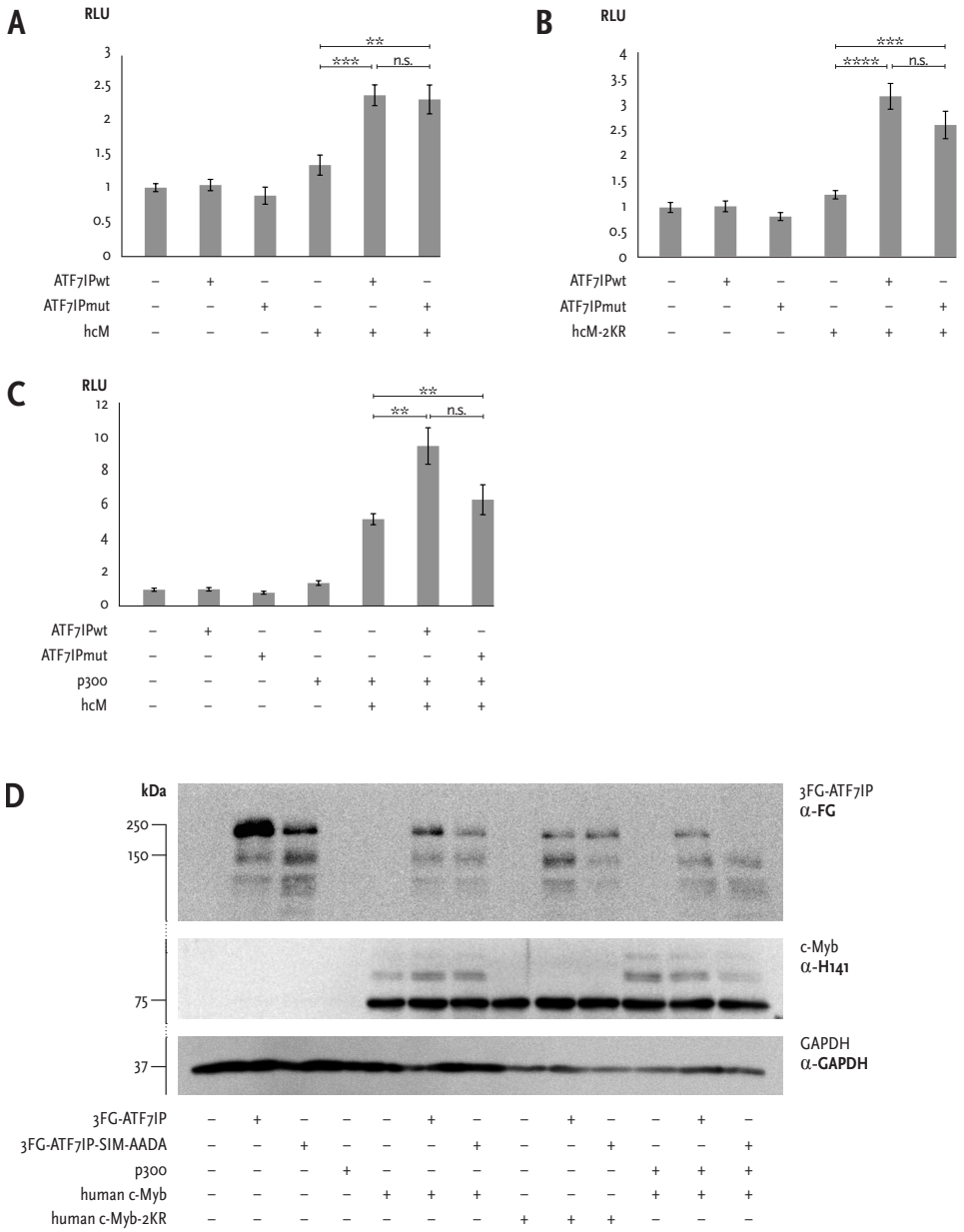

Figure 3.10 (A-D): Initial transiently transfected natural reporter assay testing the effects of ATF7IP and ATF7IP-SIM-AADA on c-Myb target gene activity. CV-1 cells were seeded into 24 well dishes ($0.2x10^5$ cells/well in 0.5 mL medium per well). After 24 hours cells were transfected with 0.8 μg plasmid DNA per well, using 0.2 μg pGL3-MYADM reporter (designed and constructed by P.I. Lorenzo). Experiments **A, B and C** are additionally transfected with: **(A)** 0.2 μg pCIneo-hcM-HA , 0.2 μg pCIneo-3FG-ATF7IP or 0.2 μg pCIneo-ATF7IP-SIM-AADA. **(B)** 0.2 μg pCIneo-hcM-HA-2KR, 0.2 μg pCIneo-3FG-ATF7IP or 0.2 μg pCIneo-ATF7IP-SIM-AADA. **(C)** 0.2μg pCIneo-hcM-HA , 0.2 μg pCIneo-3FG-ATF7IP or 0.2 μg pCIneo-ATF7IP-SIM-AADA and 0.2 μg pCneo-p300-myc. p300 is a well documented c-Myb co-activator. After 24 hours cells were lysed with passive lysis buffer for luciferase assay and in 3xSDS GLB for western blot analysis. Values are given as relative luciferase units (RLU) they represent the mean RLU ± SEM. The background is = 1 RLU. Values are calculated from three independent experiments carried out in triplicates. Statistical analysis is performed using the two-sided, unpaired Student's t-test with Welch correction. **p<0.01, ***p<0.001, ****p<0.0001. **(D)** For the western blot analysis ATF7IP was detected using primary anti-FLAG antibody and secondary anti-mouse-HRP, c-Myb was detected using primary anti-hcM antibody (H141) and secondary antibody anti-rabbit-HRP. The loading control GAPDH was detected using primary antibody anti-GAPDH and secondary antibody anti-mouse-HRP.

From the variations of the luciferase assay, testing c-Myb dependent reporter gene activation and how ATF7IP might modulate this activation (figure 3.10 A, B and C), we conclude that ectopic expression of ATF7IP leads to a significant increase in c-Myb dependent activation. The ATF7IP SIM mutant also leads to an increase in activation, albeit slightly less than ATF7IP. ATF7IP by itself had no significant effect on the reporter assay.

From the western blot (figure 3.10 D), we can confirm that ATF7IP was expressed in the cells transfected with the plasmids encoding ATF7IP wild-type and mutant. The same can be said about the expression and detection of c-Myb and c-Myb-2KR. Based on the loading control (GAPDH), we deduce that there was a relatively even cell number present in the different samples.

We conclude that this type of transient transfection assay does not support our hypothesis of ATF7IP-induced repression. On the contrary, these first reported assays indicated that ATF7IP might rather stimulate c-Myb dependent gene activation.

3.3.2. Luciferase Assays in HEK293-c1 cells containing a stably integrated reporter

As the reported repressive effect of ATF7IP is believed to be mediated through the epigenetic writer SETDB1, we decided to run a comparable assay using the HEK293-c1 system. As described in section 2.3.3 and discussed in 4.2.1, in this assay the reporter is integrated in the genome and does not need to be transfected. As a consequence, the reporter is fully chromatinized and hence should be more sensitive to epigenetic processes. The effectors (c-Myb and c-Myb-2KR) have their own DNA-binding domains replaced with that of Gal4.

Figure 3.11 shows four different variants of this assay, as well as a supporting western blot.

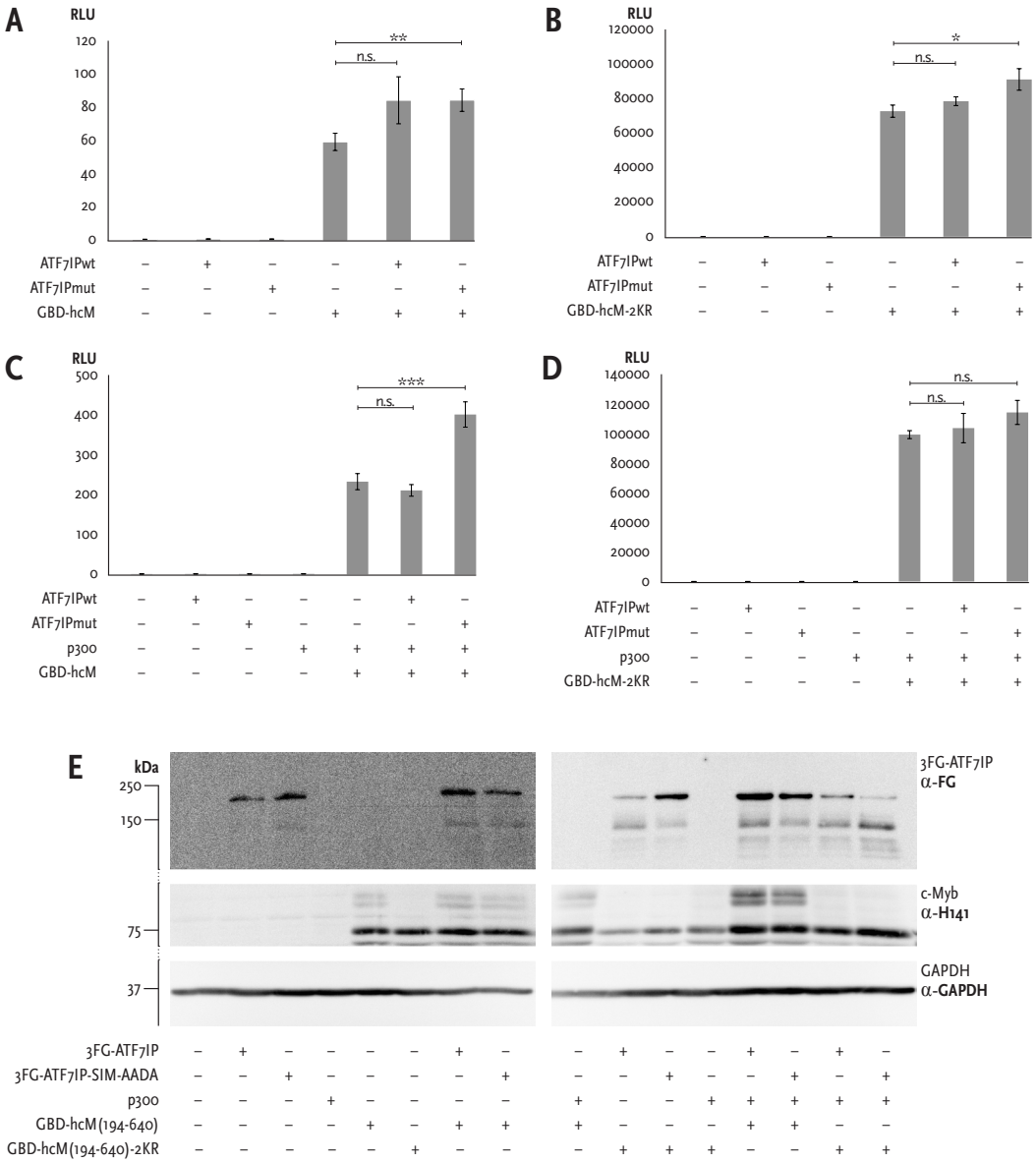

Figure 3.11 A-E: Initial stably integrated synthetic reporter assay testing the effects of ATF7IP and ATF7IP-SIM-AADA on c-Myb target gene activity. HEK293-c1 cells were seeded into 24 well dishes ($0.34x10^5$ cells/well in 0.5 mL medium per well). After 24h cells were transfected with 0.4 μg plasmid DNA per well. Experiments **A, B, C and D** were transfected with: **(A)** 0.1 μg pCIneoB-GBD-hcM(194-640) , 0.1 μg pCIneo-3FG-ATF7IP or 0.1 μg pCIneo-ATF7IP-SIM-AADA. **(B)** 0.1 μg pCIneoB-GBD-hcM(194-640)-2KR, 0.1 μg pCIneo-3FG-ATF7IP or 0.1 μg pCIneo-ATF7IP-SIM-AADA **(C)** 0.1 μg pCIneoB-GBD-hcM(194-640) , 0.1 μg pCIneo-3FG-ATF7IP or 0.1 μg pCIneo-ATF7IP-SIM-AADA and 0.1 μg pCneo-p300-myc. **(D)** 0.1 μg pCIneoB-GBD-hcM(194-640)-2KR, 0.1 μg pCIneo-3FG-ATF7IP or 0.1 μg pCIneo-ATF7IP-SIM-AADA and 0.1 μg pCneo-p300-myc. p300 is a well described c-Myb co-activator. After 24 hours cells were lysed with passive lysis buffer for luciferase assay and in 3xSDS GLB for western blot analysis. Values are given as relative luciferase units (RLU) they represent the mean RLU ± SEM, were the background is = 1 RLU. Values are calculated from three independent experiments carried out in triplicates. Statistical analysis is performed using the two-sided, unpaired Student's t-test with Welch correction. *$p<0.05$, **$p<0.01$, ***$p<0.001$. **(E)** For the western blot analysis ATF7IP was detected using primary anti-FLAG antibody and secondary anti-mouse-HRP, c-Myb was detected using primary anti-hcM antibody (H141) and secondary antibody anti-rabbit-HRP. The loading control GAPDH was detected using primary antibody anti-GAPDH and secondary antibody anti-mouse-HRP.

Again, no repression was observed. Adding wild-type ATF7IP leads in three cases to a small increase, but these changes are not statistically significant. In three of the four cases a significant increase in expression is observed upon ATF7IP-SIM-AADA addition (figures 3.11 A, B and C). From the western blot (figure 3.11 E) we conclude that the indicated proteins are expressed. Based on the GAPDH loading control an even cell number was present in the different samples.

When comparing the results between the experiments were c-Myb is used as an effector (figures 3.11 A and C) and those were c-Myb-2KR is used (figures 3.11 B and D), one can see that some of the ATF7IP-SIM-AADA effect is lost using the SUMO deficient c-Myb proteins.

Comparing the transiently transfected and stably integrated reporter assays it appears that c-Myb dependent transcription is activated by ATF7IP in the transient system (figure 3.10) and unchanged in the stable reporter system (figure 3.11). However, when using the SIM mutant ATF7IP in the stable system, an increase in transcription is observed. Could it be that ectopic ATF7IP-SIM-AADA sequesters other downstream interaction partners needed in a functioning repression complex, thereby relieving some of the hypothesized repressive effect endogenous ATF7IP would otherwise impart?

3.4. Does an increase in the SUMOylation level of c-Myb increase the functional effects of the c-Myb - ATF7IP interaction?

As the initial functional assays conducted did not result in very clear activation or repression (sections 3.3.1 and 3.3.2), we considered that this subdued functional effect might be due to the low level of c-Myb SUMOylation. As mentioned in section 1.3.2 only a small fraction of proteins in a protein pool are SUMOylated at any given time. To deal with this perceived low-level problem, we decided to design a luciferase assay using the SENP resistant SUMO1 and SUMO2 mutants discussed in subsection 3.1.3.2. The idea was that if the interaction between ATF7IP and c-Myb is significantly stabilized and increased by SUMO modification of c-Myb, then using an assay in which a larger fraction of the c-Myb protein pool is SUMOylated, might lead to a more pronounced change of c-Myb dependent transcriptional activity.

We transiently transfected CV-1 cells with the synthetic pGL4x5MRE reporter and plasmids encoding the c-Myb effector, ATF7IP, the PIASy E3 ligase and either the SUMO1 or the SUMO2 mutant. The results from this luciferase assay and the accompanying western blot are shown in figure 3.12.

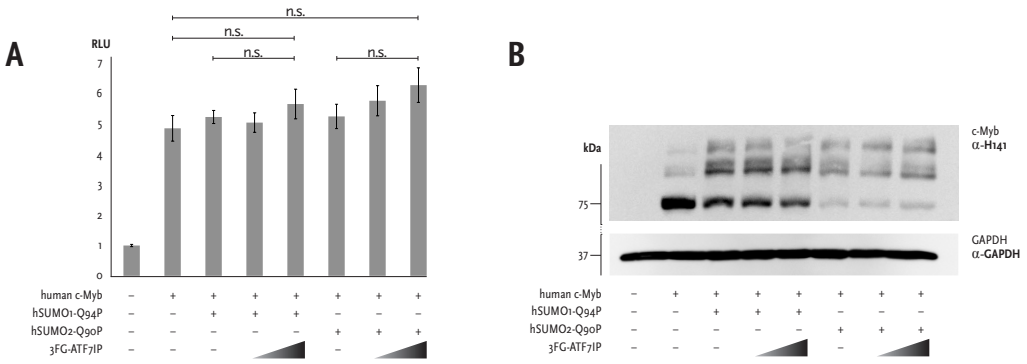

Figure 3.12 A and B: Transiently transfected synthetic reporter assay testing the effect of ATF7IP on c-Myb target gene activity. CV-1 cells were seeded into 24 well dishes ($0.2x10^5$ cells/well in 0.5 mL medium per well). After 24 h cells were transfected with 0.75 μg plasmid DNA per well. Using 0.1 μg pGL4x-5xMRE(GG)-myc as reporter, 0.2 μg pCIneo-hcM-HA as effector, 0.05 μg pCMVB-T7-PIASy, 0.2 μg of either pCIneo-hSUMO1-Q94P or pCIneo-hSUMO2-Q90P with increasing amounts of pCIneo-3FG-ATF7IP (0.1 μg or 0.2 μg). After 24 hours cells were lysed with passive lysis buffer for luciferase assay and in 3xSDS GLB for western blot analysis. Values are given as relative luciferase units (RLU) they represent the mean RLU ± SEM, were the background is = 1 RLU. Values are calculated from four independent experiments carried out in triplicates. Statistical analysis is performed using the two-sided, unpaired Student's t-test with Welch correction. **(B)** For the western blot analysis c-Myb was detected using primary anti-hcM antibody (H141) and secondary antibody anti-rabbit-HRP. The loading control GAPDH was detected using primary antibody anti-GAPDH and secondary antibody anti-mouse-HRP.

The results from the luciferase assay (figure 3.12 A) show that there is no significant change in c-Myb dependent reporter activation. This indicates that increasing the SUMOylation level of c-Myb does not enhance the functional effects of the c-Myb – ATF7IP interaction.

This result is especially surprising when considering the western blot analysis run parallel to the luciferase assay (figure 3.12 B). From the blot we can see that there is a major change in steady state of c-Myb, depending on whether it is SUMOylated by SUMO1 or SUMO2. This verifies the western blot results from the hSUMO1-Q94P and hSUMO2-Q90P dosage response trial in subsection 3.1.3.2 (figure 3.7 C). While also reinforcing that the correlation between c-Myb steady state levels and reporter activation is far from simple.

Both samples, the ones with SENP resistant SUMO1 and those with SENP resistant SUMO2, exhibited an increase in SUMOylated c-Myb forms. Yet, as seen in the last three lanes (containing the SUMO2 mutant – figure 3.12 B), much less c-Myb was present. Modification of c-Myb by SUMO2 seems to lead to degradation, while not affecting c-Myb dependent transcription levels negatively.

3.5. Does co-transfection with known ATF7IP interactants SETDB1 and MBD1 increase the functional effects of the c-Myb – ATF7IP interaction?

One of the starting hypotheses was that SUMOylated c-Myb would recruit ATF7IP, which in turn would recruit SETDB1, thereby leading to the formation of facultative heterochromatin and the silencing of c-Myb target genes (section 1.4.4). Perhaps the functional effects observed so far have been so small due to the lack of important interactants? We therefore asked whether ectopic expression of the reported ATF7IP interactant SETDB1 alter or increase the observed functional effects (sections 3.3.1 and 3.3.2) of ATF7IP on c-Myb dependent transcription?

In the literature ATF7IP mediated repression has been linked to both SETDB1 and MBD1 [35, 86], we therefore decided to also include MBD1 in the investigation.

Since both of these interactants are linked to chromatin - we decided to continue our functional assays using both a synthetic transiently transfected reporter (section 3.5.1) and a synthetic stably integrated luciferase gene reporter system (section 3.5.2), hoping that using these two different assays would give an insight into the chromatin specific contributions.

3.5.1. Luciferase Assays in CV-1 cells using a transiently transfected reporter

To test the importance of the ATF7IP partners with a transiently transfected reporter, we transfected CV-1 cells with the synthetic pGL4x5MRE reporter plasmid and plasmids encoding the c-Myb effector, ATF7IP and SETDB1. The results of the luciferase assays and the western blot analysis are seen in figures 3.13 and 3.14.

Based on the luciferase measurements (figures 3.13 A) we detect a small decrease of c-Myb dependent transcription when ATF7IP is co-transfected with c-Myb, yet based on statistical analysis this change is insignificant. When both ATF7IP and SETDB1 were co-transfected with c-Myb, no ATF7IP-SETDB1 repression of c-Myb target genes was detected (figure 3.13 A). In contrary, the larger amount of ectopic SETDB1 leads to an increase in c-Myb dependent transcription in this system.

We performed the same assay, but with ectopic expression of MBD1 instead of SETDB1 (figure 3.14). Here a significant fold change was observed (figure 3.14 A). While ATF7IP alone did not alter c-Myb dependent luciferase levels, the combination of MBD1 and ATF7IP leads to a marked increase of c-Myb dependent transcription (figure 3.14 A). Based on the western blots (figures 3.13 B and 3.14 B), there are no significant changes in c-Myb levels, suggesting that MBD1 induces a real activation of c-Myb in this model system.

We conclude that c-Myb dependent luciferase levels are not influenced much by the addition of SETDB1 to the assay. MBD1 however, leads to a significant increase in c-Myb reporter genes.

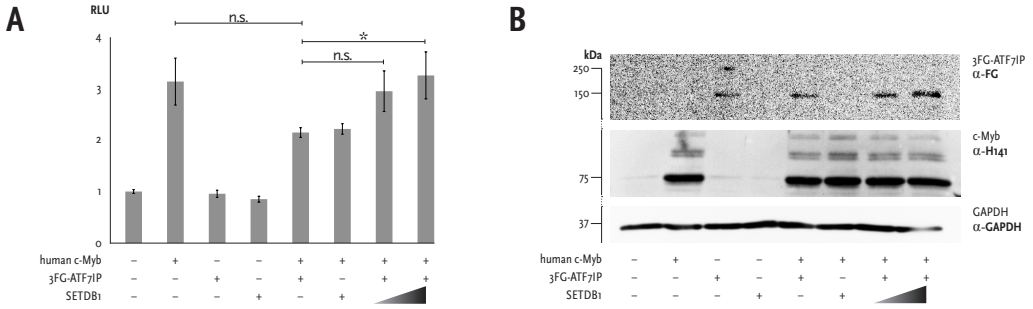

Figure 3.13 A and B: Transiently transfected synthetic reporter assay testing the effect of SETDB1 and ATF7IP on c-Myb target gene activity. CV-1 cells were seeded into 24 well dishes ($0.2x10^5$ cells/well in 0.5 mL medium per well). After 24 h cells were transfected with 0.8 µg plasmid DNA per well. Using 0.1 µg pGL4x-5xMRE(GG)-myc as reporter, 0.2 µg pCIneo-hcM-HA as effector, 0.2 µg pCIneo-3FG-ATF7IP and increasing amounts of pCIneo-SETDB1 (0.2 µg or 0.3 µg). After 24 hours cells were lysed with passive lysis buffer for luciferase assay and in 3xSDS GLB for western blot analysis. Values are given as relative luciferase units (RLU) they represent the mean RLU ± SEM, were the background is = 1 RLU. Values are calculated from three independent experiments carried out in triplicates. Statistical analysis is performed using the two-sided, unpaired Student's t-test with Welch correction. *p<0.05. **(B)** For the western blot analysis ATF7IP was detected using primary anti-FLAG antibody and secondary anti-mouse-HRP, c-Myb was detected using primary anti-hcM antibody (H141) and secondary antibody anti-rabbit-HRP. The loading control GAPDH was detected using primary antibody anti-GAPDH and secondary antibody anti-mouse-HRP.

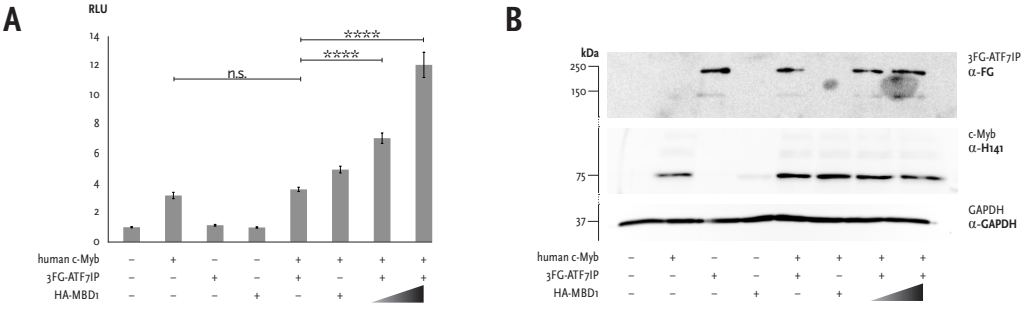

Figure 3.14 A and B: Transiently transfected synthetic reporter assay testing the effect of MBD1 and ATF7IP on c-Myb target gene activity. CV-1 cells were seeded into 24 well dishes ($0.2x10^5$ cells/well in 0.5 mL medium per well). After 24 h cells were transfected with 0.8 µg plasmid DNA per well. Using 0.1 µg pGL4x-5xMRE(GG)-myc as reporter, 0.2 µg pCIneo-hcM-HA as effector, 0.2 µg pCIneo-3FG-ATF7IP and increasing amounts of pCIneo-HA-MBD1 (0.2 µg or 0.3 µg). After 24 hours cells were lysed with passive lysis buffer for luciferase assay and in 3xSDS GLB for western blot analysis. Values are given as relative luciferase units (RLU) they represent the mean RLU ± SEM, were the background is = 1 RLU. Values are calculated from three independent experiments carried out in triplicates. Statistical analysis is performed using the two-sided, unpaired Student's t-test with Welch correction. ****p<0.0001. **(B)** For the western blot analysis ATF7IP was detected using primary anti-FLAG antibody and secondary anti-mouse-HRP, c-Myb was detected using primary anti-hcM antibody (H141) and secondary antibody anti-rabbit-HRP. The loading control GAPDH was detected using primary antibody anti-GAPDH and secondary antibody anti-mouse-HRP.

3.5.2. Luciferase Assays in HEK293-c1 cells containing a stably integrated reporter

To test the importance of the ATF7IP partners with a chromatinized reporter, we repeated the assays carried out in section 3.5.1 using the HEK293-c1 cell line. The experiments were set up similar to the parallel transient assay. Though, as the reporter is integrated in the genome, it does not need to be transfected and the c-Myb effector has a GBD instead of a DBD (figures 3.15 and 3.16). An additional test we performed in this system was aimed at exploring the effects on c-Myb dependent transcription when combining ATF7IP, MBD1 and SETDB1 (figure 3.17).

The results of the luciferase assays and the accompanying western blot analysis are shown in figures 3.15, 3.16 and 3.17.

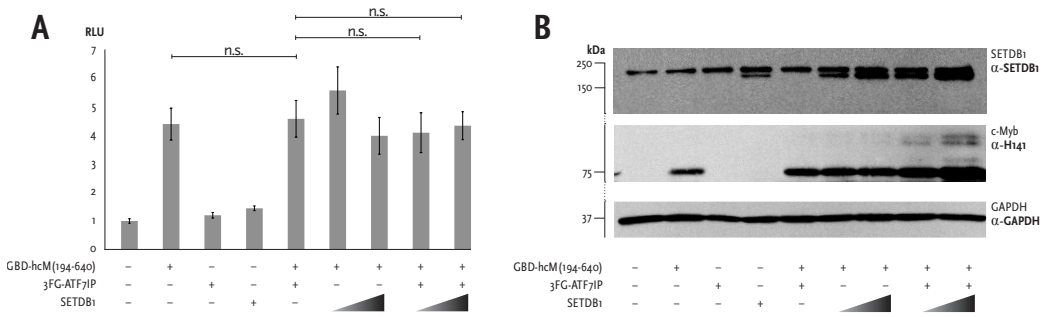

Figure 3.15 A and B: Stably integrated synthetic reporter assay testing the effect of SETDB1 and ATF7IP on c-Myb target gene activity. HEK293-c1 cells were seeded into 24 well dishes ($0.34x10^5$ cells/well in 0.5 mL medium per well). After 24h cells were transfected with 0.8 μg plasmid DNA per well. Using 0.2 μg pCIneoB-GBD-hcM(194-640), 0.2 μg pCIneo-3FG-ATF7IP and increasing amounts of pCIneo-SETDB1 (0.2 μg or 0.3 μg). After 24 hours cells were lysed with passive lysis buffer for luciferase assay and in 3xSDS GLB for western blot analysis. Values are given as relative luciferase units (RLU) they represent the mean RLU ± SEM, were the background is = 1 RLU. Values are calculated from three independent experiments carried out in triplicates. Statistical analysis is performed using the two-sided, unpaired Student's t-test with Welch correction. **(B)** For the western blot analysis SETDB1 was detected using primary anti-SETDB1 antibody and secondary anti-rabbit-HRP, c-Myb was detected using primary anti-hcM antibody (H141) and secondary antibody anti-rabbit-HRP. The loading control GAPDH was detected using primary antibody anti-GAPDH and secondary antibody anti-mouse-HRP.

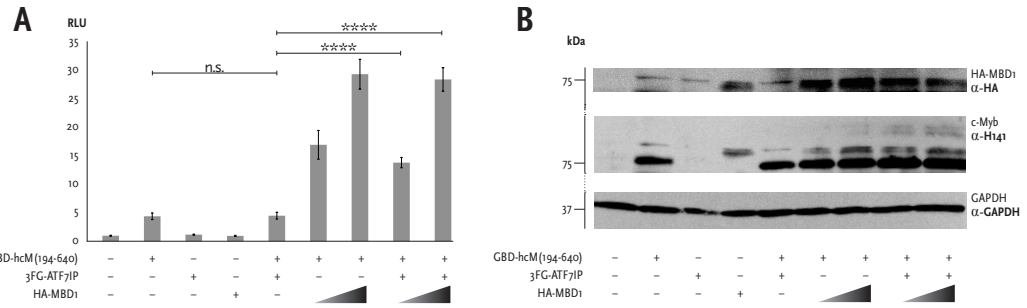

Figure 3.16 A and B: Stably integrated synthetic reporter assay testing the effect of MBD1 and ATF7IP on c-Myb target gene activity. HEK293-c1 cells were seeded into 24 well dishes ($0.34x10^5$ cells/well in 0.5 mL medium per well). After 24h cells were transfected with 0.8 µg plasmid DNA per well. Using 0.2 µg pCIneoB-GBD-hcM(194-640), 0.2 µg pCIneo-3FG-ATF7IP and increasing amounts of pCIneo-HA-MBD1 (0.2 µg or 0.3 µg). After 24 hours cells were lysed with passive lysis buffer for luciferase assay and in 3xSDS GLB for western blot analysis. Values are given as relative luciferase units (RLU) they represent the mean RLU ± SEM, were the background is = 1 RLU. Values are calculated from three independent experiments carried out in triplicates. Statistical analysis is performed using the two-sided, unpaired Student's t-test with Welch correction, (***$p<0.001$, ****$p<0.0001$). **(B)** For the western blot analysis MBD1 was detected using primary anti-HA antibody and secondary anti-rabbit-HRP, c-Myb was detected using primary anti-hcM antibody (H141) and secondary antibody anti-rabbit-HRP. The loading control GAPDH was detected using primary antibody anti-GAPDH and secondary antibody anti-mouse-HRP.

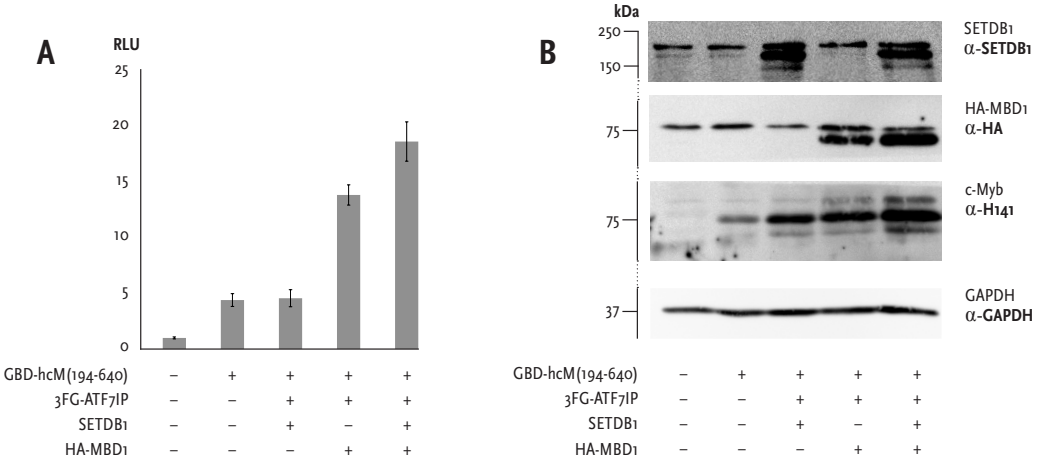

Figure 3.17 A and B: Stably integrated synthetic reporter assay testing the effect of SETDB1, MBD1 and ATF7IP on c-Myb target gene activity. HEK293-c1 cells were seeded into 24 well dishes ($0.34x10^5$ cells/well in 0.5 mL medium per well). After 24 h cells were transfected with 0.8 µg plasmid DNA per well. Using 0.2 µg pCIneoB-GBD-hcM(194-640), 0.2 µg pCIneo-3FG-ATF7IP, 0.2 µg pCIneo-SETDB1 and 0.2 µg pCIneo-HA-MBD1. After 24 hours cells were lysed with passive lysis buffer for luciferase assay and in 3xSDS GLB for western blot analysis. Values are given as relative luciferase units (RLU) they represent the mean RLU ± SEM, were the background is = 1 RLU. Values are calculated from three independent experiments carried out in triplicates. **(B)** For the western blot analysis SETDB1 was detected using primary anti-SETDB1 antibody and secondary anti-rabbit-HRP. MBD1 was detected using primary anti-HA antibody and secondary anti-rabbit-HRP. c-Myb was detected using primary anti-hcM antibody (H141) and secondary antibody anti-rabbit-HRP. The loading control GAPDH was detected using primary antibody anti-GAPDH and secondary antibody anti-mouse-HRP.

As shown in figure 3.15, ectopic expression of SETDB1 had no effect on c-Myb dependent expression in this fully chromatinized assay (figure 3.15 A), neither by itself nor in combination with ATF7IP. Overall the activational changes in this model system, as in the transient assay (figure 3.13) are negligible.

As before, the experiment was repeated using MBD1 instead of SETDB1. Combining c-Myb with MBD1 lead to a marked increase of c-Myb specific reporter activation (figure 3.16 A). This is the same trend as in the transient reporter assay (figure 3.14). However, this MBD1 dependent activation of c-Myb target genes, appears to be ATF7IP independent. The relative activational levels seem to be identical - with or without ATF7IP (figure 3.16 A).

Something we had not tested before was whether repression required the entire MBD1-ATF7IP-SETDB1 complex reported for repression by other groups [35, 86]. To determine whether ATF7IP can function as a c-Myb co-repressor in this reported complex, we carried out a luciferase assay combining c-Myb, ATF7IP, MBD1 and SETDB1. The results (figure 3.17) show that combining c-Myb with SETDB1 and ATF7IP lead to no significant change in transactivation levels. Upon adding MBD1 however, transactivation levels of c-Myb dependent reporter activation increased manifold (figure 3.17 A).

Considering these functional assays (sections 3.5.1 and 3.5.2) collectively, it appears that c-Myb dependent reporter activation is not influenced much by adding SETDB1 to the assay (figures 3.13, 3.15 and 3.17). When including MBD1 however, the transcription levels of c-Myb reporter genes increased significantly (figures 3.14, 3.16 and 3.17). This observed MBD1 co-activation of c-Myb targets is neither ATF7IP (figures 3.16 and 3.17), nor chromatin dependent (figures 3.14 and 3.16). From the western blot analysis (figures 3.15 B, 3.16 B and 3.17 B), we conclude that MBD1 has a stabilizing effect on c-Myb in the HEK293-c1 lysates, this effect is not observed in the CV-1 lysates (figures 3.13 B and 3.14 B).

3.6. Is the observed MBD1 effect c-Myb specific?

Having found that the ATF7IP partner MBD1 causes a significant activation in the c-Myb reporter assays, we asked whether this effect was c-Myb specific. One might expect MBD1 to have a rather general effect on chromatin-dependent processes. We therefore decided to test a non-related transcriptional activator in the same system.

VP16 is a herpes simplex virus trans-acting protein, known for its strong transactivation domain [14, 90]. VP16 was also selected because it contains no SUMO-conjugation sites. We decided to apply the VP16 transactivation domain fused to the same Gal4 DNA-binding domain (GBD) used in our GBD-hcM(194-640) constructs to determine whether the observed MBD1 effect (figure 3.16 A) is c-Myb specific or not. If the effect is c-Myb specific it will not be observed when using the GBD-VP16 fusion. For this experiment the HEK293-c1 cells were transfected with plasmids expressing VP16, MBD1 and ATF7IP. The results of the luciferase assay and the accompanying western blot analysis are shown in figure 3.18.

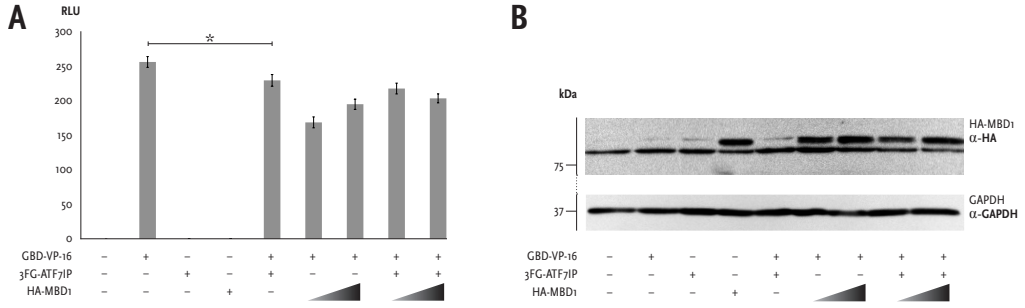

Figure 3.18 A and B: Stably integrated synthetic reporter assay testing the effect of MBD1 and ATF7IP on VP-16 target gene activity. HEK293-c1 cells were seeded into 24 well dishes ($0.34x10^5$ cells/well in 0.5 mL medium per well). After 24 h cells were transfected with 0.6 μg plasmid DNA per well. Using 0.1 μg pCIneoB-GBD-VP16, 0.2 μg pCIneo-3FG-ATF7IP and either 0.2 μg or 0.3 μg pCIneo-HA-MBD1. After 24 hours cells were lysed with passive lysis buffer for luciferase assay and in 3xSDS GLB for western blot analysis. Values are given as relative luciferase units (RLU) they represent the mean RLU ± SEM, were the background is = 1 RLU. Values are calculated from three independent experiments carried out in triplicates. Statistical analysis is performed using the two-sided, unpaired Student's t-test with Welch correction. *$p<0.05$ **(B)** For the western blot analysis MBD1 was detected using primary anti-HA antibody and secondary anti-rabbit-HRP. The loading control GAPDH was detected using primary antibody anti-GAPDH and secondary antibody anti-mouse-HRP. We have no functioning anti-GBD or anti-VP16 primary antibody at our disposal.

From the resulting luciferase measurements (figure 3.18 A) we see that MBD1 accompanied by ATF7IP does not lead to activation. It rather appears as if both ATF7IP and MBD1 lead to a slight repression of GBD-VP16 dependent reporter activation (figure 3.18 A). Based on these results, we conclude that the observed MBD1 effect on transcriptional activation is c-Myb dependent.

3.7. Is the observed activational effect of MBD1 on c-Myb regulated transcription SUMO dependent?

As we have determined that the activational effect of MBD1 is c-Myb specific (subchapter 3.6), yet does not depend on ATF7IP (subchapter 3.5), we decided to investigate whether this transcriptional regulation is SUMO dependent. To test this the SUMO-binding deficient 2KR mutant of GBD-hcM(194-640) is used.

We transfected HEK293-c1 cells with plasmids expressing this SUMOylation deficient c-Myb mutant and MBD1. The results of the luciferase assay and the western blot analysis are shown in figure 3.19.

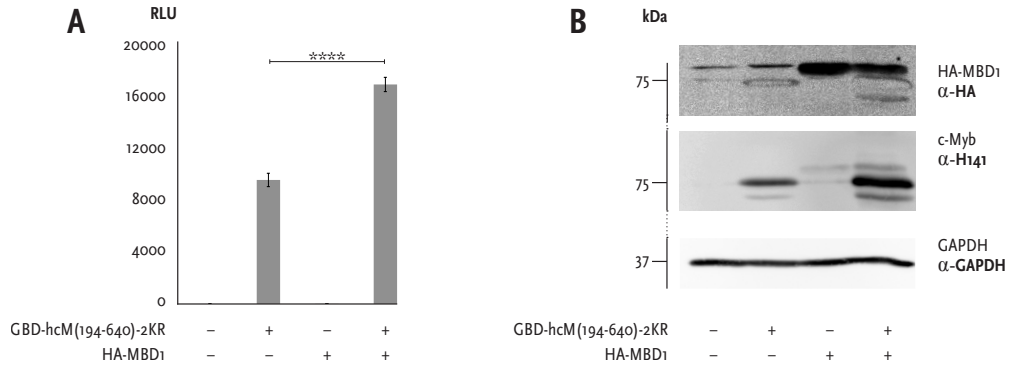

Figure 3.19 A and B: Stably integrated synthetic reporter assay testing the effect of MBD1 and ATF7IP on c-Myb-2KR target gene activity. HEK293-c1 cells were seeded into 24 well dishes ($0.34x10^5$ cells/well in 0.5 mL medium per well). After 24 h cells were transfected with 0.4 μg plasmid DNA per well. Using 0.2 μg pCIneo-GBD-hcM(194-640)2KR and 0.2 μg pCIneo-HA-MBD1. After 24 hours cells were lysed with passive lysis buffer for luciferase assay and in 3xSDS GLB for western blot analysis. Values are given as relative luciferase units (RLU) they represent the mean RLU ± SEM, were the background is = 1 RLU. Values are calculated from three independent experiments carried out in triplicates. Statistical analysis is performed using the two-sided, unpaired Student's t-test with Welch correction, (****$p<0.0001$). **(B)** For the western blot analysis MBD1 was detected using primary anti-HA antibody and secondary anti-rabbit-HRP. c-Myb was detected using primary anti-hcM antibody (H141) and secondary antibody anti-rabbit-HRP. The loading control GAPDH was detected using primary antibody anti-GAPDH and secondary antibody anti-mouse-HRP.

The results from the assay (figure 3.19 A) show that MBD1 still lead to an increase in c-Myb dependent activation. This activational increase however seems to be slightly less pronounced than when using the c-Myb version that is SUMOyable. Combining MBD1 with the wild type c-Myb triples activation of c-Myb dependent gene expression (figure 3.17 A), while combining MBD1 with the 2KR mutants approximately doubles transcriptional activation (figure 3.19 A).

When evaluating the western blot, there is a noticeable stabilizing effect of MBD1 on c-Myb (figure 3.19 B). This stabilizing effect can also be seen in some of the previous western blots containing both c-Myb and MBD1 (figures 3.16 B and 3.17 B), but not in others (figures 3.13 and 3.14). It appears as if the observed activational effect of MBD1 on c-Myb regulated transcription is not SUMO dependent, yet might be SUMO enhanced. There is some evidence in HEK293-c1 cell lysates pointing to a stabilizing of c-Myb by MBD1, which might cause the increase in c-Myb dependent transcription.

3.8. What are the functional implications of ATF7IP and MBD1 on c-Myb regulated transcription using a more endogenous assay approach?

We tried to determine the functional implications of the ATF7IP – c-Myb interaction in chromatinized (section 3.3.1) and non-chromatinized assays (section 3.3.2), using different interactants of both c-Myb (sections 3.3.1, 3.3.2) and ATF7IP (subchapters 3.4 and 3.5). In all these different functional luciferase assay versions, ATF7IP displayed either no effect or a modest degree of c-Myb dependent activation.

Both the transiently transfected and stably integrated luciferase assay systems have their limitations (as discussed in 4.2.1). We therefore decided to use a more endogenous approach to further examine possible effects of the ATF7IP-c-Myb interaction. We chose the HD11 *mim-1* reporter gene assay (section 2.3.3). The reporter in this assay is a natural and fully chromatinized c-Myb target gene, and the ectopically expressed c-Myb effector is the full-length protein with intact DBD. The cell line is a hematopoietic cell line containing all the expected partners of c-Myb,

except c-Myb itself [19], and thus represents a more natural environment for c-Myb than CV-1, COS-1 and HEK293-c1 cells.

HD11 cells were transfected with c-Myb, ATF7IP and MBD1 expressing plasmids. The cells were lysed, total mRNA extracted and cDNA synthesized (as described in sections 2.3.3, 2.1.3 and 2.1.13). The cDNA was then used in quantitative real time PCR with primers specific for *mim-1* and the reference gene *hprt* (section 2.1.11). The results were calculated using *mim-1* expression relative to *hprt* expression and determining an expression fold change in relation to empty vector transfections. The results of the HD11 *mim-1* reporter gene assay are shown in figure 3.20.

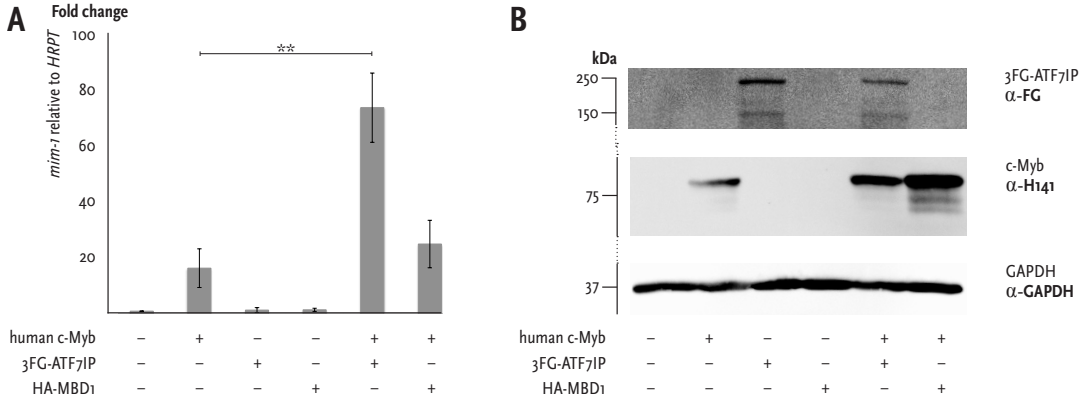

Figure 3.20 A and B: **Natural HD11 *mim-1* reporter gene assay testing the effect of ATF7IP and MBD1 on c-Myb target gene activity.** HD11 cells were seeded into 6 well dishes (5 x 10^5 cells/well in 2 mL medium per well). After 24 hours cells were transfected with 2 µg plasmid DNA per well. Using 1 µg pEF1neo-3xTy1-hcM and 1 µg of either pCIneo-3FG-ATF7IP or pCIneo-HA-MBD1. After 24 hours cells were lysed for total RNA isolation and first-strand DNA was synthesized. Activation of the endogenous c-Myb target gene was subsequently measured using qRT-PCR with primers specific for the *mim-1* and *hprt* genes. Results are given as *mim-1* expression relative to *hprt* expression. Results represent the mean ± SEM, the background is set to 1. Values are calculated from two independent experiments carried out in triplicates. Statistical analysis is performed using the two-sided, unpaired Student's t-test with Welch correction (**p<0.01). **(B)** For the western blot analysis ATF7IP was detected using primary anti-FLAG antibody and secondary anti-mouse-HRP. c-Myb was detected using primary anti-hcM antibody (H141) and secondary antibody anti-rabbit-HRP. The loading control GAPDH was detected using primary antibody anti-GAPDH and secondary antibody anti-mouse-HRP.

Measuring the activation of the endogenous c-Myb target gene, *mim-1*, one can see that ATF7IP enhances the c-Myb dependent transcription. Ectopic expression of MBD1 also leads to an activation of *mim-1* expression, but less so than ATF7IP (figure 3.20 A). From the western blot, performed from the same cell lysate used in

one of the reporter gene assays, the c-Myb stabilization by MBD1 is again evident (figure 3.20 B).

In the HD11 *mim-1* natural endogenous reporter system we can see that ATF7IP has a clear and significant effect on c-Myb dependent transcription. However, contrary to our initial hypothesis, this effect does not lead to repression of c-Myb target genes. Rather, ATF7IP appears to function as a co-activator of c-Myb dependent transcription. An unexpected finding was that one of the reported partners of ATF7IP, MBD1, in all assays operates as an independent co-activator of c-Myb function.

4. Discussion

The starting point for this research project was a recent Y2H screening identifying ATF7IP as a possible c-Myb interaction partner. This interaction has not been reported elsewhere. Since ATF7IP has strong links to both repression and activation of transcription in general, two models for its way of action have been proposed (see Introduction, subchapter 1.5). Since novel interaction partners of c-Myb could have major implications for human cancer biology, it is of great interest to expand our knowledge of this possible interaction and to investigate any functional outcomes.

The work for this thesis was divided into three main parts, as previously outlined in the introduction (subchapter 1.5).

4.1. Interaction Studies - Confirming and characterizing the interaction between c-Myb and ATF7IP

Before the work on this thesis started, ATF7IP had been identified as a potential, novel c-Myb interaction partner by Y2H screening carried out in our lab. During this screening two different ATF7IP clones were identified, one of them spanned the coding sequence for amino acids 896 to 1270 of ATF7IP (in this thesis referred to as ATF7IP-CTD), while the other was an *ATF7IP* and *Arylsulfatase B* fusion sequence. The *ATF7IP* sequence of this second clone encoded amino acid residues 958 to 980, (Master thesis - Julie Emmert Olsen). The ATF7IP-CTD protein contains both the SIM domain and Domain 2, while the amino acid residues from 958 to 980 contain little more than the SIM motif (see section 1.4.1 figure 1.4). Based on these results, the initial hypothesis was that ATF7IP interacts with c-Myb via its SIM domain, docking to the SUMO modified CRD (see subchapter 1.5 figure 1.7).

GST-pulldown studies were performed to validate the interaction between ATF7IP and c-Myb, to investigate the role of SUMO-SIM docking, and to explore whether the SIM of ATF7IP preferentially associates with SUMO1 or SUMO2 (subchapter 3.2). The questions posed and the experiments performed in that subchapter will be discussed in sections 4.1.1, 4.1.2, 4.1.3 and 4.1.4.

4.1.1. ATF7IP and c-Myb interact

In section 3.2.1 the interaction between c-Myb and ATF7IP was validated using GST-pulldown analysis (figure 3.8). What was surprising about this interaction was that SUMOylation of c-Myb was not necessary for this interaction.

Based on previous research by other groups [10, 35, 46, 11, 90] (see section 1.4.3), we know that reported interaction partners of ATF7IP appear to associate via Domain 1, Domain 2 or both. As none of the identified ATF7IP clones from the Y2H assays encoded Domain 1, it would appear reasonable to assume that ATF7IP and c-Myb interact via ATF7IPs Domain 2. Further studies using ATF7IP truncations would be required to verify this assumption (see chapter 6).

4.1.2. The interaction between ATF7IP and c-Myb is SUMO enhanced.

Based on figure 3.8 in section 3.2.1 it was possible to validate the ATF7IP – c-Myb interaction and to determine that while this interaction is not SUMO dependent (section 4.1.1), it is clearly SUMO enhanced. A fraction of unSUMOylated c-Myb is retained; this unSUMOylated fraction increases relative to the input as the SUMO state of c-Myb increases. This result is reminiscent of the reported MBD1 – ATF7IP interaction (discussed in subsection 1.4.3.4) where the TRD of MBD1 binds to Domain 2 of ATF7IP [35] while SUMOylation of MBD1 enhances this interaction via the ATF7IP SIM domain [86].

The SIM-SUMO interaction seems to supply an additional recruitment or docking mechanism. The SUMO conjugation on the CRD of c-Myb might in this manner enhance the pre-existing interaction between ATF7IP and c-Myb, or recruit ATF7IP to c-Myb where it then binds to c-Myb via its Domain 2.

4.1.3. ATF7IP shows a preference for SUMO2 over SUMO1.

It has already been reported that the SIM domain of ATF7IP has a higher affinity for SUMO2/3 over SUMO1 [86, 78]. We confirmed this preference for SUMO2 over SUMO1 using GST-SUMO1, GST-SUMO2 and GST-3xSUMO1 in a pulldown assay (section 3.2.2 figure 3.9 A and B). In this assay the preference of ATF7IP for poly-SUMO over mono-SUMO was again noticeable (sections 4.1.2 and 4.1.4).

ATF7IPs preference for SUMO2 over SUMO1 was shown to translate into a preference for c-Myb modified by SUMO2, rather than c-Myb modified by SUMO1 (figure 3.9 C). This result could be indicative of a type of switch on/off mechanism for the c-Myb and ATF7IP interaction, resonating with that of the MBD1 – ATF7IP interaction (as described below).

Research by Uchimura *et al*. has demonstrated that MBD1 is efficiently modified by either SUMO1 or SUMO2/3 *in vitro* and *in vivo*. They further demonstrated in a GST-pulldown analysis, that MBD1 modified by SUMO3 was capable of interacting with ATF7IP. The interaction between MBD1 modified by SUMO1 and ATF7IP in the same assay was significantly weaker [86]. Wang *et al.* reported in 2003 that ATF7IP is needed in order for SETDB1 to efficiently convert di-methylation of H3K9 into a repressive tri-methylation mark [89], thereby leading to the formation of facultative heterochromatin. These reported findings together with interaction studies between ATF7IP, MBD1 and SETDB1 by Ichimura *et al.* [35] culminated in the MBD1-ATF7IP-SETDB1 repression complex, schematically illustrated in figure 1.5.

Lyst *et al.* on the other hand, have shown that modification of MBD1 by SUMO1 disrupts the interaction between MBD1 and SETDB1. This disassociation leads to a depletion of the silencing H3K9me3 chromatin modification and thereby a de-repression of transcription, suggesting that SUMO1 and SUMO2/3 might have opposite effects on MBD1 functions by leading to recruitment of different cofactors [48, 49].

The question arises as to whether a similar mechanism might be at play in the c-Myb-ATF7IP interaction. Human c-Myb is a substrate for both SUMO1 and SUMO2, while ATF7IP associates significantly better with SUMO2 over SUMO1 *in vitro*.

Saitoh *et al*. reported that cells contain large pools of unconjugated SUMO2/3 and that stress stimuli (such as oxidative, heat or genotoxic stresses) lead to a depletion of these pools by conjugating the free SUMO2/3 proteins to high molecular mass proteins. This suggests a SUMO2/3 dependent cellular stress response [72]. Later, Sramko *et al*. arrived at the conclusion that c-Myb was one of those proteins modified by SUMO2/3 in response to these protein-damaging stresses. In their paper they

claimed that c-Myb is modified by SUMO1 under normal physiological conditions and that cellular stress induces a switch replacing SUMO1 with SUMO2/3 in the highly dynamic SUMOylation turnover [80]. Data presented in this thesis (subsection 3.1.3.2 figure 3.7 C and subchapter 3.4 figure 3.12 B) re-enforces the suggestion of a regulation mechanism leading to SUMOylation of c-Myb by either SUMO1 or SUMO2/3. Based on these western blots there is a clear difference depending on which SUMO molecule modifies c-Myb. SUMO2 modification appears to significantly change the steady state of c-Myb.

Considering that the c-Myb – ATF7IP interaction is enhanced by SUMO2 modification, these findings could suggest a method of ATF7IP interaction regulation. Hypothetically, when the switch between SUMO1 and SUMO2 modification takes place, ATF7IP might be recruited to c-Myb, where ATF7IP (probably Domain 2) would bind to an unspecified region of c-Myb. This idea is illustrated in figure 4.1.

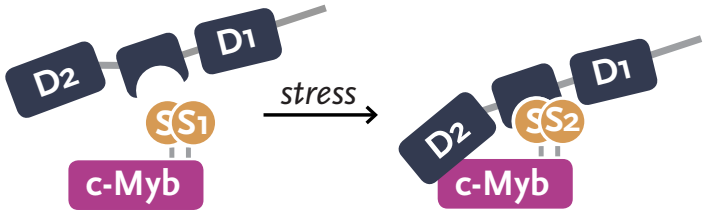

Figure 4.1: Schematic representation for the proposed recruitment of ATF7IP to c-Myb. Under stress conditions c-Myb is modified increasingly by SUMO2/3, leading to the recruitment of the transcriptional cofactor ATF7IP via its SIM domain. This ultimately leads to the binding of ATF7IP (here suggested to be via ATF7IP-Domain 2) to an unspecified region of c-Myb.

4.1.4. ATF7IP shows a preference for poly-SUMO over mono-SUMO

As mentioned before (sections 4.1.2 and 4.1.3) there are clear indications that ATF7IP preferentially associates with poly-SUMO over mono-SUMO. This preference was experimentally demonstrated in various GST-pulldown assays (section 3.2.1 figure 3.8 and section 3.2.2 figure 3.9).

In one of the GST-pulldown assays SENP resistant SUMO mutants were used to test the interaction between ATF7IP and c-Myb modified by either SUMO1 or SUMO2. This set-up resulted in a visualisation of additional c-Myb modifications (figure 3.9 C). From this blot it appears as if the interaction increase that is due to an increase in SUMO-modification, is decreased again by an additional modification of the SUMO-modified c-Myb proteins. Based on research conducted in our lab (Matre *et al*., manuscript submitted) it is likely that this modification is a phosphorylation. These results would add an additional level to the previously discussed model of ATF7IP recruitment or docking to c-Myb.

From this data two plausible models can be proposed:

1) The SUMOylation of the lysine residues on the c-Myb CRD leads to the additional modifications on c-Myb, thereby preventing the association of ATF7IP to c-Myb.
2) Alternatively, c-Myb might be diSUMOylated leading to the recruitment of and association with ATF7IP. In order for this association to disassemble, c-Myb needs to be modified by the additional modifications – breaking the interaction between ATF7IP and c-Myb. Model 2 is illustrated in figure 4.2.

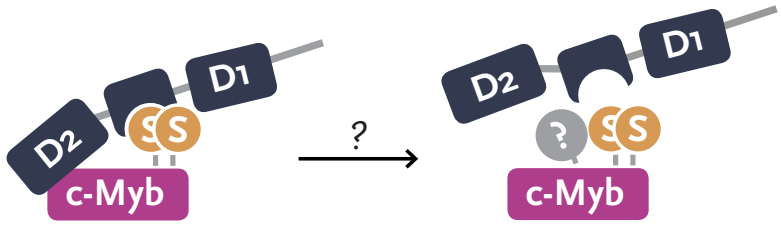

Figure 4.2: Schematic representation for the proposed disassociation of ATF7IP from c-Myb.

Incorporating the previously stated experimental findings, we would like to suggest an overall model of ATF7IP recruitment and disassociation from c-Myb containing foci (schematically illustrated in figure 4.3).

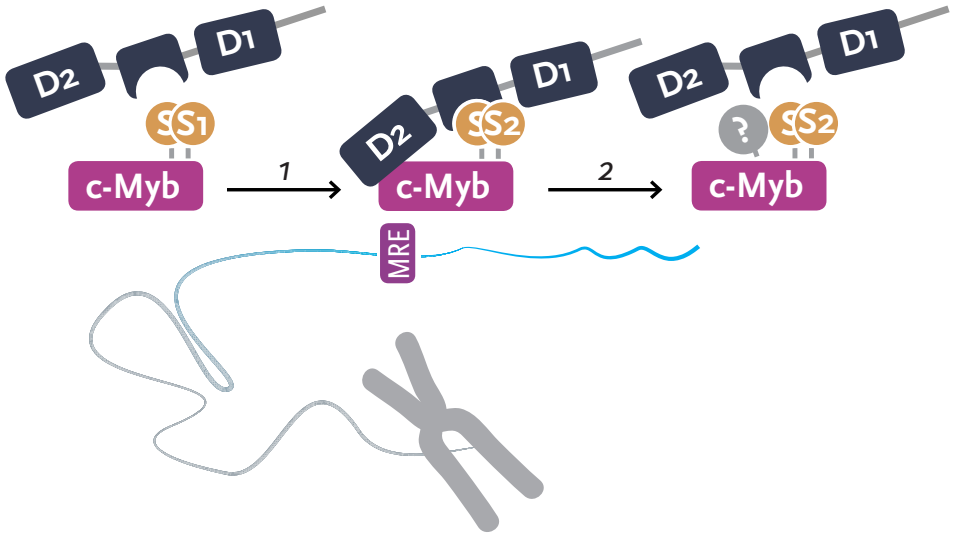

Figure 4.3: Schematic representation for the proposed model of ATF7IP recruitment and disassociation from c-Myb containing foci. c-Myb is SUMO1 modified under normal physiological conditions. Due to some stimuli (possibly stress induction) SUMO1 modification is outcompeted by SUMO2/3 modification. SUMO2/3 modification of c-Myb leads to recruitment of ATF7IP, increasing the pre-existing affinity between c-Myb and ATF7IP. The proteins bind to each other via so far unknown regions (possibly Domain 2 of ATF7IP is involved as hypothesized previously – see text). This interaction between c-Myb and ATF7IP modulates c-Myb dependent target gene expression. When this modulatory effect is no longer needed, additional unknown modifications of c-Myb lead to the disassociation between c-Myb and ATF7IP.

4.2. Functional Studies – The effect ATF7IP has on c-Myb

After validating the interaction between c-Myb and ATF7IP we asked what biological effects this interaction imposes on c-Myb dependent transcription (and thereby the cell/organism). Different approaches were used to assess these functional implications.

This subchapter starts with an examination of the different types of functional assays used throughout this project and their respective experimental advantages and disadvantages (section 4.2.1). Subsequently the results from the assays testing the effects of ATF7IP on c-Myb are discussed (section 4.2.2). During the experimental stages of the work for this thesis some discrepancies were observed in relation to ATF7IP (these are discussed in sections 4.2.3 and 4.2.4)

4.2.1. Choice of different functional reporter gene assays

During the work for this thesis, transiently transfected, stably integrated and endogenous reporter gene assays were used to assess the influence of ATF7IP on c-Myb dependent expression. These different assays are briefly described in the methods (subchapter 2.2, sections 2.3.2 and 2.3.3). Further discussion concerning their advantages and limitations are presented here.

The expression in these different systems is driven by regulatory elements; promoters and enhancers. Here one refers to synthetic and natural promoters. Synthetic promoters are promoters that consist of a set of primary elements needed for accurate transcription, in particular a set of multimerized response elements for a specific transcription factor, such as c-Myb. Natural promoters, on the other hand, are (as the name implies) naturally occurring promoters.

For this project, transiently transfected luciferase reporters with natural and synthetic promoters that are c-Myb responsive, were used (see figure 4.4 A and B), while the stably integrated assay made use of a synthetic promoter region that is Gal4-responsive (see figure 4.4 C). The last reporter gene assay, the HD11 *mim-1* system, is special in this context as both the reporter gene and its natural promoter are used in their endogenous setting. The *mim-1* promoter contains three closely spaced MREs

[59], driving *mim-1* gene expression. In addition, an upstream *mim-1* enhancer region also contains MREs contributing to its responsiveness [12, 91]. This reporter gene naturally occurs in the HD11 genome. While c-Myb is not endogenously expressed, its cooperating partner C/EBPβ is expressed, as well as other hematopoietic coactivators. Therefor the *mim-1* gene is only expressed after transfection with a c-Myb encoding plasmid (schematic of the system is illustrated in figure 4.4 D).

Transient reporter gene assays refer to reporter plasmids containing the regulatory elements and the reporter genes these elements drive. The plasmid is transiently co-transfected into the cell, along with plasmids encoding the effector and possible cofactors. These transient reporter plasmids associate with the four core histones and the linker histone H1. However, the stoichiometry of the linker histones is altered [30]. There are fewer H1 histones on the transient templates compared to stable templates. Hebbar and Archer reported that this lead to only intermediate levels of nucleosome formation [30]. The results from Mladenova *et al.* showed nucleosome-like structures of transfected plasmids, albeit anomalous when compared to stable template [54]. This lack, or intermediate level of chromatin formation, is a major concern when using transient transfection in these types of assays [79].

Based on these reports and on the initial hypothesis that the c-Myb – ATF7IP complex associates with SETDB1, leading to silencing of c-Myb target genes by propagating facultative heterochromatin, we decided to perform functional studies in both transient and stable reporter gene assays. Doing this would allow us to use any divergent results to shed light on the importance of chromatinization in ATF7IP dependent c-Myb activity modulation.

The chromatinized reporter gene assays used for this thesis were the HEK293-c1 and the HD11 *mim-1* systems. In the first system a luciferase gene is stably integrated in the HEK293 cell line, driven by five Gal4 responsive elements. The derived cell line is called HEK293-c1 and was generated by the Suske group [81] (see figure 4.4 C). The c-Myb effector used for this chromatinized assay is not a full-length protein. In this system a Gal4-binding domain able to interact with the GREs driving the integrated luciferase gene replaces the DNA-binding domain of c-Myb. This is not

always ideal, as any effects mediated via the DBD region of c-Myb will be lost or altered. The other fully chromatinized assay used was the HD11 *mim-1* system. HD11 cells are a hematopoietic chicken cell line, which do not express c-Myb endogenously. In this cell-line however, it is possible to express the c-Myb target gene *mim-1* if c-Myb is overexpressed ectopically. The *mim-1* transcript levels can subsequently be quantified using qRT-PCR, making the HD11 *mim-1* system an excellent system for studying c-Myb cofactors (the schematic illustration can be seen in figure 4.4 C).

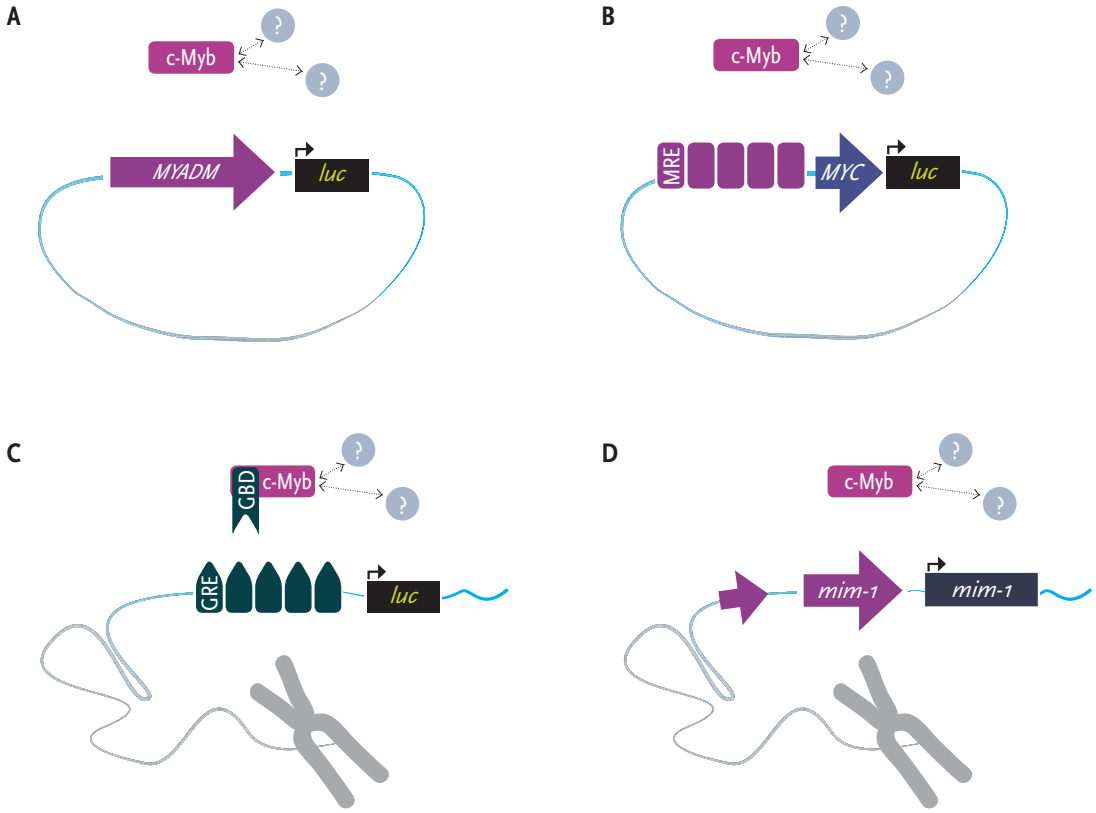

Figure 4.4 (A to D): Schematic illustrations of the different reporter gene assays used in this thesis. (A) The pGL3-MYADM transient reporter plasmid, luciferase expression from this plasmid is controlled by the natural *MYADM* promoter region, containing 7 MREs. **(B)** The pGL4x5MRE is a transient reporter plasmid with a synthetic promoter region. **(C)** In the HEK293-c1 reporter system a synthetic promoter and the luciferase gene are stably integrated into the cellular genome. **(D)** In the HD11 *mim-1* system the reporter gene, the promoter and the enhancer are all natural and endogenous to the macrophage cell-line.

4.2.2. Disproving Model 1 - The interaction between c-Myb and ATF7IP does not lead to repression of c-Myb target genes

One of the starting points for this thesis was the hypothesis that ATF7IP might be the co-repressor necessary for the formation of facultative heterochromatin generated by SUMOylated c-Myb. This in turn would lead to the repression of c-Myb activity that has been observed when c-Myb is in its SUMOylated state.

A number of different functional assays were performed to determine how ATF7IP modulates c-Myb activity. In subchapters 3.3, 3.4, 3.5 and 3.8, we were able to show that the effect of ATF7IP on c-Myb activity is not repressive in any of the model systems. Contrary to the initial repression hypothesis, we established that ATF7IP enhances full-length c-Myb dependent activation of target genes (see figures 3.10 and 3.20).

It is well established that c-Myb activity and levels are highest in immature progenitor cells (keeping cells in a proliferative stage) and that these levels and activity decline as cells commit [59]. As previously mentioned (see section 4.1.3), researchers from the Bies Lab claim that c-Myb is modified by SUMO1 under physiological conditions and that this SUMO1 modification is exchanged with SUMO2/3 modification in response to cellular stresses [80]. Molvaersmyr *et al*. in our lab, have reported that the modification of c-Myb by SUMO exerts a negative regulatory function on the activation of target genes by the c-Myb CRD [56] (also see section 1.2.1). The question remains whether this negative regulation by SUMO on c-Myb activity is SUMO variant specific or unspecific. As c-Myb can be modified by either SUMO1 or SUMO2/3, and as the SIM regions of different proteins have varying affinities for SUMO1, SUMO2/3, or both, it would be reasonable to assume that different variants of SUMO lead to altered protein-protein interactions.

Another finding that should be taken under consideration is that overexpression of ATF7IP is reported as manifesting in cancerous tissues and cells. This has been reported by Liu *et al*. who confirmed the overexpression of ATF7IP in cancer originating from various tissue sources and also reported that this overexpression was not present in non-cancerous tissue samples [46]. As previously discussed in the

Introduction and reviewed by Zhou and Ness [93], c-Myb over-expression and deregulation has recently also been detected in a wide range of human cancers. In view of these reports, a picture emerges that could possibly explain the seemingly contradictory results reported by Molvaersmyr *et al*. [56] and this thesis.

It might be the synergistic interplay of a SUMO2/3 versus SUMO1 switch, coupled with an overexpression of ATF7IP and c-Myb leading to the ATF7IP – c-Myb complex formation as stipulated in subsection 4.1.4. This would imply that under normal physiological conditions, when c-Myb is modified by SUMO1 and neither c-Myb, nor ATF7IP are overexpressed, SUMOylation of the CRD represses the activation that would otherwise be imparted on c-Myb target genes. Under stress situations however, SUMO2/3 replaces SUMO1 on the c-Myb CRD. One of the ways in which the oncogenic potential of a cell increases, leading to the progression of tumourigenesis, is due to aberrations in the cells stress response. One might argue, if stress induces the SUMO1, SUMO2/3 switch and ATF7IP is overexpressed, it might be recruited to c-Myb (as previously described), leading to an increased c-Myb activity and thereby retaining the cells in their proliferative state.

4.2.3. Expression levels - Endogenous versus transfected ATF7IP

One of the concerns during the work for this thesis was the possibility of too low ATF7IP levels. Detecting ectopic 3FLAG-tagged ATF7IP from cell lysates with anti FLAG primary antibody required very long exposure times, and was not very robust.

Listed below are two likely scenarios explaining how this perceived low–level problem might impact on observations of functional effects imparted by the ATF7IP - c-Myb complex.

1) The ectopically expressed amount of 3FG-ATF7IP is so low in comparison to the endogenous ATF7IP pool that it might not lead to any significant functional changes, as it does not change the overall ATF7IP levels.
2) ATF7IP might be so tightly regulated that even though cells are transfected, intracellular ATF7IP levels are kept stable.

To address these concerns the primary anti-ATF7IP antibody was bought and used on HEK293-c1 and CV-1 cell lysates transfected with plasmids encoding 3FG-ATF7IP and empty vectors respectively.

In CV-1 cell lysates (results not shown), we experienced what we believe to be unspecific binding. This made the detection of ATF7IP using the anti-ATF7IP antibody impossible. We did however verify that 3FG-ATF7IP was successfully expressed using an anti-FG antibody. Due to the unspecific binding we were not able to compare endogenous versus endogenous plus ectopic ATF7IP levels in the CV-1 cell line.

In the HEK293-c1 cell line we were able to show that there is a significantly higher level of ATF7IP in the cells transfected with the plasmids encoding 3FG-ATF7IP, compared to the control cells (see figure 3.2), thereby eliminating the above listed concerns, in experiments using this cell line.

4.2.4. PTMs of ATF7IP - The migration paradox

ATF7IP spans 1270 amino acid residues and has a theoretical molecular weight of 136.4 kDa. In expression and detection experiments the ectopically expressed 3FG-ATF7IP is, when using the primary anti-FG antibody, usually detected as two strong bands migrating at 250 kDa and 150 kDa with a number of additional weaker bands (see for example figures 3.3, 3.10 and 3.11). From the experiments comparing levels of endogenous and ectopic ATF7IP in HEK293-c1 cells (figure 3.2 B), one can see that endogenous ATF7IP also migrates at 250 kDa and that the increase in size due to the 3FG tag appears minimal on the western blot. Collectively this means that the upper band is migrating at a speed characteristic for a protein approximately 100 kDa larger than ATF7IP.

This unexpected migration pattern has been observed by other labs (see table 1), but has never been extensively discussed or reported on. Uchimura *et al.* went so far as to say that the band seen at 240 kDa in their blots was the full-length unmodified ATF7IP protein [86]. As the Uchimura *et al.* paper is one of the most-cited sources for ATF7IP information; it could explain why many of the subsequent reports have

seemingly not further examined the migration speed of ATF7IP. Liu *et al.* for example referred to the fast migrating band, often seen in ATF7IP blots as a degradation product [46].

Table 1: Reported migration of ATF7IP. A light blue field indicates studies in which the sizes were not explicitly stated, but could be gathered from displayed western blots.

Size observed, kDa	Type	Authors	Reference
213	endogenous	Fujita *et al*. (2003).	23
200	ectopic	Chang *et al.* (2005).	10
~200	endogenous	Ichimura *et al*. (2005).	35
240	endogenous	Uchimura *et al.* (2006).	86
~220	endogenous	Liu *et al.* (2009).	46
~250	endogenous	Chang *et al.* (2010).	11
~200	endogenous	Lin *et al.* (2014).	43
220	endogenous	Minkovsky *et al.* (2014).	52

ATF7IP has a number of reported PTMs (see section 1.4.2), none of which initially appear to be large enough to warrant a migratory shift of 100 kDa.

In subsection 3.1.2.3, we investigated whether phosphorylation might be at the root of the unexpected migration pattern. We concluded that although there appears to be some λ-PPase sensitive phospho-modifications, these were not responsible for the 250 kDa band. In section 1.4.2, we suggested that ATF7IP might be additionally O-GlcNAc modified. This modification has been reported on a number of ATF7IP interactants [15], as well as on the murine homologue [57]. Of course, this idea of O-GlcNAc modifications on ATF7IP is highly speculative. What is not speculative is that ATF7IP is consistently found to migrate at a speed uncharacteristic for a protein of its size. As ATF7IP has become more prominent over the past couple of years (7 new articles in 2014 [27, 40, 43, 52, 28], two of which in Nature [63, 90]), investigating potential ATF7IP post-translational modifications would arguably be of quite some interest (see chapter 6).

4.3. Functional studies - How ATF7IP interaction partners affect c-Myb

During our investigations into the cofactor potential of ATF7IP, we showed that SETDB1 did not modulate the activity of the ATF7IP – c-Myb complex (see figures 3.13, 3.15 and 3.17). However, carrying out the same experiments with MBD1 lead to a significant increase in activation function (see figures 3.14, 3.16, 3.17, 3.19 and 3.20). Furthermore, we were able to show that this activation by MBD1 is not ATF7IP dependent (see figure 3.16), but c-Myb specific (figure 3.18). Additionally we revealed that although the activation by MBD1 did not rely on SUMOylation of c-Myb, it was enhanced by it (see figure 3.19).

All of the functional assays in this thesis are supported by western blot analysis. From these western blots one can see that although MBD1 leads to c-Myb dependent reporter activation in all of the experiments (see figures 3.14 A, 3.16 A, 3.17 A, 3.19 A and 3.20 A), it stabilizes c-Myb only in the experiments using the HEK293-c1 and HD11 cell lines (figures 3.16 B, 3.17 B, 3.19 B and 3.20 B). This stabilizing effect is not seen in the experiments using the CV-1 cell line (see figures 3.14 B). Changes of protein stability are frequently observed in protein-protein interactions. This could be due to a number of different mechanisms. Stabilization (as in our case) could for example result from shielding of Ubiquitin PTMs of c-Myb, thereby inhibiting the 26S proteasome degradation pathway. Considering the results from the cell lines tested, it seems plausible that MBD1 is a c-Myb co-activator. Additional studies would need to be carried out, testing if c-Myb and MBD1 interact (see chapter 6).

4.4. Functional Studies - Model 1 versus Model 2

The epigenetic repressive model (Model 1) is not supported by any of the experiments in this work. The Mediator-like activator model (Model 2) is supported by some, albeit with changing levels of activation response from the different experimental setups. We asked which experimental parameters correlate when comparing the experiments exhibiting low ATF7IP-induced activation and those that exhibit high activation.

When comparing the transiently transfected reporter assays (figure 3.10) with the stably integrated assays (figures 3.11 and 3.20), we observed a high ATF7IP-induced

activation from the MYADM reporter as well as from the endogenous *mim-1* reporter, but no activation in the stably integrated HEK293-c1 reporter system. Based on these results it appears that the observed phenomenon is not dependent on the degree of reporter chromatinization.

We further asked whether the levels of ATF7IP-induced activation correlate with the use of simple versus complex promoters. The reporter gene assay systems from which activation was detected were the ones with the natural *MYADM* and *mim-1* promoters (figures 3.10 and 3.20). Both of these are more complex then the synthetic promoters used during this investigation. This observation is interesting as the Mediator-like model (Model 2, figure 1.8) is based on the assumption that ATF7IP functions as a bridge between c-Myb and the basal transcription machinery. Bridging is more critical in complex promoters.

5. Summary of findings

In the introduction (subchapter 1.5), we outlined the aims of this study, dividing them into three parts. In chapter 3 we showed our results and discussed them in chapter 4, in this chapter we will briefly summarize these results, relating them back to the initial aim of the work.

5.1. Conclusions - Part 1

Part 1 was an investigation of the interaction between c-Myb and ATF7IP. The validity of this interaction was addressed, as well as the role of SUMO-SIM.

- We validated the interaction between ATF7IP and c-Myb.
- We showed that the interaction is not SUMO dependent, but SUMO enhanced.
- We confirmed that the SIM of ATF7IP has higher affinity for SUMO2, than SUMO1.
- We revealed that ATF7IP has a higher affinity for poly-SUMO, than mono-SUMO.

An additional finding in part 1 of this study, although unrelated to ATF7IP, was the noticeable difference of c-Myb steady-state depending on which SUMO variant is conjugated to it.

5.2. Conclusions - Part 2

In Part 2 we explored the functional implications of the ATF7IP – c-Myb interaction complex.

- We disproved the hypothesized Model 1 (figure 1.7).
- We showed that ATF7IP functions as a c-Myb co-activator, thereby implicating Model 2 (figure 1.8) as a plausible mechanism of c-Myb target gene modulation.

5.3. Conclusions - Part 3

In Part 3 we investigated known ATF7IP interaction partners implicated in the hypothesized Model 1 complex, SETDB1 and MBD1, in relation to c-Myb target gene expression.

- We showed that SETDB1 had no noticeable c-Myb dependent effects in our model systems, consistent with the rejection of Model 1 (figure 1.7).
- We exposed MBD1 as a potential, novel, coactivator of c-Myb.

6. Future Work

6.1. Further studies - Part 1

Although we were able to validate the interaction between c-Myb and ATF7IP, we still have to map this interaction to specific parts of the proteins. In the discussion (subchapter 4.1) we have deliberated the probable involvement of ATF7IP's Domain 2, this has not yet been proven. GST-fusion proteins of various c-Myb and ATF7IP deletion mutants would be needed to pinpoint and validate the exact interaction regions on both proteins involved.

Using the SENP resistant SUMO mutants, we were able to show that modification of c-Myb with different SUMO variants affects c-Myb's steady state. This is a finding, which to our knowledge has not been reported in relation to c-Myb before. We discussed how STUbLs might be involved (subchapter 3.1), but have so far not researched this further.

6.2. Further studies - Part 2

We were able to show that ATF7IP lead to an increase in c-Myb dependent activation using reporter gene assays. In the introduction and the discussion (sections 1.43 and 4.2.2), we briefly mentioned that ATF7IP has been reported to interact with the components of the basal transcription machinery, culminating in our proposed Model 2 (figure 1.8). However, it is unclear which regions of ATF7IP interact with RNAPII, studying this interaction by GST-pulldown assays would be of interest.

If the complexity of the promoter is a determinant for ATF7IP-dependence, one might also design a series of model promoter-enhancer constructs with different spacing to evaluate the bridging role of ATF7IP.

So far, it is unclear which c-Myb responsive genes are modulated by the interaction with the ATF7IP co-activator *in vivo*. There are indications that complex promoters are likely candidates, but we did not conduct experiments, which could implicate ATF7IP more directly in specific c-Myb target gene activation. Based on the experiments presented by Sasai *et al.* [76] it does not seem like knock-down of

ATF7IP is a good option when studying targets of ATF7IP. The cofactor has many cellular targets, and from the knock-down experiments presented in that paper it appears that knock-down has a global effect, leading to premature cell-death. It would be interesting to study target genes using chromatin immunoprecipitation (ChiP), investigating which target genes of c-Myb are modulated by an interaction with ATF7IP.

In Part 2, we also discussed the necessity to have a closer look at ATF7IP and its possible post-translational modifications. ATF7IP has been consistently described as migrating at a speed uncharacteristic for a protein of its size. Mass spectrometry analysis of ATF7IP expressed in mammalian cells could shed light on this migration paradox.

6.3. Further studies - Part 3

We showed that MBD1 leads to an increase in c-Myb depending activation and that this activation is ATF7IP independent. We further showed that although this activation does not depend on SUMO, SUMOylation of c-Myb does enhance it. It would be interesting to conduct interaction studies to determine whether c-Myb and MBD1 interact in a direct manner. If there is no direct interaction, it would be interesting to see if MBD1 sequesters a protein that would otherwise lead to repression of c-Myb activity, as well as which protein this might be.

7. References

1. Adams, M. D. *et al*. *The Genome Sequence of Drosophila melanogaster*. Science, 2000. **287**(5461): p. 2185-2195.
2. Alm-Kristiansen, A.H., Lorenzo, P. I., Molvaersmyr, A. K., Matre, V., Ledsaak, M., Saether, T., Gabrielsen, O. S. *PIAS1 interacts with FLASH and enhances its co-activation of c-Myb*. Molecular Cancer, 2011. **10**(21): p. 21.
3. Andersson, K.B., Kowenz-Leutz, E., Brendeford, E. M., Tygsett, A. H., Leutz, A., Gabrielsen, O. S. *Phosphorylation-dependent down-regulation of c-Myb DNA binding is abrogated by a point mutation in the v-myb oncogene*. Journal of Biological Chemistry, 2003. **278**(6): p. 3816-3824.
4. Berge T., Bergholtz S.T., Brevik Andersson K., Gabrielsen O.S. *A novel yeast system for in vivo selection of recognition sequences: defining an optimal c-Myb-responsive element.* Nucleic Acids Research, 2001. **29**(29 e99).
5. Bergholtz, S., Andersen, T. Ø., Andersson, K. B., Borrebæk, J., Lüscher, B., Gabrielsen, O. S. *The highly conserved DNA-binding domains of A-, B- and c-Myb differ with respect to DNA-binding, phosphorylation and redox properties*. Nucleic Acids Research, 2001. **29**(17): p. 3546-3556.
6. Biedenkapp, H., Borgmeyer, U., Sippel, A. E., Klempnauer, K. H. *Viral myb oncogene encodes a sequence-specific DNA-binding activity.* Nature, 1988. **335** (27), 835–837.
7. Bies, J. and L. Wolff. *Oncogenic activation of c-Myb by carboxyl-terminal truncation leads to decreased proteolysis by the ubiquitin-26S proteasome pathway*. Oncogene, 1997. **14**: p. 203 – 212.
8. Bies, J., Markus, J. and Wolff, L. *Covalent attachment of the SUMO-1 protein to the negative regulatory domain of the c-Myb transcription factor modifies its stability and transactivation capacity*. The Journal of Biological Chemistry, 2002. **277**(11): p. 8999-9009.
9. Brivanlou, A.H. and Darnell, J.E. Jr., *Signal transduction and the control of gene expression*. Science, 2002. **295**(5556): p. 813-818.
10. Chang, L.K., Chung, J. Y., Hong, Y. R., Ichimura, T., Nakao, M., Liu, S. T. *Activation of Sp1-mediated transcription by Rta of Epstein-Barr virus via an interaction with MCAF1*. Nucleic Acids Research, 2005. **33**(20): p. 6528-6539

11. Chang, L.K., Chuang, J. Y., Nakao, M., Liu, S. T. *MCAF1 and synergistic activation of the transcription of Epstein-Barr virus lytic genes by Rta and Zta.* Nucleic Acids Research, 2010. **38**(14): p. 4687-4700.
12. Chayka, O., Kintscher, J., Braas, D., Klempnauer, K. H. *v-Myb mediates cooperation of a cell-specific enhancer with the mim-1 promoter.* Molecular and Cellular Biology, 2005. **25**(1): p. 499-511
13. Clappier E, Cuccuini W, Kalota A, Crinquette A, Cayuela JM, Dik WA, Langerak AW, Montpellier B, Nadel B, Walrafen P, Delattre O, Aurias A, Leblanc T, Dombret H, Gewirtz AM, Baruchel A, Sigaux F, Soulier J. *The C-MYB locus is involved in chromosomal translocation and genomic duplications in human T-cell acute leukemia (T-ALL), the translocation defining a new T-ALL subtype in very young children*. Blood, 2007. **110** (4): p. 1251–1261.
14. Clouaire, T., de Las Heras, J. I., Merusi, C., Stancheva, I. *Recruitment of MBD1 to target genes requires sequence-specific interaction of the MBD domain with methylated DNA.* Nucleic Acids Research, 2010. **38**(14): p. 4620-4634.
15. Comer, F.I. and Hart, G.W. *O-Glycosylation of nuclear and cytosolic proteins. Dynamic interplay between O-GlcNAc and O-phosphate*. The Journal of Biological Chemistry, 2000. **275**(38): p. 29179-29182.
16. Corradini, F., Cesi, V., Bartella, V., Pani, E., Bussolari, R., Candini, O., Calabretta, B. *Enhanced proliferative potential of hematopoietic cells expressing degradation-resistant c-Myb mutants*. The Journal of Biological Chemistry, 2005. **280**(34): p. 30254-30262.
17. COS-1 ATCC ® CRL-1650™ Cercopithecus aethiops kidney
18. CV-1 ATCC ® CCL-70™ Cercopithecus aethiops kidney Normal
19. Dahle, Ø., Andersen, T. O., Nordgard, O., Matre, V., Del Sal, G., Gabrielsen, O. S. *Transactivation properties of c-Myb are critically dependent on two SUMO-1 acceptor sites that are conjugated in a PIASy enhanced manner.* European Journal of Biochemistry, 2003. **270**(6): p. 1338-1348.
20. Dai, P., Akimaru, H., Tanaka, Y., Hou, D. X., Yasukawa, T., Kanei-Ishii, C., Takahashi, T., Ishii, S. *CBP as a transcriptional coactivator of c-Myb*. Genes & Development, 1996. **10**(5): p. 528-540.

21. Daujat, S., Bauer, U. M., Shah, V., Turner, B., Berger, S., Kouzarides, T. *Crosstalk between CARM1 Methylation and CBP Acetylation on Histone H3.* Current Biology, 2002. **12**: p. 2090-2097.
22. De Graeve F., B.A., Chatton B., and Kedinger C., *A murine ATFa-associated factor with transcriptional repressing activity.* Oncogene, 2000. **19**: p. 1807-1819.
23. Fujita, N., Watanabe, S., Ichimura, T., Ohkuma, Y., Chiba, T., Saya, H., Nakao, M. *MCAF Mediates MBD1-Dependent Transcriptional Repression.* Molecular and Cellular Biology, 2003. **23**(8): p. 2834-2843.
24. Gabrielsen, O.S., Sentenac, A. and Fromageot, P. *Specific DNA binding by c-Myb: evidence for a double helix-turn-helix –related motif.* Science, 1991. **253**: p. 1140-1143.
25. Geiss-Friedlander, R. and Melchior F. *Concepts in sumoylation: a decade on.* Nature Reviews: Molecular Cell Biology, 2007. **8**(12): p. 947-956.
26. Gunther M., Laithier M. and Brison O. *A set of proteins interacting with transcription factor Sp1 identified in a two-hybrid screening.* Molecular and Cellular Biochemistry, 2000. **210**: p. 131-142.
27. Hameed, U. F., Lim, J., Zhang, Q., Wasik, M. A., Yang, D., Swaminathan, K. *Transcriptional Repressor Domain of MBD1 is Intrinsically Disordered and Interacts with its Binding Partners in a Selective Manner.* Scientific Reports, 2014. **4**: p. 4896.
28. Hanufsa, T. *Function of Aire in central and peripheral immune tolerance*. Japanese Journal of Clinical Immunology, 2014. **37**(3): p. 133 – 138.
29. Hay, R.T. *SUMO: a history of modification.* Molecular Cell, 2005. **18**(1): p. 1-12.
30. Hebbar, P. B. and T. K. *Altered histone H1 stoichiometry and an absence of nucleosome positioning on transfected DNA.* The Journal of Biological Chemistry, 2008. **283**(8): p. 4595-4601.
31. HEK-293 ATCC ® CRL-1573™ Homo sapiens embryonic kidney
32. Hooper, J., Maurice, D., Argent-Katwala, M. J., Weston, K. *Myb proteins regulate expression of histone variant H2A.Z during thymocyte development.* Immunology, 2008. **123**(2): p. 282-289.
33. Hornbeck PV.*et al.* Nucleic Acids Research, 2012 40:D261-70.

34. Howe K. M., Reakes C. F., Watson R. J. *Characterization of the sequence-specific interaction of mouse c-myb protein with DNA*. The EMBO Journal, 1990. **9**(1): p. 161–169.
35. Ichimura, T., Watanabe, S., Sakamoto, Y., Aoto, T., Fujita, N., Nakao, M. *Transcriptional repression and heterochromatin formation by MBD1 and MCAF/AM family proteins.* The Journal of Biological Chemistry, 2005. **280**(14): p. 13928-13935.
36. Introna, M. and Golay, J. *How can oncogenic transcription factors cause cancer: a critical review of the myb story.* Leukemia, 1999. **13**: p. 1301–1306.
37. Kaiser, P and Davison, F. *Appendix 2: Resources available for studying avian immunology*. Avian Immunology, 2008. Elsevier, London, p. 459-465.
38. Kauraniemi, P., Hedenfalk, I., Persson, K., Duggan, D. J., Tanner, M., Johannsson, O., Olsson, H., Trent, J. M., Isola, J., Borg, Å. *MYB oncogene amplification in hereditary BRCA1 breast cancer.* Cancer Research, 2000. **60**(19): p. 5323-5328.
39. Klempnauer K.H., Gonda T.J., Bishop J.M. *Nucleotide sequence of the retroviral leukemia gene v-myb and its cellular progenitor c-myb: the architecture of a transduced oncogene.* Cell, 1982. **31**: p. 453–463.
40. Kobayashi, K., Mitsui, K., Ichikawa, H., Nakabayashi, K., Matsuoka, M., Kojima, Y., Takahashi, H., Iijima, K., Ootsubo, K., Oboki, K., Okita, H., Yasuda, K., Sakamoto, H., Hata, K., Yoshida, T., Matsumoto, K., Kiyokawa, N., Ohara, A. *ATF7IP as a novel PDGFRB fusion partner in acute lymphoblastic leukaemia in children.* British Journal of Haematology, 2014. **165**(6): p. 836 – 841.
41. Leverson, J.D., Koskinen, P. J., Orrico, F. C., Rainio, E.-M., Jalkanen, K. J., Dash, A. B., Eisenman, R. N., Ness, S.A. *Pim-1 Kinase and p100 Cooperate to Enhance c-Myb Activity.* Molecular Cell, 1998. **2**: p. 417-425.
42. Levine, M. and Tjian, R. *Transcription regulation and animal diversity.* Nature, 2003. **424**: p. 147-151.
43. Lin, T., Chu, Y., Yang, Y., Hsu, S., Liu, S., Chang, L. *MCAF1 and Rta-Activated BZLF1 Transcription in Epstein- Barr Virus.* PLoS One, 2014. **9**(3):e90698.
44. Lipsick, J.S. and Wang, D.-M. *Transformation by v-Myb*. Oncogene, 1999. **18**: p. 3047 - 3055.

45. Liu, F., Lei, W., O'Rourke, J. P., Ness, S. A. *Oncogenic mutations cause dramatic, qualitative changes in the transcriptional activity of c-Myb*. Oncogene, 2006. **25**(5): p. 795-805.
46. Liu, L., Ishihara, K., Ichimura, T., Fujita, N., Hino, S., Tomita, S., Watanabe, S., Saitoh, N., Ito, T., Nakao, M. *MCAF1/AM is involved in Sp1-mediated maintenance of cancer-associated telomerase activity.* The Journal of Biological Chemistry, 2009. **284**(8): p. 5165-5174.
47. Lüscher, B. and Eisenman, R.N. *New light on Myc and Myb. Part II. Myb.* Genes & Development, 1990. **4**: p. 2235-2241.
48. Lyst, M. J. and Stancheva I. *A role for SUMO modification in transcriptional repression and activation.* Biochemical Society Transactions, 2007. **35**(Pt 6): p. 1389-1392.
49. Lyst, M. J., Nan, X., Stancheva, I. *Regulation of MBD1-mediated transcriptional repression by SUMO and PIAS proteins*. The EMBO Journal, 2006. **25**: p. 5317-5328.
50. Ma X.-P. and Calabretta B. *DNA binding and transactivation activity of A-myb, a c-myb-related gene.* Cancer Research, 1994. **54**: p. 6512–6516.
51. Matre, V., Nordgard, O., Alm-Kristiansen, A. H., Ledsaak, M., Gabrielsen, O. S. *HIPK1 interacts with c-Myb and modulates its activity through phosphorylation*. Biochemical and Biophysical Research Communications, 2009. **388**(1): p. 150-154.
52. Minkovsky, A., Sahakyan, A., Rankin-Gee, E., Bonora, G., Patel, S., Plath, K. *The Mbd1-Atf7ip-Setdb1 pathway contributes to the maintenance of X chromosome inactivation.* Epigenetics & Chromatin, 2014. **7**:12.
53. Mizuguchi G., N.H., Nagase T., Nomura N., Date T., Ueno Y., and Ishii S., *DNA binding activity and transcriptional activator function of the human B-myb protein compared with c-MYB.* The Journal of Biological Chemistry, 1990. **265**(16): p. 9280-9284.
54. Mladenova, V., Nakagoshi H., Nagase T., Nomura N., Date T., Ueno Y., Ishii S. *Organization of Plasmid DNA into Nucleosome-Like Structures after Transfection in Eukaryotic Cells*. Biotechnology & Biotechnological Equipment, 2014. **23**(1): p. 1044-1047.

55. Mo, X., Kowenz-Leutz, E., Laumonnier, Y., Xu, H., Leutz, A. *Histone H3 tail positioning and acetylation by the c-Myb but not the v-Myb DNA-binding SANT domain.* Genes & Development, 2005. **19**(20): p. 2447-2457.
56. Molvaersmyr, A.K., Saether, T., Gilfillan, S., Lorenzo, P. I., Kvaloy, H., Matre, V., Gabrielsen, O. S. *A SUMO-regulated activation function controls synergy of c-Myb through a repressor-activator switch leading to differential p300 recruitment.* Nucleic Acids Research, 2010. **38**(15): p. 4970-4984.
57. Myersa S. A., Panningb B., Burlingamea, .A. L., *Polycomb repressive complex 2 is necessary for the normal site-specific O-GlcNAc distribution in mouse embryonic stem cells.* Proceedings of the National Academy of Sciences, 2011. **108**(23): p. 9490–9495.
58. Narlikar G.J., Fan H.Y., Kingston, R.E. *Cooperation between complexes that regulate chromatin structure and transcription*. Cell, 2002. **108**: p. 475–487
59. Ness, S. A., Marknell, Å., Graf, T. *The v-myb Oncogene Product Binds to and Activates the Promyelocyte-Specific mim-1 Gene.* Cell, 1989. **59**: p. 1115-1125.
60. Ness, S.A., *Myb binding proteins: regulators and cohorts in transformation.* Oncogene, 1999. **18**: p. 3039-3046.
61. Oh, I.H. and E.P. Reddy, *The myb gene family in cell growth, differentiation and apoptosis*. Oncogene, 1999. **18**: p. 3017-3033.
62. Ording, E., Kråvik, W., Bostad, A., Gabrielsen, O. S. *Two functionally distinct half sites in the DNA-recognition sequence of the Myb oncoprotein*. European Journal of Biochemistry, 1994. **222**: p. 113-120.
63. Papaemmanuil, E., *et al. RAG-mediated recombination is the predominant driver of oncogenic rearrangement in ETV6-RUNX1 acute lymphoblastic leukemia.* Nature Genetics, 2014. **46**: p. 116–125.
64. Persson, M., Andren, Y., Mark, J., Horlings, H.M., Persson, F., Stenman, G. *Recurrent fusion of MYB and NFIB transcription factor genes in carcinomas of the breast and head and neck*. Proceedings of the National Academy of Sciences, 2009. **106**(44): p. 18740–18744.

65. Poulsen, S. L., Hansen, R. K., Wagner, S. A., van Cuijk, L., van Belle, G. J., Streicher, W., Wikstrom, M., Choudhary, C., Houtsmuller, A. B., Marteijn, J. A., Bekker-Jensen, S., Mailand, N. *RNF111/Arkadia is a SUMO-targeted ubiquitin ligase that facilitates the DNA damage response.* Journal of Cell Biology, 2013. **201**(6): p. 797-807.
66. Prouse M. B., Campbell M. M. *The interaction between MYB proteins and their target DNA binding sites.* Biochimica et Biophysica Acta, 2012. **1819**(1): p. 67–77.
67. Ramsay, R.G., Thompson, M.A., Hayman, J.A., Reid, G., Gonda, T.J., Whitehead, R.H. *Myb expression is higher in malignant human colonic carcinoma and premalignant adenomatous polyps than in normal mucosa.* Cell Growth & Differentiation, 1992. **3**: p. 723–730.
68. Ramsay, R.G. and Gonda, T.J. *MYB function in normal and cancer cells*. Nature Reviews: Cancer, 2008. **8**(7): p. 523-534.
69. Ruvkun, G. and Hobert, O. *The taxonomy of developmental control in Caenorhabditis elegans.* Science, 1998. **282**(5396): p. 2033–2041.
70. Saether, T., Pattabiraman, D. R., Alm-Kristiansen, A. H., Vogt-Kielland, L. T., Gonda, T. J., Gabrielsen, O. S. *A functional SUMO-interacting motif in the transactivation domain of c-Myb regulates its myeloid transforming ability.* Oncogene, 2011. **30**(2): p. 212-222.
71. Saether, T., Berge, T., Ledsaak, M., Matre, V., Alm-Kristiansen, A. H., Dahle, Ø., Aubry, F., Gabrielsen, O. S. *The chromatin remodeling factor Mi-2alpha acts as a novel co-activator for human c-Myb.* The Journal of Biological Chemistry, 2007. **282**(19): p. 3994-4005.
72. Saitoh, H. *Functional Heterogeneity of Small Ubiquitin-related Protein Modifiers SUMO-1 versus SUMO-2/3.* Journal of Biological Chemistry, 2000. **275**(9): p. 6252-6258.
73. Sakamoto, H., Dai, G., Tsujino, K., Hashimoto, K., Huang, X., Fujimoto, T., Mucenski, M., Frampton, J., Ogawa, M. *Proper levels of c-Myb are discretely defined at distinct steps of hematopoietic cell development.* Blood, 2006. **108**: p. 896–903

74. Sakura, H., Kanei-Ishi, C., Nagase, T., Nakagoshi, H., Gonda, T., Ishii S. *Delineation of three functional domains of the transcriptional activator encoded by the c-myb protooncogene.* Proceedings of the National Academy of Sciences, 1989. **86**: p. 5758-5762.
75. Sano, Y. and Ishii, S. *Increased affinity of c-Myb for CREB-binding protein (CBP) after CBP-induced acetylation.* The Journal of Biological Chemistry, 2001. **276**(5): p. 3674-3682.
76. Sasai, N., Saitoh, N., Saitoh, H., Nakao, M. *The Transcriptional Cofactor MCAF1/ATF7IP Is Involved in Histone Gene Expression and Cellular Senescence.* PLoS One, 2013. **8**(7):e68478.
77. Schultz, D. C., Ayyanathan, K., Negorev, D., Maul, G. G., Rauscher, F. J. *SETDB1: a novel KAP-1-associated histone H3, lysine 9-specific methyltransferase that contributes to HP1-mediated silencing of euchromatic genes by KRAB zinc-finger proteins.*" Genes & Development, 2002. **16**(8): p. 919-932.
78. Sekiyama, N., Ikegami, T., Yamane, T., Ikeguchi, M., Uchimura, Y., Baba, D., Ariyoshi, M., Tochio, H., Saitoh, H., Shirakawa, M. *Structure of the small ubiquitin-like modifier (SUMO)-interacting motif of MBD1-containing chromatin-associated factor 1 bound to SUMO-3.* The Journal of Biological Chemistry, 2008. **283**(51): p. 35966 - 35975.
79. Smith, C. L. and Hager, G. L. *Transcriptional Regulation of Mammalian Genes in Vivo: A Tale of two Templates.* Journal of Biological Chemistry, 1997. **272**(44): p. 27493-27496.
80. Sramko, M., Markus, J., Kabat, J., Wolff, L., Bies, J. *Stress-induced inactivation of the c-Myb transcription factor through conjugation of SUMO-2/3 proteins.* The Journal of Biological Chemistry, 2006. **281**(52): p. 40065-40075.
81. Stielow, B., Sapetschnig, A., Wink, C., Kruger, I., Suske, G. *SUMO-modified Sp3 represses transcription by provoking local heterochromatic gene silencing*. EMBO Reports, 2008. **9**(9): p.899-906.
82. Streubel, G., Bouchard, C., Berberich, H., Zeller, M. S., Teichmann, S., Adamkiewicz, J., Muller, R., Klempnauer, K. H., Bauer, U. M. *PRMT4 is a novel coactivator of c-Myb-dependent transcription in haematopoietic cell lines.* PLoS Genetics, 2013. **9**(3): e1003343.

83. Tatham, M. H., Geoffroy, M. C., Shen, L., Plechanovova, A., Hattersley, N., Jaffray, E. G., Palvimo, J. J., Hay, R. T. *RNF4 is a poly-SUMO-specific E3 ubiquitin ligase required for arsenic-induced PML degradation.* Nature Cell Biology, 2008. **10**(5): p. 538-546.
84. Tomita, A., Towatari M., Tsuzuki S., Hayakawa F., Kosugi H., Tamai K., Miyazaki T., Kinoshita T., Saito H. *c-Myb acetylation at the carboxyl-terminal conserved domain by transcriptional co-activator p300.* Oncogene, 2000. **19**: p. 444-451
85. Torelli, G., Venturelli, D. Colo, A., Zanni, C., Seller, L., Moretti, L., Calabretta, B.,Torelli, U. *Expression of c-myb Protooncogene and Other Cell Cycle-related Genes in Normal and Neoplastic Human Colonic Mucosa*. Cancer Research, 1987. **47**: p. 5266-5269.
86. Uchimura, Y., Ichimura, T., Uwada, J., Tachibana, T., Sugahara, S., Nakao, M., Saitoh, H. *Involvement of SUMO modification in MBD1- and MCAF1-mediated heterochromatin formation.* The Journal of Biological Chemistry, 2006. **281**(32): p. 23180 – 23190.
87. Udeshi, N. D., Svinkina, T., Mertins, P., Kuhn, E., Mani, D. R., Qiao, J. W., Carr, S. A. *Refined preparation and use of anti-diglycine remnant (K-epsilon-GG) antibody enables routine quantification of 10,000s of ubiquitination sites in single proteomics experiments.* Molecular & Cellular Proteomics, 2013. **12**(3): p. 825-831.
88. Wallrapp, C., Muller-Pillasch, F., Solinas-Toldo, S., Lichter, P., Friess, H., Buchler, M., Fink, T., Adler, G., Gress, T.M. *Characterization of a high copy number amplification at 6q24 in pancreatic cancer identifies c-myb as a candidate oncogene.* Cancer Research, 1997. **57**: p. 3135–3139.
89. Wang, H., An, W., Cao, R., Xia, L., Erdjument-Bromage, H., Chatton, B., Tempst, P., Roeder, R.G., Zhang, Y. *mAM Facilitates Conversion by ESET of Dimethyl to Trimethyl Lysine 9 of Histone H3 to Cause Transcriptional Repression.* Molecular Cell, 2003. **12**(2): p. 475-487.

90. Waterfield, M., Khan, I. S., Cortez, J. T., Fan, U., Metzger, T., Greer, A., Fasano, K., Martinez-Llordella, M., Pollack, J. L., Erle, D. J., Su, M., Anderson, M. S. *The transcriptional regulator Aire coopts the repressive ATF7ip-MBD1 complex for the induction of immunotolerance*. Nature Immunology, 2014. **15**(3): 258-265.
91. Wilczek, C., Chayka, O., Plachetka, A., Klempnauer, K. H. *Myb-induced chromatin remodeling at a dual enhancer/promoter element involves non-coding rna transcription and is disrupted by oncogenic mutations of v-myb.* The Journal of Biological Chemistry, 2009. **284**(51): p. 35314-35324.
92. Xu, L., Glass, K., Rosenfeld, M. *Coactivator and corepressor complexes in nuclear receptor function*. Current Opinion in Genetics & Development, 1999. **9**: p. 140–147.
93. Zhou, Y. and Ness, S.A. *Myb proteins: angels and demons in normal and transformed cells.* Frontiers of Bioscience, 2011. **16**: p. 1109 – 1131.
94. Zor, T., De Guzman, R. N., Dyson, H. J., Wright, P. E. *Solution structure of the KIX domain of CBP bound to the transactivation domain of c-Myb*. Journal of Molecular Biology, 2004. **337**(3): p. 521-534.

Appendices

Appendix 1: Abbreviations

2KR mutant	c-Myb variant with lysine residues 503 and 527 mutated into arginine
A	Absorbance
aa	Amino acid
AMV	Avian myeblastosis virus
APS	Ammonium persulfate
ATF7IP	Activating transcription factor 7 – interacting protein
ATP	Adenosine triphosphate
AU	Absorbance unit
b	Path length in cm
BB	Binding buffer
bp	Base pair
BSA	Bovine serum albumin
c	Nucleic acid concentration in ng/ µL
CBP	CREB binding protein
cDNA	Complementary DNA
ChiP	Chromatin immunoprecipitation
COS	**C**V-1 **O**rigin and carrying the **S**V40 genetic material
CRD	c-Myb domain: Carboxy-terminal regulatory domain
CREB	cAMP response element binding protein
DBD	c-Myb domain: DNA-binding domain
dH2O	Distilled water
DMEM	Dulbecco's Modified Eagle Medium
DMSO	Dimethyl sulfoxide
DNA	Deoxyribonucleic acid
Domain 1	ATF7IP domain
Domain 2	ATF7IP domain
DPBS	Dulbecco's phosphate buffered saline
DTT	Dithithreitol
E1, E2, E3	Enzymes of the SUMOylation machinery
EDTA	Ethylenediaminetetraacetic acid
EtBR	Ethidium bromide

EVES	c-Myb CRD motif
FAETL/LZ	c-Myb CRD motif
FBS	Fetal bovine serum
FCS	Fetal calf serum
FG tag	FLAG tag
GLB	Gel loading buffer
GS	Glutathione sepharose
GST	Glutathione S-transferase
GTF	General transcription factor
H3K9	Histone 3 lysine 9
HA tag	Hemagglutinin tag
hcM	Human c-Myb
HEK	Human embryonal kidney
HRP	Horseradish peroxidase
HTH	Helix-turn-helix
IMDM	Iscove's Modified Dulbecco's Medium
Kac	Potassium acetate
kb	Kilo base
kDa	Kilo Dalton
KIX	p300/CPB domain
l-PPase	Lambda protein phosphatase
LB	Lysogeny broth
LC-96	LightCycler® 96 Real-Time PCR System
MCS	Multiple cloning site
Mim-1	Myb-induced myeloid protein 1
Model 1	Epigenetic repressor model
Model 2	Mediator-like activator model
MRE	Myb-recognition element
mRNA	Messenger RNA
MYB domains	R1, R2 and R3
NEM	N-ethylmalemide
p300	CBP homologue (300 kDa)
PAGE	Polyacrylamide gel electrophoresis
PCR	Polymerase chain reaction
PS	Penicillin / streptomycin
PTM	Post-translational modification

PVDF	Polyvinylidene fluoride
R1, **R2, R3**	c-Myb DBD repeats
rcf	Relative centrifugal force
rcm	Revolutions per minute
RLU	Relative luciferase units
RNA	Ribonucleic acid
RNAPII	RNA polymerase II
SDS	Sodium dodecyl sulphate
SENP	Sentrin-specific protease
SIM	SUMO-interacting motif
SRAF	SUMO-regulated activation function
STUbLs	SUMO-targeted ubiquitin ligases
SUMO	Small ubiquitin-related modifier
TAD	c-Myb domain: Transactivation domain
TBS-T	Tris-buffered saline-Tween-20
TE	Tris-EDTA
TEMED	Tetramethylethylenediamine
TF	Transcription factor
TP	c-Myb CRD region rich in threonine and proline
U	Enzyme unit
UV	Ultraviolet
WB	Western blot
WT	Wild-type
Y2H	Yeast two-hybrid

Amino Acid Abbreviations		
One letter code	Three letter code	Name
G	Gly	glycine
A	Ala	alanine
V	Val	valine
I	Ile	isoleucine
L	Leu	leucine
S	Ser	serine
T	Thr	threonine
C	Cys	cysteine
M	Met	methionine
D	Asp	aspartate
E	Glu	glutamate
N	Asn	asparagine
Q	Gln	glutamine
K	Lys	lysine
R	Arg	arginine
H	His	histidine
F	Phe	phenylalanine
Y	Tyr	tyrosine
W	Trp	tryptophan
P	Pro	proline
Ψ	large hydrophobic amino acid residue	
x	any amino acid residue	

Nucleotide Abbreviations	
One letter code	Name
A	Adenine
G	Guanine
C	Cytosine
T	Thymine
U	Uracil
R	Purine (A or G)
Y	Pyrimidine (C or T)
N	Any nucleotide
W	Weak (A or T)
S	Strong (G or C)
M	Amino (A or C)
K	Keto (G or T)
B	Not A (G, C or T)
H	Not G (A, C or T)
D	Not C (A, G or T)
V	Not T (A, G or C)

Appendix 2: Recipes

Appendix 2.1: Solutions for general use

100x Complete protease inhibitor (500 µL)
1 tablet complete protease inhibitor is dissolved in 500 µL sdH_2O

1 M DTT (20 mL)
3.09 g DTT
20 mL 0.01 M sodium acetate pH 5.2
Sterile filtrate
Store at -20^{0}C

0.5 M EDTA (250 mL)
46.53g $NA_2EDTA*2H_2O$
200 mL dH_2O
5g NaOH pellets (the pH must be just above 7 for EDTA to be dissolved)
Adjust pH to 8.0 with 1 M NaOH
Adjust volume to 250 mL with dH_2O
Autoclave

50% Glycerol (100 mL)
50 mL 99.5% Glycerol
50 mL dH_2O
Autoclave

5 M KAc (250 mL)
122.6 g KAc
250 mL dH_2O
Autoclave

LB medium (1000 mL)
10 g Trypton
5.0 g Yeast extract
10 g NaCl
dH_2O to 1000 mL
Adjust pH to 7.2 with 1 M NaOH
Autoclave

LB plates (20 plates)
400 mL LB medium
6.0 g agar
Autoclave

When the temperature is approximately 50°C antibiotics can be added (e.g. Ampicillin 100 μL/ mL or Chloramphenicol 25 μL/ mL). Use approximately 20 mL medium for each petri dish.

2 M $MgSO_4$ (250 mL)
123.24 g $MgSO_4$
250 mL dH_2O

5M NaCl (500 mL)
146.1 g NaCl
500 mL dH_2O
Autoclave

10 M NaOH (50 mL)
20 g NaOH pellets
50 mL dH_2O

50 mM PMSF (10 mL)
87 mg PMSF
10 mL isopropanol
freeze at -20°C

SOB medium (1000 mL)
20 g trypton
5.0 g yeast extract
0.5 g NaCl
dH_2O to 800 mL

50x TAE (500mL)
121 g Tris-base
50 mL 0.5 M EDTA
28.5 mL acetic acid
dH_2O to 500 mL

1x TE buffer (500 mL)
5 mL 1 M Tris-HCl pH 8.0
1 mL 0.5 M EDTA
dH_2O to 500 mL
Autoclave

0.5 M Tris HCl pH 6.8 (500 mL) – Upper buffer
30.28 g Tris base
400 ml dH_2O
Adjust pH to 6.8 with HCl
dH_2O to 500 ml
Autoclave

1 M Tris HCl pH 8 (1000 mL)
121.15 g Tris base
800 ml dH_2O
Adjust pH to 8.0 with HCl
dH_2O to 1000 mL
Autoclave

1.5 M Tris HCl pH 8.8 (500 mL) – Lower buffer
90.9 g Tris base
400 mL dH_2O
Adjust pH to 8.8 with HCl
dH_2O to 500 mL
Autoclave

10% Triton X-100 (50 mL)
5 mL 100% Triton X-100
dH_2O to 50 mL

Appendix 2.2: Solutions for SDS-PAGE

10% APS (10 mL)
1 g APS
10 mL H_2O
store at -20°C

10% SDS (500 mL)
50 g SDS
H_2O to 500 mL

1x SDS electrophoresis buffer (1000 mL)
15 g glycine
3 g Tris base
10 mL 10% SDS
dH_2O to 1000 mL

3x SDS loading buffer (10 mL)
3.75 mL 0.5 M Tris HCl pH 6.8
0.69 g SDS
3 mL 99.5% glycerol
dH_2O to 10 mL
Add a few grains bromphenol blue. Before use add 10% 1 M DTT.

10 % SDS polyacrylamide gel
Separating gel:
8 mL 40% acrylamide
8 mL 1.5 M Tris HCl pH 8.8
16 mL dH2O
320 µL 20% SDS
100 µL 10 % APS
20 µL TEMED

Stacking gel:
2.5 mL 40% acrylamide
5 ml 0.5 M Tris HCl pH 8.8
12.5 mL dH2O
200 µL 20% SDS
60 µL 10 % APS
20 µL TEMED

Appendix 2.3: Solutions for WB

Minus buffer (500 mL)
500 mL plus buffer
2.62 g e-amino-n-caproic acid

Plus buffer (1000 mL)
3.0 g Tris base 20% methanol
dH_2O to 1000 mL

10x TBS-T (500 mL)
50 mL 1 M Tris HCl pH 8.0
150 mL 5 M NaCl
2.5 mL Tween 20
dH_2O to 500 mL

1x TBS-T with 5% milk (500 mL)
25.0 g skim milk powder
50 mL 10x TBS-T
dH_2O to 500 mL

Appendix 2.4: Solutions for GST-pulldown and phosphatase treatment

Binding buffer
50 mM Tris HCl pH 8
150 mM NaCl
5 mM EDTA
1% Triton X-100
Prior to use add DTT and Complete protease inhibitor to final concentrations:
- 1 mM DTT
- 1x Complete protease inhibitor

KAc buffer (1000 mL)
20 mM HEPES pH 7.6
10% Glycerol
0.2% Triton X-100
150 mM KAc
Prior to use add DTT and Complete protease inhibitor to final concentrations:
- 1 mM DTT
- 1x Complete protease inhibitor

PTP buffer (100 mL)
33 mL 150 mM HEPES pH 7.6
2 mL 500 mM EDTA
4 mL 250 mM EGTA
dH_2O to 100 mL
Prior to use add PMSF, Leupeptin and Aprotinin:
- 1 mM PMSF
- 10 μg / mL Leupeptin
- 10 μg / mL Aprotinin

Appendix 3: Primers

Appendix 3.1: Primers for site-directed mutagenesis

SIM-VIDL to AADA

M167	GGCAGTGATTCAAGTGGTGcCgcgGATgcCACAATGGATGATGAAGAG
M168	CTCTTCATCATCCATTGTGgcATCcgcGgCACCACTTGAATCACTGCC

Appendix 3.2: Primers for sequencing

S068	rev pCIneo	CTCCCCCTGAACCTGAAACA
S082	fwd pCIneo	GACATCCACTTTGCCTTTCTCTCC
S140	rev pcDNA3-R1	CAACAGATGGCTGGCCAACTA
S182	fwd pBS	GTAAAACGACGGCCAGTG
S183	rev pBS	GAAACAGCTATGACCATG
S239	fwd CMV - S2	CCACTGCTTACTGGCTTATCG
S248	rev BGH	TAGAAGGCACAGTCGAGGC
hMBD1_F_end	fwd MBD1	TACCCATGATCTTCGCTTCC
hMBD1_R210	rev MBD1	ACGTGAGCCACCTCAGATTC
hSETDB1_F_end	fwd SETDB1	CCAGGTGAAGCAAGAGAAGG
hSETDB1_R233	rev SETDB1	GCACAAGATGCCTTGTTTGA

Appendix 3.3: Primers for quantitative real-time PCR

LC-mim-F	GCAACAGTGTATGCTCCCTTTT
LC-mim-R2	ATCTGAGCGATCGCAGTTCT
LC-GgHPRT1-F568	GGATACGCCCTCGACTACAA
LC-GgHPRT1-R772	GGGCTGGGGTGTTCTACAAT
LC-hcM-F1438	AAATACGGTCCCCTGAAGATGCTA
LC-hcM-R1653	GTCTGCGTGAACAGTTGGGTATTC

Appendix 4: Plasmids

Appendix 4.1: Miscellenious plasmids

Bluescript SKII+ (pBS)
pCIneo-HA
pCIneo-HA-hMBD1
pCIneo-hSETDB1
pCIneo-hSUMO1-Q94P
pCIneo-hSUMO2-Q90P
pCIneo-RfA
pCIneoB-GBD-VP16
pCMVB-T7-PIASy
pCneo-p300-myc
pGEX-KG-hMBD1
pOTB7-MBD1
pOTB7-SETDB1

Appendix 4.2: c-Myb plasmids

pCIneo-3FG-hcM
pCIneo-3FG-hcM-SUMO1
pCIneo-hcM-HA
pCIneo-hcM-HA-2KR
pCIneoB-GBD-hcM(194-640)
pCIneoB-GBD-hcM(194-640)-2KR
pEF1neo-3xTy1-hcM

Appendix 4.3: ATF7IP plasmids

pBS-ATF7IP-EcoNot
pBS-ATF7IP-EcoNot SIM-AADA
pcDNA3-FG-ATF7IP
pCIneo-3FG-ATF7IP
pCIneo-3FG-ATF7IP-CTD
pCIneo-3FG-ATF7IP-SIM-AADA
pCIneo-myc-ATF7IP
pCIneo-myc-ATF7IP-SIM-AADA

Appendix 4.4: Reporter plasmids

pGL3-MYADM
pGL4x-5xMRE(GG)-myc
pGL4x-5xMRE(GG)-myc enhancer

Appendix 5: Materials

Material	Producer	Product nr.
Enzymes		
EcoRI	New England BioLabs®	R0101S
NcoI	New England BioLabs®	R0193S
NotI	New England BioLabs®	R0189S
PpuMI	New England BioLabs®	R0506S
SacII	New England BioLabs®	R0157S
SalI	New England BioLabs®	R0138S
SmaI	New England BioLabs®	R0141S
XhoI	New England BioLabs®	R0146S
Various other NEB restriction enzymes, not specified here.		
Gateway® LR Clonase® Enzyme mix	Invitrogen	11791-019
Vent Polymerase	New England BioLabs®	M0254L
Pfu Ultra Hotstart DNA polymerase	Stratagene	600390
T4 DNA ligase	New England BioLabs®	M0202L
CIP	New England BioLabs®	M0290S
SAP	Affymetrix	78390
λ-PPase	New England BioLabs®	P0753S
Buffers		
EcoRI buffer	New England BioLabs®	Supplied
NEB 1.1	New England BioLabs®	Supplied
NEB 2.1	New England BioLabs®	Supplied
NEB 3.1	New England BioLabs®	Supplied
CutSmart	New England BioLabs®	Supplied
Vent Polymerase	New England BioLabs®	Supplied
Pfu Ultra buffer	Stratagene	Supplied
T4 DNA ligase buffer	New England BioLabs®	Supplied
λ-PPase buffer	New England BioLabs®	Supplied
Ladders		
1 kb DNA ladder	Invitrogen	15615-024
Precision Plus Protein dual color	Bio-Rad	161-0374
Extras		
2.5 mM dNTP Mix	Invitrogen	R72501
Complete Protease Inhibitor Tablets	Roche	11836145001
Antibiotics		
Ampicilin	Sigma-Aldrich	A0166
Kanamycin	Sigma-Aldrich	K4000
Chloramphenicol	Sigma-Aldrich	C3175
Pyromycin	Sigma-Aldrich	P9620
Cell culture		
Countess™ slides	Invitrogen	C10228
DMEM	Gibco® Invitrogen	41965-039
DPBS	Gibco® Invitrogen	14190-094

FBS	Gibco® Invitrogen	10106-169
IMDM	Gibco® Invitrogen	12440-053
PenStrep	Gibco® Invitrogen	15140-122
TransIT® -LT1	Mirus	MIR 2300
Tryphan blue	Invitrogen	T10282
Trypsin-EDTA	Gibco® Invitrogen	25300-054
GST-pulldown		
Glutathione Sepharose 4B	GE- healthcare	17-0756-01
SDS-PAGE and WB		
Amersham Hybond-P	GE- healthcare	RPN303F
Criterion XT 4-12% Bis-Tris gel	Bio-Rad	345-0123
Restore Western Blot Stripping Buffer	Thermo Scientific	21062
SuperSignal West Dura Extend Duration Substrate	Thermo Scientific	34076
Whatman filter paper	Whatman GE- healthcare	3017-915
XT MOPS running buffer	Bio-Rad	161-0788
Antibodies		
α-ATF7IP/MCAF1 rabbit	Bethyl Laboratories	A300-169A
α-FLAG mouse	Sigma-Aldrich	F1804
α-GAPDH mouse	Invitrogen	AM4300
α-HA rabbit	Sigma-Aldrich	H9658
α-Myb H-141 mouse	Santa Cruz Biotechnology	Sc-7874
α-SETDB1 rabbit	Abcam	ab12317
HRP-α-mouse donkey	Jackson ImmunoResearch Laboratories	715-035-150
HRP-α-rabbit donkey	Jackson ImmunoResearch Laboratories	711-035-152
Commercial kits		
AffinityScript QPCR cDNA Synthesis	Agilent	600559
Gateway® LR Clonase® Enzyme mix	Invitrogen	11791019
Luciferase Assay System	Promega	E4530
NucleoBond®Xtra	Macherey-Nagel	740414.5
NucleoSpin®ExtractII	Macherey-Nagel	740609.5
NucleoSpin®Plasmid	Macherey-Nagel	740588.25
RNeasy Mini Kit	Qiagen	74104
Software		
Carestream Molecular Imaging	Carestream Health	
CLC main workbench 6.5	CLC bio	
GraphPad Prism	GraphPad Software, Inc.	
LC-96 Software	Roche	
NanoDrop 2000	Thermo Scientific	